Suzuki–Miyaura cross-coupling based synthesis and characterization of fluorescent and chemiluminescent boron dipyrromethene dyes spanning near-infrared region

(近赤外領域にわたるボロンジピロメテン蛍光および化学発光色素の鈴木–宮浦クロスカップリングを活用した合成とその特性評価)

Guanglei Li

Division of Environmental Materials Science

Graduate School of Environmental Science

Hokkaido University

A dissertation submitted for
the degree of Doctor of Philosophy

2018

Table of Contents

Chapter 1 General Introduction

Fluorescence has been used extensively in diverse fields, such as clinical diagnostics, life science, materials, food analysis and environmental sciences[1,2]. Compared to traditional measurement methods, such as magnetic resonance imaging, computed tomography, X-ray, ultrasound and radiography, fluorescence imaging offers an optional way which possesses incomparable merits, especially for cellular sensing and imaging of living systems[3-6]. For instance, fluorescence imaging is a non-invasive measurement, and it does not consume or destroy the specimens, which is essential for live systems[6,7]. The high sensitivity and specificity enable the detection even in single molecule level[8], what's more, the rapid development of fluorescence microscopy and spectroscopy, as well as fluorescent labeling techniques, make it possible to provide detailed information about the kinetics, dynamics and 3D architecture of the various analytes simultaneously[9]. In addition, fluorescence does not include radioactive risks, it is a safe detection method for both analytes and analysts. Thus, fluorescence technology has a bright perspective in the future.

As fluorophores, which correspond to convert the information of analytes to detectable fluorescence signals, are the essential elements of the fluorescence sensing systems. The rapid growth of using fluorescence technology call for design, development, and characterization of many fluorophores featuring various properties.

1.1. Near-infrared (NIR) fluorescent dyes

Fluorescent dyes have been widely used as an indispensable tool to obtain relevant biological information. However, for imaging of deep tissues (>500 μm to cm) require the use of NIR light. As shown in **Figure 1.1**, visible and infrared light could be absorbed efficiently by oxy- and deoxyhemoglobin and water, the major absorbers in tissue[10]. Thus, the light region around 650-900 nm is considered as NIR window, which has been recognized to be the optimal range for

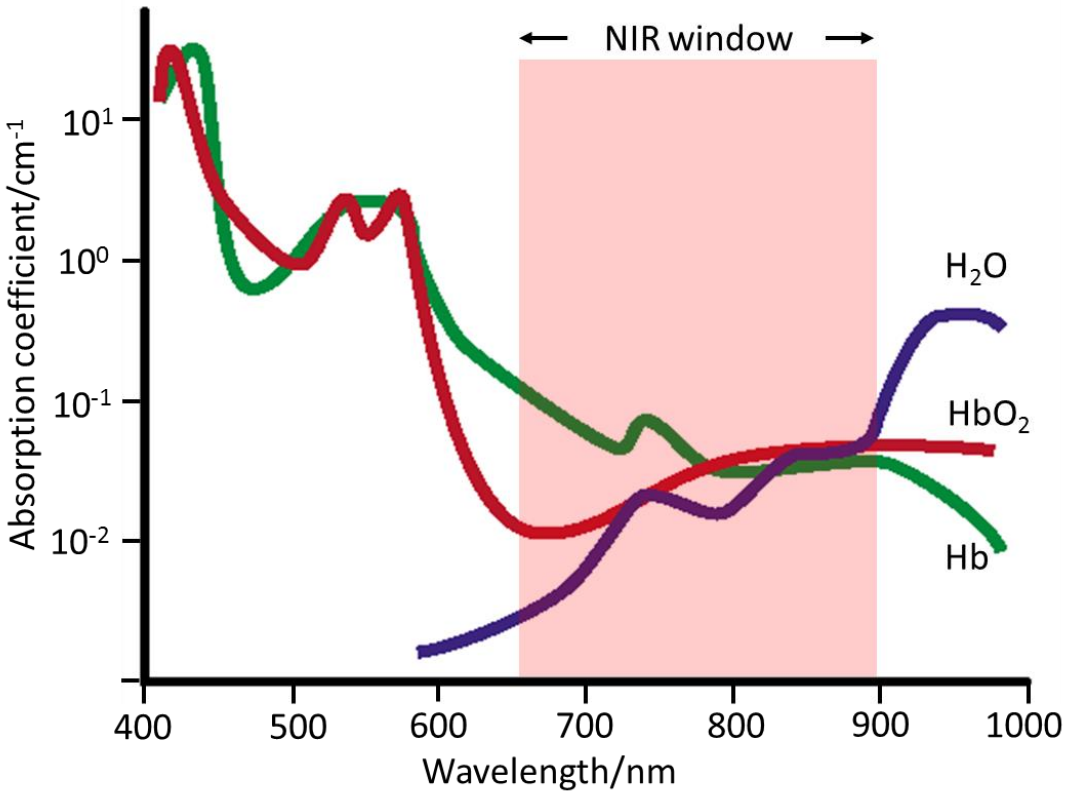

Figure 1.1. The NIR window is ideally suit for *in vivo* imaging due to minimal absorption by deoxyhemoglobin (Hb), oxyhemoglobin (HbO_2) and H_2O in this region. *Image: Nature Biotechnology volume 19, pages 316–317 (2001).*

in vivo imaging. What's more, phototoxicity to the organism, light scattering[11,12] and autofluorescence[13,14] from biological samples could be dramatically reduced. Therefore, dyes excited and emit light in the NIR region, have attracted ongoing interesting for their diverse application in biological and medical applications[15-17].

Cyanine is one of the most studied NIR fluorescent dyes. They are a unique class of charged chromophores containing an odd number of sp2 carbon atoms bridge between two electronegative centers, typically nitrogen or oxygen atoms (**Figure 1.2**)[18], they cover a wide range of spectrum from ultraviolet (UV) to NIR depending on the structure. Applied some modifications could induce an effective decrease of the HOMO-LUMO energy gap, and hence prolong the wavelengths to NIR region, for example, 1) increase the length of methane chain by an addition of vinylene groups, 2) modification the terminal groups with new heterocycles with branched electron system[19]. Cyanine derivatives have been studied extensively over more than 150 years, which are the most commonly used NIR dyes in biology[20]. However, the cyanine dyes also have some drawbacks, such as low solubility in water, the trend to aggregate in aqueous solution and low fluorescence quantum yield[6]. These problems can be alleviated by introducing some water-soluble parts, such as sulfonate groups, which increase the solubility of the dye in water and hence reduce the fluorescence quenching[6]. To date, the inherent defect, low fluorescence quantum yield, has still not fixed well and continuously restrict their practical application. Nowadays, there are plenty of NIR

cyanine dyes are available, one Cy5.5 dye as shown in **Figure 1.3** for example. Cy represents 'cyanine', the first digit ‘5’ identifies the number of carbon atoms between the two indolenine groups, and the postfix of .5 means the benzo-fused analogs.

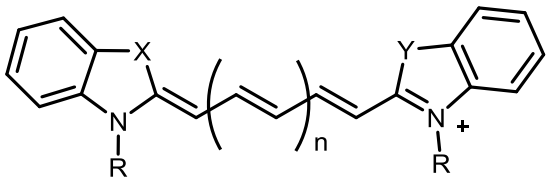

Figure 1.2. The basic structure of cyanine. (X, Y = O, S, C, C(CH_2) or C=CH_2).

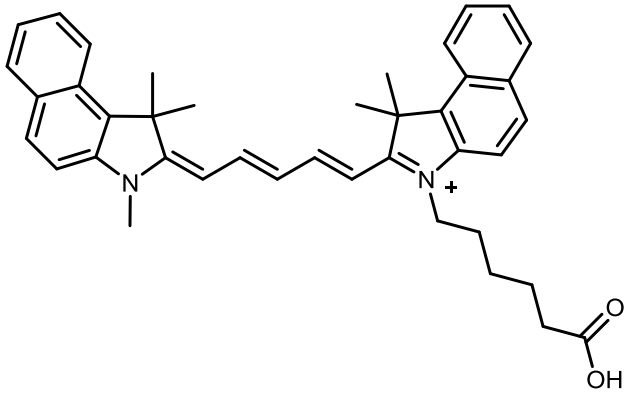

Figure 1.3. The structure of one commercially available Cy5.5 dye (Lumiprobe corporation, MD, USA).

1.2. NIR bio/chemiluminescent dyes

Unlike fluorescence, bio/chemiluminescence is generated through a certain reaction instead of excitation light, therefore high signal-to-noise ratio is achieved due to no background noise arising from autofluorescence. High sensitivity makes bio/chemiluminescence assay widely used in various chemical and biological

applications[21,22].

There are many types of bioluminogenic systems in nature (such as certain species of jellyfish, firefly, and squid)[23], and considerable efforts have been devoted to design and synthesize longer wavelength bio/chemiluminescent dyes. Recently, a new type of NIR bioluminescent probes has been developed, named AkaLumine-HCl (**Figure 1.4**)[24]. It emits light in the NIR region (λ_{max} = 677 nm) in the reaction with firefly luciferase. Compared to D-luciferin and cyclic alkylaminoluciferin (CycLuc1) (λ_{max} = 604 nm), AkaLumine-HCl has been proved to be better suited for the detection of deep tissue by tissue imaging experiments on mice.

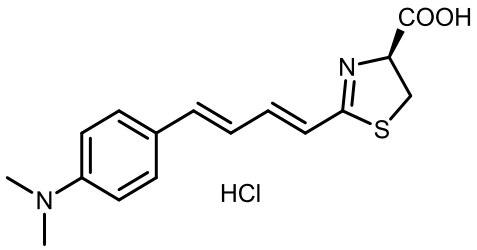

Figure 1.4. The structure of AkaLumine-HCl.

Innately, bioluminescence analysis is restricted by cells that are engineered to express the enzyme luciferase, while chemiluminescence light is initiated by a specific chemical reaction without enzymatic dependence. It could offer some advantages over bioluminescence analysis due to its ability for wider application.[25-27].

Purely organic and nonbiological chemiluminogens are rare[23], and can be classified mainly into several groups as oxalate ester, acridinium ester, dioxetanes

and luminol derivatives[26,27]. Some efforts have been made to prepare longer wave longer wavelength chemiluminescent dyes, however, most of them are still in the visible wavelength ranges[23,28-32]. Recently, a dioxetane based NIR chemiluminescent dye has been synthesized by composing of dioxetane tethered with the quinone-cyanine (**Figure 1.5**)[33]. Removal of the galactose (trigger) by β-galactosidase initiates the chemically initiated electron exchange luminescence (CIEEL) mechanism, which leads to energy transfer from the excited benzoate to the quinone-cyanine and resulting in the excitation of the fluorophore[33]. The chemiluminescent dye emits NIR light with a maximum wavelength of 714 nm. What's more, the emitted light can be varied by exchanging the quinone-cyanine to other fluorophores, such as fluorescein (λ = 535 nm). However, dioxetanes are prone to decompose by heat and/or light. Both dyes decomposed completely lees in 13 hours under normal room illumination condition at room temperature.

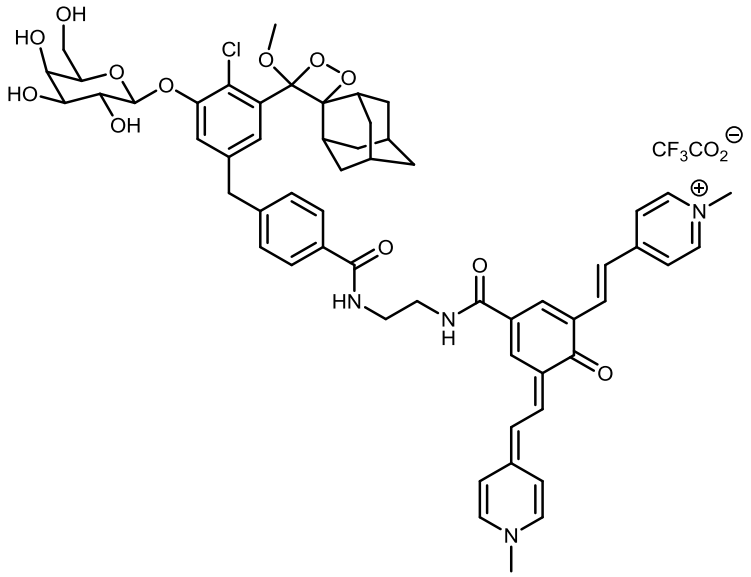

Figure 1.5. The molecular structure of dioxetane based NIR chemiluminescent dye.

1.3. BODIPY derivatives

BODIPYs (IUPAC name: 4,4-difluoro-4-bora-3a,4a-diaza-s-indacene derivatives), also known as boron dipyrromethene, is a class of organic fluorescence dyes which share the same core composed of dipyrromethene typically complexed with a BF_2 unit. The BODIPYs was first reported by A. Treibs and F.-H. Kreuzer in 1968[1,34] and have attracted constant enthusiasm from chemists. Mostly due to their inherent excellent features: high molar absorption coefficients and quantum yields, stability against chemical reagents and extreme temperatures, and tuneable spectroscopic and photophysical properties[1,35]. However, the excitation and emission maxima of most BODIPY chromophores are less than 600 nm, the relatively short wavelengths limit hinder their practical application in living systems[36]. Thus, it is crucial to prolong the wavelengths of BODIPY chromophore to the NIR region.

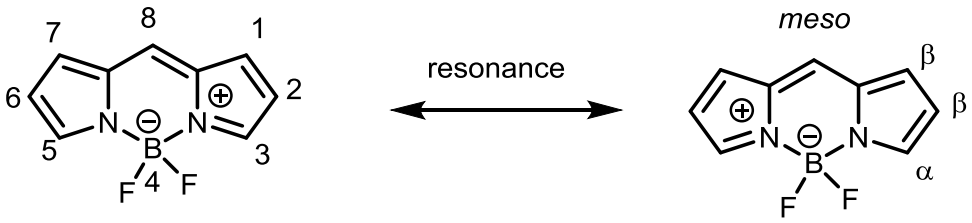

Figure 1.6. The molecular structure of BODIPY and its IUPAC numbering system. Delocalized resonance structures are provided with the formal charges indicated.

1.4. NIR BODIPYs

As mentioned above, one of the merits of BODIPY chromophores is the spectroscopic and photophysical properties are possible to be turned by slight

chemical modifications. A wide range of modification method has been performed to synthesize NIR BODIPY dyes, such as the extension of π-conjugation length [37,38], the formation of a "push-pull" motif[39,40], rigidification of rotatable moieties[36,41] and exchange the *meso*-carbon atom to nitrogen atom to form aza-BODIPY dyes[42-44]. A summary of the modification strategies and some selected NIR BODIPY chromophores will be briefly discussed herein.

1.4.1. Extension of π-conjugation of BODIPYs

Extension of π-conjugation of BODIPYs is an efficient way to decrease the HOMO-LUMO energy gap and prolong the absorption and emission wavelength to the longer region. However, generally 4-position is not favorable for this kind of modification, and many authors have reported that these changes have little effect on the optical properties[45,46]. 1,7-positions were also described as not favorable for promoting the spectra[47]. K. Yamada et al. have stated that rotatable substituents at *meso*-position are poorly conjugate with BODDIPY core and what's wore they could decrease the fluorescence quantum yield[48]. Since there is a nodal plane at the *meso*-carbon of BODIPY core, the substituted π-systems has a minor effect on the BODIPY core[49]. Hence, the extension of π-conjugation of BODIPYs usually carried out on α-position (3,5-positions) and β-position (2,6-positions) of BODIPYs instead of *meso*- and 4- positions.

Many far-red and NIR BODIPYs have been developed via these ways, some of them are very interesting, here are some typical examples. Directly connect phenyl (**1.2**)[50], pyrrole (**1.3**)[51] and thiophene (**1.4**)[50] substituents at these positions lead to appreciable bathochromic shifts. As the results are shown in **Figure 1.7**, although the spectroscopies of these compounds were not measured in the same solvent, we can still calculate some conclusions: 1) phenyl could prolong the wavelengths, but the red-shift is limited. 2) hetero-aromatic rings, such as pyrrole and thiophene units could lead to longer red-shift than phenyl did. These conclusions were supported by another study, furan (**1.7**) also induce a larger redshift than phenyl (**1.6**) did. Comparing compound **1.8** and **1.9**, more thiophene rings led to a further redshift in wavelengths. These spectral differences were aroused by 1) the degree of steric hindrance between the substitution groups and BF_2 unit decreasing from a 6- to a 5- membered ring 2) 5- membered aromatic rings are electron rich. Oligothienyl-BODIPYs (**Figure 1.8**) were synthesized by connecting many thiophene units at the 3,5-positions, increasing the number of thiophene units pronged the wavelengths longer.

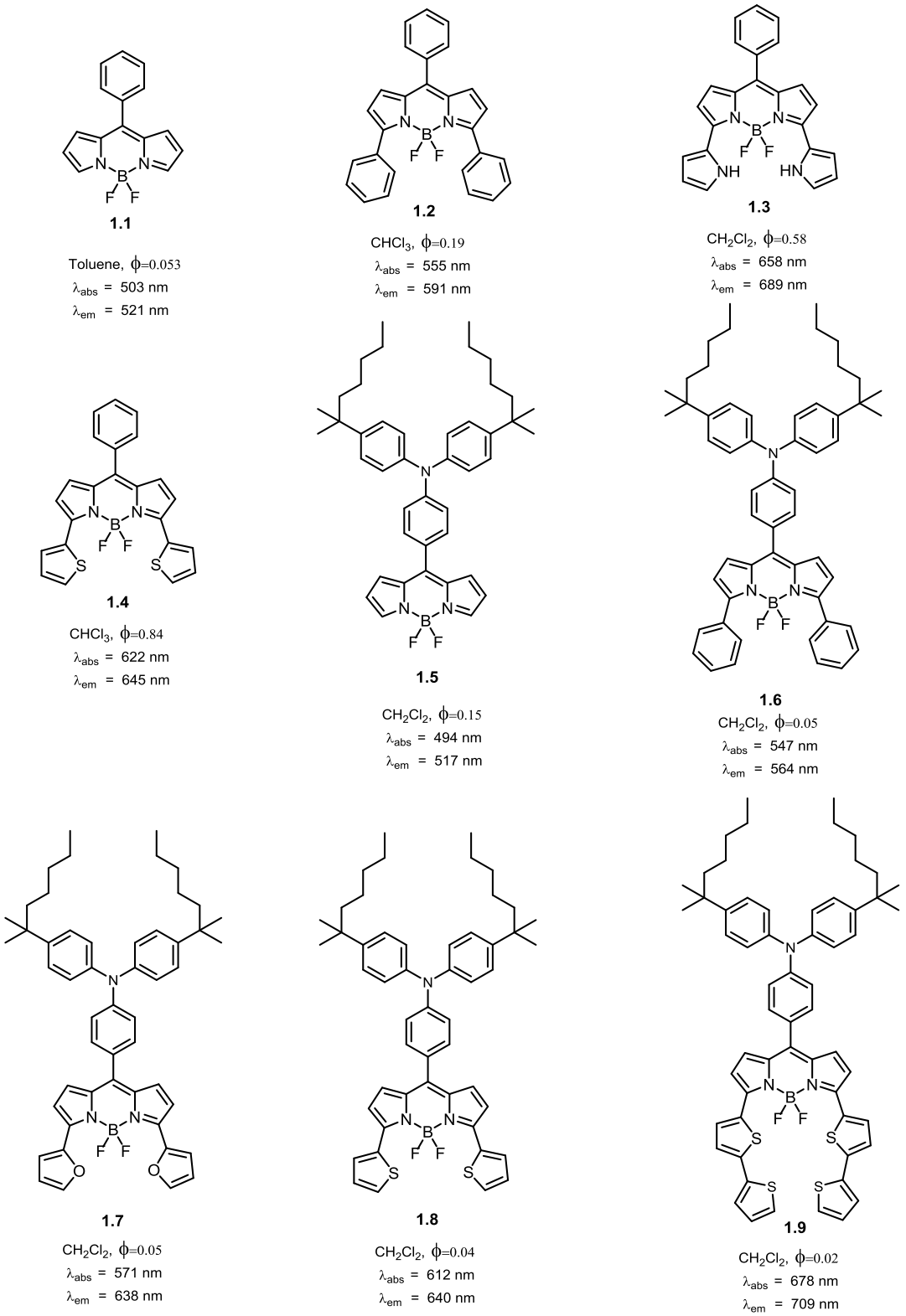

Figure 1.7. Examples of aryl and heteroaryl substituted BODIPYs. (The optical data in the figure are from the previous publications [50-53])

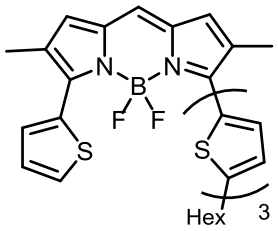

1.10

CH_2Cl_2, ϕ=0.1
λ_{abs} = 645 nm
λ_{em} = 725 nm

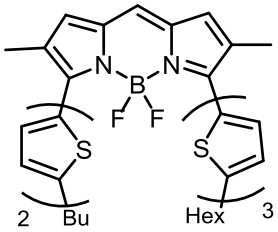

1.11

CH_2Cl_2, ϕ=0.14
λ_{abs} = 677 nm
λ_{em} = 769 nm

Figure 1.8. Examples of α-Oligothienyl substituted BODIPYs (The optical data in the figure are from the previous publications[54])

Similar modification strategies have been applied to modify on 2,6-positions of BODIPYs. As shown in **Figure 1.9**, compound **1.12** and **1.13** almost showed same absorption maxima, that because the dihedral angles between the least square plane of the thiophene ring and that of the adjacent pyrrole ring were similar for these two compounds[50]. Although, thiophene substituted at 2,6-positions lead much further bathochromic shift (c.a. 40 nm), at the cost of fluorescence quantum yield. Compared to the thienyl groups of **1.12**, which is restricted by the fluorine atom via hydrogen bond (C—H--F) of BF_2 unit[55], the thienyl groups of **1.13** are flexible, the geometry relaxation induced larger Stokes shift[56]. Compound **1.14**, a BODIPY with four 2-thienyl substituted at 2,3,5,6-positions, exhibit a slight redshift. The relative short bathochromic shift is predictable for the multiple substitutions give rise to high steric hindrance and unfavorable to the extension of π-conjugation[50].

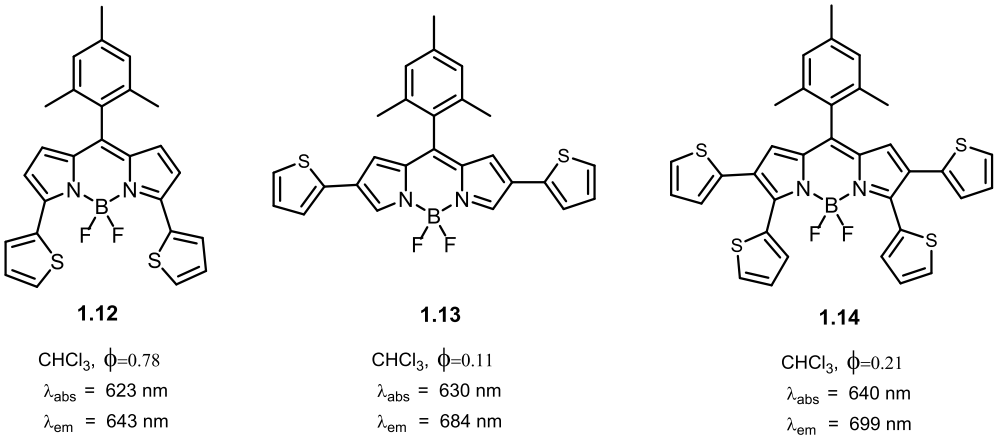

Figure 1.9. Examples of thienyl substituted BODIPYs**.** (The optical data in the figure are from the previous publication[50])

The strategy to extend the π-conjugation of BODIPYs is not limited to the aromatic substitution groups, alkenyl and alkynyl were also applied to elongate the π-conjugation of BODIPYs. Alkenyl and alkynyl can be efficiently introduced at 3,5- positions of BODIOYs via the Heck and Sonogashira coupling reactions. Introduction of styryl groups at the 3,5- positions in compound **1.15** causes larger redshift than that of compound **1.16**, both the absorption and emission maxima of **1.15** were red-shifted by ~20 nm compared to **1.16**, however, still not extend to the NIR region[57]. Compound **1.17**, bearing a thiophene at each end of alkynyl groups, exhibited absorption and emission maxima in the NIR regions. Cellular staining experiments showed **1.17** was possible to permeate through cell-membrane, and readily taken up by human carcinoma HEp2 cells, meanwhile, it was found to localize mainly within the endoplasmic reticulum[58].

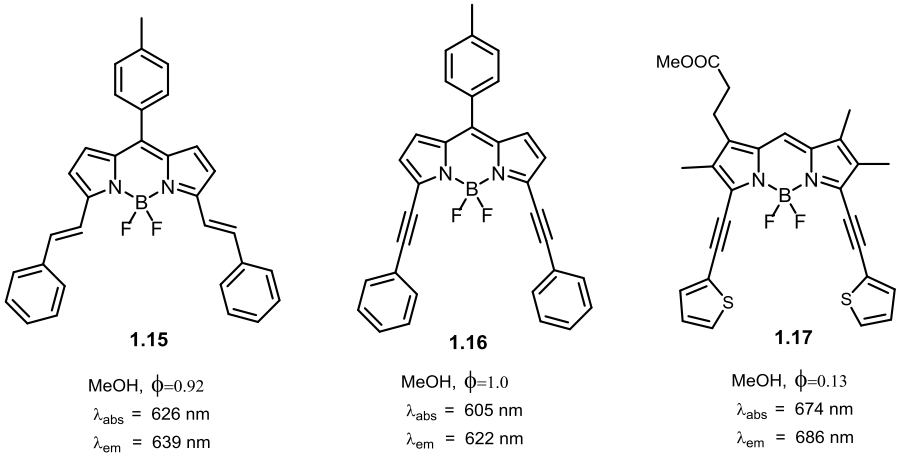

Figure 1.10. Examples of 3,5-alkenyl and alkynyl substituted BODIPYs (The optical data in the figure are from the previous publications[57,58])

Regioselective borylation was achieved by the iridium catalyzed reaction on the *meso*-substituted dipyrromethane and boron dipyrrin (BODIPY) dyes[59]. The regioselective borylation enabled various modification at the α- or/and β- positions via the rhodium-catalyzed Heck-type addition. Several polymethine-substituted BODIPYs were prepared, and two typical compounds (**1.8**, **1.9**) showed a remarkable bathochromic shift in both absorption and emission spectra. Compared to **1.9**, the 3,5-disubstituted BODIPY **1.8** displayed slight redshift, but much higher fluorescence quantum yield. These studies revealed that the properties of parent BODIPYs could be finely tuned both by the substitution groups and their modification positions.

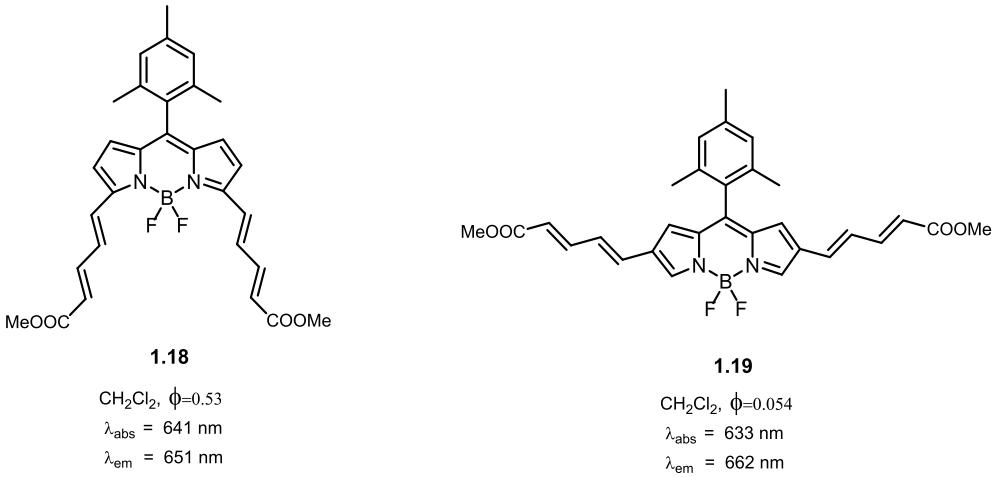

Figure 1.11. Dimethine ester substituted BODIPYs (The optical data in the figure are from the previous publication[59]

1.4.2. Formation of a "push-pull" motif

Generation of a "push-pull" motif is an efficient way to push the absorption and emission spectra to longer wavelength regions. The larger molecular orbitals (MO) coefficient of the HOMO of 3,5-positions was found, the electron-donating groups were expected to increase the energy of HOMO, hence decrease the energy gap between the two front molecular orbitals[49]. The BODIPY core is usually regarded as electron deficient, therefore the addition of electron-donating groups onto the BODIPY core leads to an intramolecular push-pull effect[60] and expected to low the energy gap between the HOMO and LUMO by activation of the intramolecular photophysical process, such as charge transfer and electron transfer[61]. Compound **1.20** and **1.21** which bearing electron-donating moieties (methoxy and dimethylamino groups, respectively) at the para-position of phenyls

exhibited different bathochromic shifts in both absorption and emission spectra. The stronger electron-donating group (dimethylamino, Hammett parameter σ= -0.84) led a larger red-shifts than that of the weaker electron-donating group (methoxy, σ= -0.268). The absorption and emission maxima of **1.20** and **1.21** were in the NIR regions.

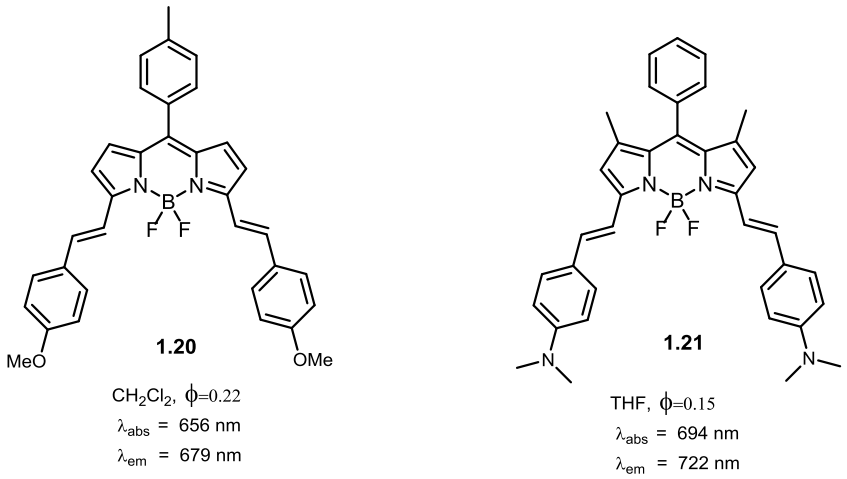

Figure 1.12. Examples of push-pull BODIPYs (The optical data in the figure are from the previous publications[62,63])

Addition of electron-donating and electron-withdrawing groups onto the BODIPY core simultaneously could further enhance the push-pull effect, the spectroscopic and photochemical would change dramatically[64]. Two thienyls were installed in at the 2- and 6- positions of **1.2**, the electron-rich donors induced a pronounced bathochromic shift.

Although, there is a nodal plane at the *meso*-position and the π-system attached at the *meso*-position hardly alter the energy gap between the two frontier π-MOs. There is a large MO coefficient of the LUMO at the meso-positions,

therefore the introduction of electron-withdrawing groups at the position is expected to decrease the energy of LUMO[49]. The further red shift was observed for **1.23**, after attaching the electron-withdrawing cyano group (−CN) and electron-donating methoxy groups (−OMe) onto the *meso*- and 3,5-positions of **1.22**, respectively. Multiple sets of push-pull in the compound **1.24** lead to a remarkable red shift as expected. However, one un-negligible drawback was encountered, the "push-pull" style dyes showed very low fluorescence quantum yields which could be due to the intramolecular charge transfer (ITC) resulting from the donors and acceptors[64,65].

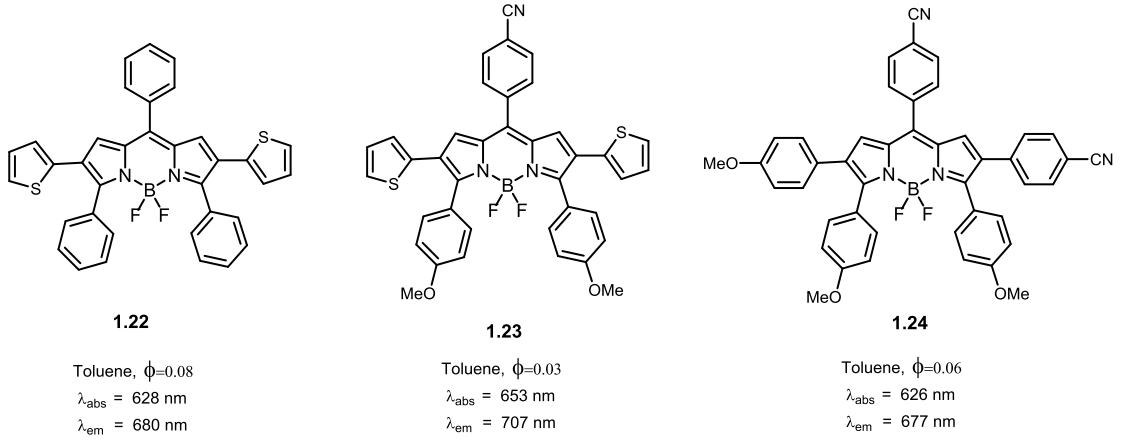

Figure 1.13. Examples of push-pull BODIPYs (The optical data in the figure are from the previous publication[39])

1.4.3. Other modification strategies

Rigidification of rotatable moieties

To increase the degree of co-planarity between the BODIPY core and substituents and decrease the energy loss from the thermal rotation of the aromatic substituents, various strategies have been applied to rigidify the rotatable moieties

with sp^3 hybridized carbon (**1.27**, **1.28**, **1.29**) and heteroatoms (**1.25**, **1.26**, **1.30**, **1.31**, **1.32**).

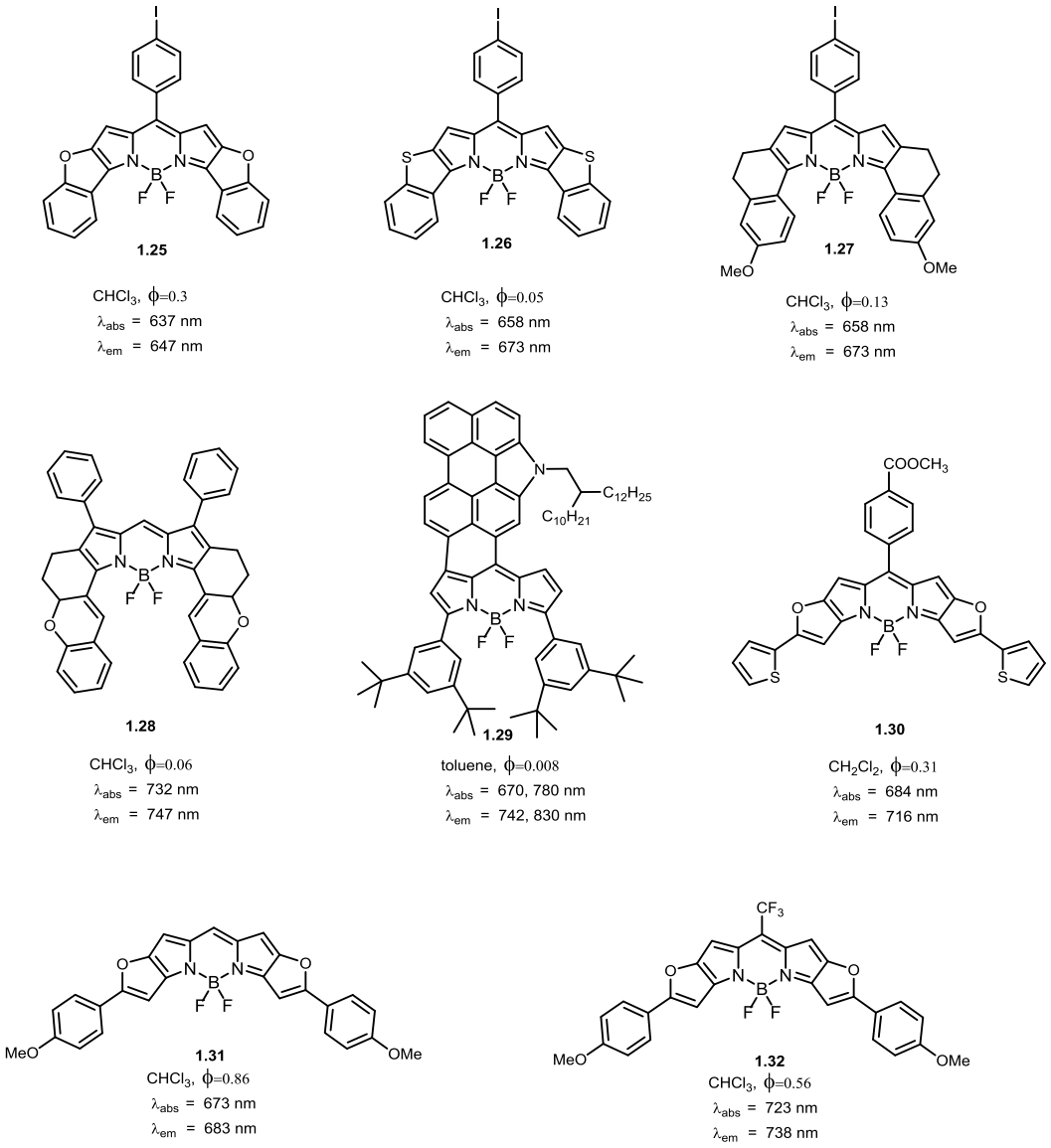

Figure 1.14. Examples of rigidified BODIPYs. (The optical data in the figure are from the previous publications[66-70])

Formation of AzaBODIPYs

Replacement of the *meso*-carbon with nitrogen atom generates an aza-difluoroboradiaza-*s*-indacene (aza-BODIPY). Electrochemical measurements and molecular-orbital calculation confirmed that the nitrogen lone pair at the *meso*-position greatly reduces the HOMO-LUMO energy gap of the actual framework[35]. A typical aza-BODIPY dye, 1,3,5,7-tetraphenyl-azaBODIPY, showed absorption and emission maxima in the NIR region (compound **1.25**). The azaBODIPY possess high molar absorption coefficient and insensitive to the polarity of solvents. In comparison to BODIPY, the fluorescence quantum yield of azaBODIPY decreased enormously, however, still at the moderate level. A further modification, for instance, substitution with electron donating groups, the formation of push-pull motif and rigidification of rotatable moieties could prolong the wavelengths to longer regions.

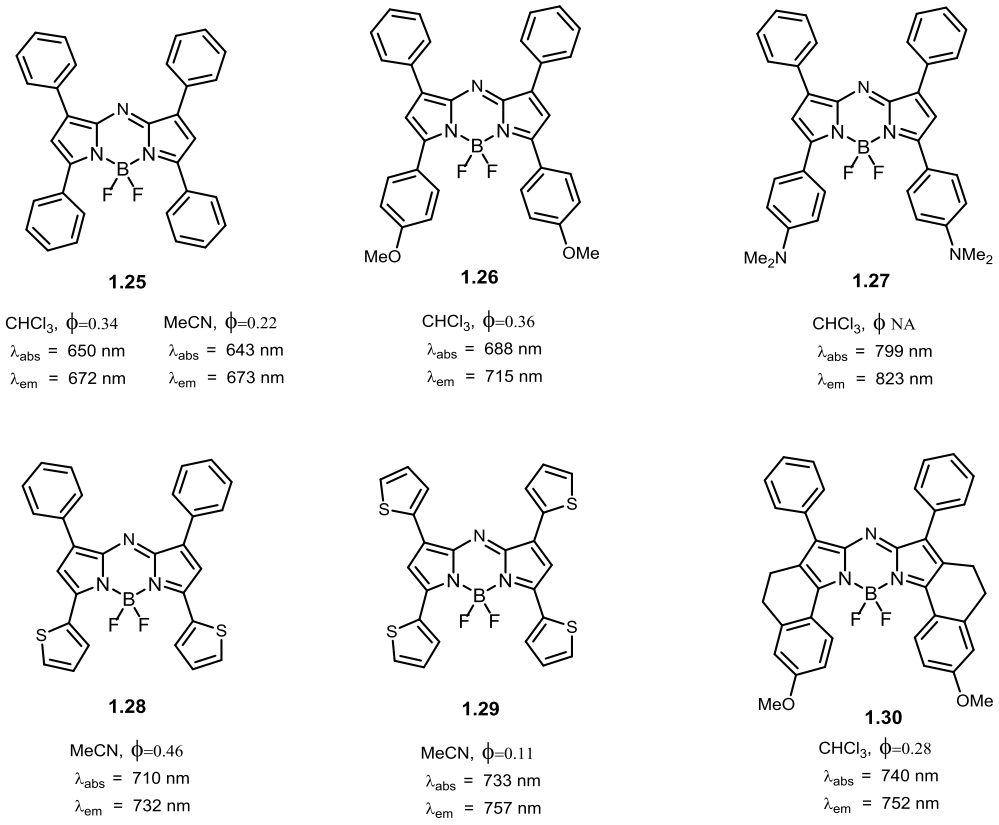

Figure 1.15. Examples of NIR azaBODIPYs. (The optical data in the figure are from the previous publications)

1.5. Objective and outline of the thesis

1.5.1. Objective of the thesis.

NIR fluorophores have been proved to be as versatile tools in diverse fields. However, synthesis of NIR fluorophores generally requires a sophisticated design that involves tedious modification steps and low synthesis yield. What's more, various synthesized NIR dyes, as for example typified by cyanines, many of them fail to show sufficient optical properties, such as high fluorescence quantum yield, stability. Therefore, it is crucial to develop a simple and systematic approach to prepare NIR fluorophore with sufficient optical properties.

Unlike fluorophore, bio/chemiluminescence was generated through a specific reaction and no excitation light is required. Bio/chemiluminescence assays have been widely utilized in chemical and biological applications due to their high sensitivity. Furthermore, chemiluminescence assay offers a more flexible method, because the light generation of chemiluminescent dye is no further enzymatic dependency. Up to date, considerable efforts have been devoted to synthesis long-wavelength chemiluminescent dye, however, only a few NIR chemiluminescent dyes have been reported. Hence, it is necessary to develop a way to prepare NIR chemiluminescent dyes.

1.5.2. The outline of the thesis.

This thesis consists of five chapters. In **chapter 1**, the general properties of NIR fluorophore, NIR chemiluminescent dyes, and BODIPYs derivatives are described. Many representatives and most recently developed NIR dyes are also briefly introduced. **Chapter 2** described a facial way to synthesize NIR BODIPY fluorophores by using a one-step Suzuki–Miyaura cross-coupling. The details of the experimental methods, photophysical properties of the NIR dyes and characteristic information are all included. In **chapter 3**, three kinds of luminol-based NIR chemiluminescent dyes were developed by further modification of the NIR fluorescent dyes described in chapter 2, the details of the experimental procedure, spectroscopic and photophysical properties of the NIR chemiluminescent dyes and characteristic information are all described. In **chapter 4**, cellular imaging of NIR fluorescent BODIPY dyes was conducted using bovine

cumulus cells. And the performance of the dyes in cellular staining was stated. Finally, in **chapter 5**, the findings of each chapter were summarized, and a general conclusion was described.

References

1. Boens, N.; Leen, V.; Dehaen, W. Fluorescent indicators based on bodipy. *Chemical Society Reviews* **2012**, *41*, 1130-1172
2. Liu, M.; Lin, Z.; Lin, J.-M. A review on applications of chemiluminescence detection in food analysis. *Analytica Chimica Acta* **2010**, *670*, 1-10
3. Perlette, J.; Tan, W. Real-time monitoring of intracellular mrna hybridization inside single living cells. *Analytical chemistry* **2001**, *73*, 5544-5550
4. Kues, T.; Peters, R.; Kubitscheck, U. Visualization and tracking of single protein molecules in the cell nucleus. *Biophysical Journal* **2001**, *80*, 2954-2967
5. Demchenko, A.P. *Introduction to fluorescence sensing*. Springer Science & Business Media: 2008.
6. Pansare, V.J.; Hejazi, S.; Faenza, W.J.; Prud'homme, R.K. Review of long-wavelength optical and nir imaging materials: Contrast agents, fluorophores, and multifunctional nano carriers. *Chemistry of materials* **2012**, *24*, 812-827
7. Weissleder, R.; Pittet, M.J. Imaging in the era of molecular oncology. *Nature* **2008**, *452*, 580
8. Lakowicz, J.R. Principles of fluorescence spectroscopy, (1999). Kluwer Academic/Plenum Publishers, New York: 2004.
9. Liu, Z.; Lavis, L.D.; Betzig, E. Imaging live-cell dynamics and structure at the single-molecule level. *Molecular cell* **2015**, *58*, 644-659
10. Weissleder, R. A clearer vision for in vivo imaging. Nature Publishing Group: 2001.
11. Escobedo, J.O.; Rusin, O.; Lim, S.; Strongin, R.M. Nir dyes for bioimaging applications. *Current opinion in chemical biology* **2010**, *14*, 64-70
12. Ghoroghchian, P.P.; Therien, M.J.; Hammer, D.A. In vivo fluorescence imaging: A personal perspective. *Wiley Interdisciplinary Reviews: Nanomedicine and Nanobiotechnology* **2009**, *1*, 156-167
13. Kobayashi, H.; Ogawa, M.; Alford, R.; Choyke, P.L.; Urano, Y. New strategies for fluorescent probe design in medical diagnostic imaging. *Chemical reviews* **2009**, *110*, 2620-2640
14. Frangioni, J.V. In vivo near-infrared fluorescence imaging. *Current opinion in*

chemical biology **2003**, *7*, 626-634

15. Gómez-Hens, A.; Aguilar-Caballos, M. Long-wavelength fluorophores: New trends in their analytical use. *TrAC Trends in Analytical Chemistry* **2004**, *23*, 127-136
16. Yuan, L.; Lin, W.; Zheng, K.; He, L.; Huang, W. Far-red to near infrared analyte-responsive fluorescent probes based on organic fluorophore platforms for fluorescence imaging. *Chemical Society Reviews* **2013**, *42*, 622-661
17. Hilderbrand, S.A.; Weissleder, R. Near-infrared fluorescence: Application to in vivo molecular imaging. *Current opinion in chemical biology* **2010**, *14*, 71-79
18. Le Guennic, B.; Jacquemin, D. Taking up the cyanine challenge with quantum tools. *Accounts of chemical research* **2015**, *48*, 530-537
19. Bricks, J.L.; Kachkovskii, A.D.; Slominskii, Y.L.; Gerasov, A.O.; Popov, S.V. Molecular design of near infrared polymethine dyes: A review. *Dyes and Pigments* **2015**, *121*, 238-255
20. Luo, S.; Zhang, E.; Su, Y.; Cheng, T.; Shi, C. A review of nir dyes in cancer targeting and imaging. *Biomaterials* **2011**, *32*, 7127-7138
21. Roda, A.; Guardigli, M. Analytical chemiluminescence and bioluminescence: Latest achievements and new horizons. *Analytical and bioanalytical chemistry* **2012**, *402*, 69-76
22. Roda, A.; Guardigli, M.; Pasini, P.; Mirasoli, M.; Michelini, E.; Musiani, M. Bio- and chemiluminescence imaging in analytical chemistry. *Analytica chimica acta* **2005**, *541*, 25-35
23. Degirmenci, A.; Algi, F. Synthesis, chemiluminescence and energy transfer efficiency of 2, 3-dihydrophthalazine-1, 4-dione and bodipy dyad. *Dyes and Pigments* **2017**, *140*, 92-99
24. Kuchimaru, T.; Iwano, S.; Kiyama, M.; Mitsumata, S.; Kadonosono, T.; Niwa, H.; Maki, S.; Kizaka-Kondoh, S. A luciferin analogue generating near-infrared bioluminescence achieves highly sensitive deep-tissue imaging. *Nature communications* **2016**, *7*, 11856
25. Green, O.; Gnaim, S.; Blau, R.; Eldar-Boock, A.; Satchi-Fainaro, R.; Shabat, D. Near-infrared dioxetane luminophores with direct chemiluminescence emission mode. *Journal of the American Chemical Society* **2017**, *139*, 13243-13248

26. Dodeigne, C.; Thunus, L.; Lejeune, R. Chemiluminescence as diagnostic tool. A review. *Talanta* **2000**, *51*, 415-439
27. Kricka, L. Clinical applications of chemiluminescence. *Analytica chimica acta* **2003**, *500*, 279-286
28. Bag, S.; Tseng, J.-C.; Rochford, J. A bodipy-luminol chemiluminescent resonance energy-transfer (cret) cassette for imaging of cellular superoxide. *Organic & biomolecular chemistry* **2015**, *13*, 1763-1767
29. Han, J.; Jose, J.; Mei, E.; Burgess, K. Chemiluminescent energy‐transfer cassettes based on fluorescein and nile red. *Angewandte Chemie International Edition* **2007**, *46*, 1684-1687
30. Yamagishi, Y.; Son, S.-H.; Yuasa, M.; Yamada, K. Design and synthesis of a chemiluminescent solvatochromic dye. *Chemistry Letters* **2012**, *41*, 504-506
31. Sekiya, M.; Umezawa, K.; Sato, A.; Citterio, D.; Suzuki, K. A novel luciferin-based bright chemiluminescent probe for the detection of reactive oxygen species. *Chemical communications* **2009**, 3047-3049
32. Watanabe, N.; Kino, H.; Watanabe, S.; Ijuin, H.K.; Yamada, M.; Matsumoto, M. Synthesis of bicyclic dioxetanes tethering a fluororescer through an ω-carbamoyl-substituted linker and their high-performance chemiluminescence in an aqueous system. *Tetrahedron* **2012**, *68*, 6079-6087
33. Hananya, N.; Eldar Boock, A.; Bauer, C.R.; Satchi-Fainaro, R.; Shabat, D. Remarkable enhancement of chemiluminescent signal by dioxetane–fluorophore conjugates: Turn-on chemiluminescence probes with color modulation for sensing and imaging. *Journal of the American Chemical Society* **2016**, *138*, 13438-13446
34. Treibs, A.; Kreuzer, F.H. Difluorboryl‐komplexe von di‐und tripyrrylmethenen. *Justus Liebigs Annalen der Chemie* **1968**, *718*, 208-223
35. Ulrich, G.; Ziessel, R.; Harriman, A. The chemistry of fluorescent bodipy dyes: Versatility unsurpassed. *Angewandte Chemie International Edition* **2008**, *47*, 1184-1201
36. Loudet, A.; Burgess, K. Bodipy® dyes and their derivatives: Syntheses and spectroscopic properties. In *Handbook of porphyrin science (volume 8) with applications to chemistry, physics, materials science, engineering, biology and*

medicine, World Scientific: 2010; pp 1-164.

37. Descalzo, A.B.; Xu, H.-J.; Xue, Z.-L.; Hoffmann, K.; Shen, Z.; Weller, M.G.; You, X.-Z.; Rurack, K. Phenanthrene-fused boron− dipyrromethenes as bright long-wavelength fluorophores. *Organic letters* **2008**, *10*, 1581-1584
38. Jiao, L.; Yu, C.; Liu, M.; Wu, Y.; Cong, K.; Meng, T.; Wang, Y.; Hao, E. Synthesis and functionalization of asymmetrical benzo-fused bodipy dyes. *The Journal of organic chemistry* **2010**, *75*, 6035-6038
39. Xuan, S.; Zhao, N.; Ke, X.; Zhou, Z.; Fronczek, F.R.; Kadish, K.M.; Smith, K.M.; Vicente, M.G.H. Synthesis and spectroscopic investigation of a series of push–pull boron dipyrromethenes (bodipys). *The Journal of organic chemistry* **2017**, *82*, 2545-2557
40. Yu, Y.H.; Descalzo, A.B.; Shen, Z.; Röhr, H.; Liu, Q.; Wang, Y.W.; Spieles, M.; Li, Y.Z.; Rurack, K.; You, X.Z. Mono‐and di (dimethylamino) styryl‐substituted borondipyrromethene and borondiindomethene dyes with intense near‐infrared fluorescence. *Chemistry–An Asian Journal* **2006**, *1*, 176-187
41. Hayashi, Y.; Obata, N.; Tamaru, M.; Yamaguchi, S.; Matsuo, Y.; Saeki, A.; Seki, S.; Kureishi, Y.; Saito, S.; Yamaguchi, S. Facile synthesis of biphenyl-fused bodipy and its property. *Organic letters* **2012**, *14*, 866-869
42. Zhao, W.; Carreira, E.M. Conformationally restricted aza‐bodipy: A highly fluorescent, stable, near‐infrared‐absorbing dye. *Angewandte Chemie* **2005**, *117*, 1705-1707
43. Zhao, W.; Carreira, E.M. Conformationally restricted aza‐bodipy: Highly fluorescent, stable near‐infrared absorbing dyes. *Chemistry–A European Journal* **2006**, *12*, 7254-7263
44. McDonnell, S.O.; O'Shea, D.F. Near-infrared sensing properties of dimethlyamino-substituted bf2− azadipyrromethenes. *Organic letters* **2006**, *8*, 3493-3496
45. Goze, C.; Ulrich, G.; Ziessel, R. Tetrahedral boron chemistry for the preparation of highly efficient “cascatelle” devices. *The Journal of organic chemistry* **2007**, *72*, 313-322
46. Ulrich, G.; Goze, C.; Guardigli, M.; Roda, A.; Ziessel, R. Pyrromethene dialkynyl

borane complexes for “cascatelle” energy transfer and protein labeling. *Angewandte Chemie* **2005**, *117*, 3760-3764

47. Leen, V.; Miscoria, D.; Yin, S.; Filarowski, A.; Molisho Ngongo, J.; Van der Auweraer, M.; Boens, N.; Dehaen, W. 1, 7-disubstituted boron dipyrromethene (bodipy) dyes: Synthesis and spectroscopic properties. *The Journal of organic chemistry* **2011**, *76*, 8168-8176
48. Yamada, K.; Toyota, T.; Takakura, K.; Ishimaru, M.; Sugawara, T. Preparation of bodipy probes for multicolor fluorescence imaging studies of membrane dynamics. *New Journal of Chemistry* **2001**, *25*, 667-669
49. Lu, H.; Mack, J.; Yang, Y.; Shen, Z. Structural modification strategies for the rational design of red/nir region bodipys. *Chemical Society Reviews* **2014**, *43*, 4778-4823
50. Saino, S.; Saikawa, M.; Nakamura, T.; Yamamura, M.; Nabeshima, T. Remarkable red-shift in absorption and emission of linear bodipy oligomers containing thiophene linkers. *Tetrahedron Letters* **2016**, *57*, 1629-1634
51. Jiang, T.; Zhang, P.; Yu, C.; Yin, J.; Jiao, L.; Dai, E.; Wang, J.; Wei, Y.; Mu, X.; Hao, E. Straightforward synthesis of oligopyrroles through a regioselective snar reaction of pyrroles and halogenated boron dipyrrins. *Organic letters* **2014**, *16*, 1952-1955
52. Wagner, R.W.; Lindsey, J.S. Boron-dipyrromethene dyes for incorporation in synthetic multi-pigment light-harvesting arrays. *Pure and Applied Chemistry* **1996**, *68*, 1373-1380
53. Liao, J.; Wang, Y.; Xu, Y.; Zhao, H.; Xiao, X.; Yang, X. Synthesis, optical and electrochemical properties of novel meso-triphenylamine-bodipy dyes with aromatic moieties at 3, 5-positions. *Tetrahedron* **2015**, *71*, 5078-5084
54. Poirel, A.; De Nicola, A.; Ziessel, R. Oligothienyl-bodipys: Red and near-infrared emitters. *Organic letters* **2012**, *14*, 5696-5699
55. Afonin, A.V.; Ushakov, I.A.; Pavlov, D.V.; Petrova, O.V.; Sobenina, L.N.; Al’bina, I.M.; Trofimov, B.A. Structural studies of meso-cf3-3 (5)-aryl (hetaryl)-and 3, 5-diaryl (dihetaryl)-bodipy dyes by 1h, 13c and 19f nmr spectroscopy and dft calculations. *Journal of Fluorine Chemistry* **2013**, *145*, 51-57
56. Chen, Y.; Zhao, J.; Guo, H.; Xie, L. Geometry relaxation-induced large stokes

shift in red-emitting borondipyrromethenes (bodipy) and applications in fluorescent thiol probes. *The Journal of organic chemistry* **2012**, *77*, 2192-2206

57. Rohand, T.; Qin, W.; Boens, N.; Dehaen, W. Palladium‐catalyzed coupling reactions for the functionalization of bodipy dyes with fluorescence spanning the visible spectrum. *European journal of organic chemistry* **2006**, *2006*, 4658-4663
58. Jiao, L.; Yu, C.; Uppal, T.; Liu, M.; Li, Y.; Zhou, Y.; Hao, E.; Hu, X.; Vicente, M.G.H. Long wavelength red fluorescent dyes from 3, 5-diiodo-bodipys. *Organic & biomolecular chemistry* **2010**, *8*, 2517-2519
59. Chen, J.; Mizumura, M.; Shinokubo, H.; Osuka, A. Functionalization of boron dipyrrin (bodipy) dyes through iridium and rhodium catalysis: A complementary approach to α‐ and β‐substituted bodipys. *Chemistry–A European Journal* **2009**, *15*, 5942-5949
60. Flores-Rizo, J.O.; Esnal, I.; Osorio-Martínez, C.A.; Gómez-Durán, C.s.F.; Bañuelos, J.; López Arbeloa, I.i.; Pannell, K.H.; Metta-Magaña, A.J.; Peña-Cabrera, E. 8-alkoxy-and 8-aryloxy-bodipys: Straightforward fluorescent tagging of alcohols and phenols. *The Journal of organic chemistry* **2013**, *78*, 5867-5877
61. Ni, Y.; Wu, J. Far-red and near infrared bodipy dyes: Synthesis and applications for fluorescent ph probes and bio-imaging. *Organic & biomolecular chemistry* **2014**, *12*, 3774-3791
62. Lakshmi, V.; Ravikanth, M. Synthesis of conjugated bodipys via the wittig reaction. *The Journal of organic chemistry* **2013**, *78*, 4993-5000
63. Kulyk, B.; Taboukhat, S.; Akdas-Kilig, H.; Fillaut, J.-L.; Boughaleb, Y.; Sahraoui, B. Nonlinear refraction and absorption activity of dimethylaminostyryl substituted bodipy dyes. *RSC Advances* **2016**, *6*, 84854-84859
64. Nano, A.; Ziessel, R.; Stachelek, P.; Harriman, A. Charge‐recombination fluorescence from push–pull electronic systems constructed around amino‐substituted styryl–bodipy dyes. *Chemistry–A European Journal* **2013**, *19*, 13528-13537
65. Sutter, A.; Retailleau, P.; Huang, W.-C.; Lin, H.-W.; Ziessel, R. Photovoltaic performance of novel push–pull–push thienyl–bodipy dyes in solution-processed bhj-solar cells. *New Journal of Chemistry* **2014**, *38*, 1701-1710

66. Chen, J.; Burghart, A.; Derecskei-Kovacs, A.; Burgess, K. 4, 4-difluoro-4-bora-3a, 4a-diaza-s-indacene (bodipy) dyes modified for extended conjugation and restricted bond rotations. *The Journal of organic chemistry* **2000**, *65*, 2900-2906
67. Jiang, X.-D.; Gao, R.; Yue, Y.; Sun, G.-T.; Zhao, W. A nir bodipy dye bearing 3, 4, 4 a-trihydroxanthene moieties. *Organic & biomolecular chemistry* **2012**, *10*, 6861-6865
68. Jiao, C.; Huang, K.-W.; Wu, J. Perylene-fused bodipy dye with near-ir absorption/emission and high photostability. *Organic letters* **2011**, *13*, 632-635
69. Yang, Y.; Guo, Q.; Chen, H.; Zhou, Z.; Guo, Z.; Shen, Z. Thienopyrrole-expanded bodipy as a potential nir photosensitizer for photodynamic therapy. *Chemical Communications* **2013**, *49*, 3940-3942
70. Umezawa, K.; Nakamura, Y.; Makino, H.; Citterio, D.; Suzuki, K. Bright, color-tunable fluorescent dyes in the visible− near-infrared region. *Journal of the American Chemical Society* **2008**, *130*, 1550-1551

Chapter 2 Synthesis and photophysical properties of NIR fluorescent boron dipyrromethene dyes

2.1. Abstract

In this chapter, a series of red and near-infrared (NIR) dyes derived from boron dipyrromethene (BODIPY) were prepared by introducing thiophene and its derivatives to the 3- and 5- positions of the dichloroBODIPY core. For the first time, cyclictriol boronates and MIDA boronate were used as organoboron species to couple with 3,5-dichloroBODIPY via the one-step Suzuki–Miyaura cross-coupling. Six kinds of thieno-expended BODIPY dyes were synthesized in acceptable yields ranging from 31% to 79%. All six dyes showed different absorption and emission wavelengths spanning a wide range (c.a. 600–850 nm) in the red and NIR regions with relatively high quantum yields (19–85%). All six dyes were characterized using 1H-NMR and mass spectrometry.

2.2. Introduction

Long-wavelength dyes, which absorb and emit light in the far-red and NIR region, have found extensive applications in biology [1] as the spectra in the NIR region has many advantages, such as enhanced sensitivity owing to high contrast and low background noise, deep penetration in tissue, and less damage to organisms. The demand for NIR dyes has greatly stimulated the interest in the design of various novel NIR chromophores that feature optimized properties.

Cyanine is one of the most studied fluorescent dyes. However, its fluorescence tends to be weak and presents low quantum yields except for a few examples [2,3], hence impeding its application in biology. Many NIR dyes have

similar drawbacks, while some of them are difficult to synthesize. Therefore, the development of alternative NIR dyes and a straightforward modification strategy are imperative.

BODIPY derivatives—also known as boron dipyrromethene—have been widely used over the past two decades due to their outstanding characteristics, such as high molar absorption coefficients, intense fluorescence quantum yields, high stability, and tunable spectroscopic and photophysical properties [4,5]. However, the relatively short wavelength of excitation and emission maxima (generally within 500–600 nm) limit the application of BODIPY chromophores.

Various strategies have been employed to promote the absorption and emission wavelengths of BODIPY dyes to the far-red and NIR regions. Some examples include the extension of π-conjugation length [6,7], rigidification of rotatable moieties [8,9], the introduction of a nitrogen atom in the *meso*-position to form aza-BODIPY dyes [10,11], and the formation of a "push-pull" motif [12,13].

It has been known that introduction of thiophene subunits to BODIPY results in a remarkable bathochromic shift, and many of them exhibit some interesting optical properties [14-16]. Strikingly, in previous research, the author found that solvatochromic dyes containing thiophene emitted longer wavelength than other well-known solvatochromic dyes [17], such as *N*-(2-aminoethyl)-4-[5-[4-(dimethylamino)phenyl]-2-oxazolyl]benzenesulfonamide (Dapoxyl SEDA) [18], *N*,*N*-dimethyl-6-propionyl-2-naphthylamine (PRODAN) [19], and 1-

anilinonaphthalene-8-sulfonate (ANS) [20]. Therefore, the author expects to tune the absorption and emission wavelengths of BODIPYs by introducing different moieties of solvatochromic dyes on the BODIPY core.

The development of NIR dyes generally requires a sophisticated design that involves tedious modification steps. Therefore, it is crucial to develop a simple and systematic approach to tune the wavelengths of BODIPY dyes spanning the NIR region, essentially with high quantum yield.

A few examples of thienyl groups-modified 3,5-disubstituted BODIPY dyes using Stille coupling have been reported [21-24]. However, organotin compounds are highly toxic, and it is very hard to purify organotin substrates due to their instability on silica or alumina columns. This hinders the extensive application of the organotin compounds.

Suzuki–Miyaura cross-coupling—one of the most efficient methods for the construction of C-C bonds—has been employed to couple BODIPY core with phenyl or thienyl subunits [25,26]. To the best of our knowledge, only two examples of modified thiophene units have been reported to couple with 3,5-dihaloBODIPY using Suzuki–Miyaura cross-coupling; however, they were obtained in low yield (~14%) [27]. Basically, there is no available information showing the successful introduction of electron donating group-modified thiophene to the 3- and 5- positions of BODIPY core via the cross-coupling reaction. This is mostly due to two reasons: (1) the Suzuki–Miyaura cross-coupling of five-membered boronic acid could be problematic [28,29]; and (2) the first

cross-coupling reaction would significantly reduce the reactivity of the remaining halogen.

In this chapter, the author reports a straightforward method to introduce thienyl and thienyl derivatives onto a specific 3,5-dichloroBODIPY scaffold via a one-step Suzuki–Miyaura cross-coupling to tune the wavelengths toward the red and NIR regions. Using cyclictriol boronates and *N*-methyliminodiacetic acid (MIDA) boronate as organoboron species, a set of red and NIR BODIPY dyes were synthesized in acceptable yields ranging from 31% to 51% under mild reaction conditions, all of which exhibited relatively high quantum yields in the range of 0.19 to 0.85. This is the first time that electron donating group-modified thiophene parts were efficiently introduced onto the 3- and 5- positions of the BODIPY core via Suzuki–Miyaura cross-coupling.

2.3. Materials and Methods

2.3.1. General Experimental

All commercially available solvents and reagents were purchased from suppliers (Sigma-Aldrich Chemical Company (St. Louis, MO, USA), Wako Pure Chemical Industries (Osaka, Japan) or Tokyo Chemical Industry (Tokyo, Japan)), and were used as received unless otherwise noted. Reactions were monitored with high-performance thin-layer chromatography (HPLC; silica gel 60, 0.25mm, F-254, Merck KGaA, Darmstadt, Germany), which were visualized with UV light or/and by a color reaction staining with a phosphomolybdic acid solution (5% *w*/*v*

in ethanol). Column chromatography was performed using silica gel 60 mesh 230–400 (Wako Pure Chemical Industries, Osaka, Japan).

^{1}H-NMR spectra were recorded on a JEOL 400 (400 MHz) spectrometer (JEOL Ltd., Tokyo, Japan) at room temperature. Chemical shifts were expressed in parts per million (ppm) relative to the standard reference tetramethylsilane (TMS) (0 ppm). Coupling constants (*J*) were expressed in Hertz. Mass spectra were carried out on a Thermo Scientific Exactive (Thermo Fisher Scientific K.K., Tokyo, Japan) under electrospray ionization (ESI) or atmospheric pressure chemical ionization (APCI) conditions. UV-visible absorption spectra were performed on a JASCO V-560 spectrophotometer (JASCO Corporation, Tokyo, Japan), and fluorescence spectra and fluorescence quantum yields were measured with Hamamatsu Photonics Quantaurus-QY Absolute PL quantum yield spectrometer C11347 (Hamamatsu Photonics K.K., Hamamatsu, Japan);

*2.3.2. Synthesis of BODIPY dyes **2.1–2.6***

General Procedure: Synthesis of dyes **2.1–2.4**

The starting material—3,5-dichloroBODIPY core (compound **2.7**)—was synthesized according to the previously published method [30]. Compound **2.7** (1 equiv), Palladium (II) acetate [$Pd(OAc)_2$] (10 mol %), 2-Dicyclohexylphosphino-2′,6′-dimethoxybiphenyl (SPhos) (20 mol %), CuCl (0.4 equiv) and respective boronates (3 equiv) were placed in a two-necked round bottom flask. Prior to the addition of *N*,*N*-dimethylformamide (DMF), the flask was purged with N_2 three

times. The reaction was stirred at 60 °C for 24 h, and the mixture was cool to room temperature, then extracted with ethyl acetate and washed with H_2O and brine (saturated NaCl solution) successively. The organic layer was collected and dried over Na_2SO_4 and evaporated to dryness under reduced pressure. The crude sample was purified by silica gel column chromatography using eluent gradients with the eluent pair hexane/ethyl acetate.

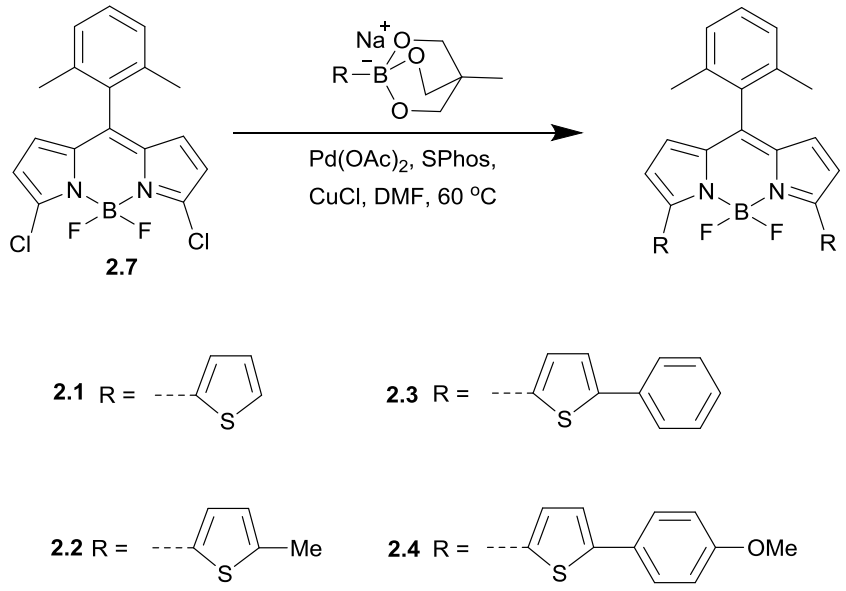

Figure 2.1. Synthesis scheme of dyes **2.1–2.4**

Synthesis of 8-(2,6-Dimethylphenyl)-3,5-di(2-thienyl)-BODIPY (**2.1**)

Prepared according to the general procedure using compound **2.7** (91 mg, 0.25 mmol), (2-thiophene) cyclic-triolborate sodium salt (175 mg, 0.75 mmol), $Pd(OAc)_2$ (6 mg, 0.025 mmol), SPhos (21 mg, 0.05 mmol), CuCl (10 mg, 0.1 mmol) and DMF (2.5 ml) to afford the desired product **2.1** as a dark green solid

(54 mg, 47%). ^{1}H-NMR (400 MHz, $CDCl_3$): δ (ppm) = 8.24 (dd, *J* = 3.8 Hz, *J* = 1 Hz, 2H), 7.49 (dd, *J* = 5.4 Hz, *J* = 1 Hz, 2H), 7.31~7.27 (m, 1H), 7.21 (dd, *J* = 4.9 Hz, *J* = 3.9 Hz, 2H), 7.15 (d, *J* = 7.8 Hz, 2H), 6.76 (d, *J* = 4.3 Hz, 2H), 5.54 (d, *J* = 3.9 Hz, 2H), 2.20 (s, 6H). ESI-FTMS (*m*/*z*): $[M+H]^+$ calculated for $C_{25}H_{20}BF_2N_2S_2$: 461.11; found: 461.12.

Synthesis of 8-(2,6-Dimethylphenyl)-3,5-di(5-methyl-2-thienyl)-BODIPY (**2.2**)

Prepared according to the general procedure using compound **2.7** (182 mg, 0.5 mmol), 2-(5-methylthiophene) cyclic-triolborate sodium salt (372 mg, 1.5 mmol), $Pd(OAc)_2$ (11 mg, 0.05 mmol), SPhos (41 mg, 0.1 mmol), CuCl (20 mg, 0.2 mmol) and DMF (5 ml) to afford the desired product **2.2** as a dark green solid (125 mg, 51%). ^{1}H-NMR (400 MHz, $CDCl_3$): δ (ppm) = 8.01 (d, *J* = 3.4 Hz, 2H), 7.33–7.24 (m, 1H), 7.13 (d, *J* = 7.3 Hz, 2H), 6.86 (d, J = 3.9 Hz 2H), 6.67 (d, *J* = 4.4 Hz, 2H), 6.48 (d, *J* = 4.4 Hz, 2H), 2.56 (s, 6H), 2.19 (s, 6H). ESI-FTMS (*m*/*z*): $[M + H]^+$ calculated for $C_{27}H_{24}BF_2N_2S_2$: 489.14; found: 489.15.

Synthesis of 8-(2,6-Dimethylphenyl)-3,5-di[(5-phenyl(2-thienyl)]-BODIPY (**2.3**)

Prepared according to the general procedure using compound **2.7** (91 mg, 0.25 mmol), compound **2.9** (240 mg, 0.75 mmol), $Pd(OAc)_2$ (6 mg, 0.025 mmol), SPhos (21 mg, 0.05 mmol), CuCl (10 mg, 0.1 mmol) and DMF (2.5 ml) to afford the

desired product **2.3** as a dark green solid (54 mg, 35%). ^{1}H-NMR (400 MHz, $CDCl_3$): δ (ppm)= 8.27 (d, *J* = 3.9 Hz, 2H), 7.69 (d, *J* = 7.4 Hz, 4H), 7.45-7.40 (m, 6H), 7.34 (d, *J* = 7.3 Hz, 2H), 7.31~7.26 (m, 1H), 7.16 (d, *J* = 7.6 Hz, 2H), 6.80 (d, *J* = 4.3 Hz, 2H), 6.54 (d, *J* = 4.3 Hz, 2H), 2.22 (s, 6H). ESI-FTMS (*m*/*z*): $[M]^+$ calculated for $C_{37}H_{27}BF_2N_2S_2$: 612.17; found: 612.17.

Synthesis of 8-(2,6-Dimethylphenyl)-3,5-di[(5-phenyl(2-thienyl)]-BODIPY (**2.4**)

Prepared according to the general procedure using compound **2.7** (182 mg, 0.5 mmol), compound **2.13** (510 mg, 1.5 mmol), $Pd(OAc)_2$ (11 mg, 0.05 mmol), SPhos (41 mg, 0.1 mmol), CuCl (20 mg, 0.2 mmol) and DMF (5 ml) to afford the desired product **2.4** as a purple solid (129 mg, 38%). ^{1}H-NMR (400 MHz, $CDCl_3$): δ (ppm) = 8.24 (d, *J* = 4.1 Hz, 2H), 7.62 (d, *J* = 8.8 Hz, 4H), 7.33 (d, *J* = 4.0 Hz, 2H), 7.30~7.26 (m, 1H), 7.15 (d, *J* = 7.7 Hz, 2H), 6.95 (d, *J* = 8.8 Hz, 4H), 6.78 (d, *J* = 4.4 Hz, 2H), 6.52 (d, *J* = 4.4 Hz, 2H), 3.86 (s, 6H), 2.21 (s, 6H). ESI-FTMS (*m*/*z*): $[M]^+$ calculated for $C_{39}H_{31}BF_2N_2O_2S_2$: 672.19, found: 672.19.

Synthesis of dyes **2.5** and **2.6**

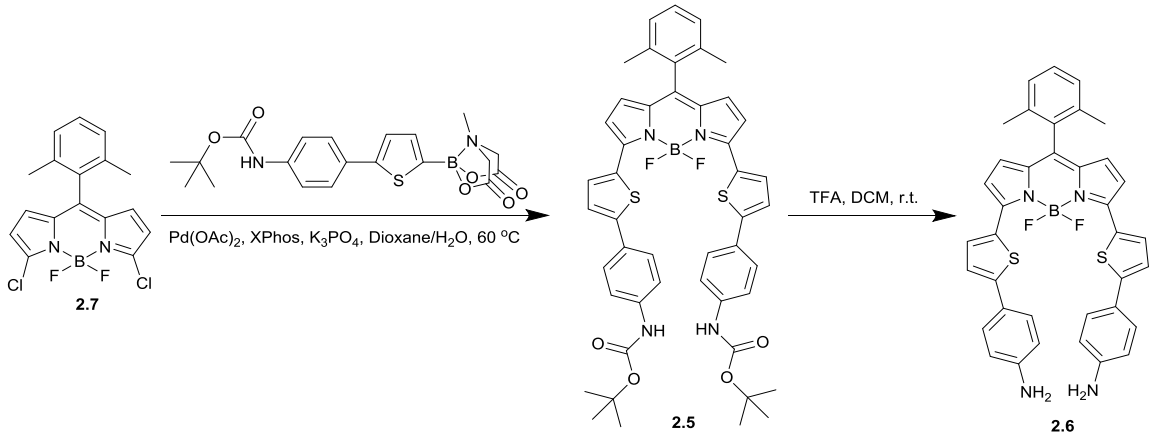

Figure 2.2. The synthesis scheme of dyes **2.5–2.6**

Synthesis of 8-(2,6-Dimethylphenyl)-3,5-di[5-(4-BOC-aminophenyl)-2-thienyl)]-BODIPY (**2.5**)

Compound **2.7** (25 mg, 0.07 mmol), $Pd(OAc)_2$ (2 mg, 0.007 mmol), 2-Dicyclohexylphosphino-2′,4′,6′-triisopropylbiphenyl (XPhos) (7 mg, 0.014 mmol), and MIDA boronate **2.17** (88 mg, 0.21 mmol) were placed in a two-necked round bottom flask. The flask was then purged with N_2 three times before addition of dioxane (5 ml). The mixture was stirred at ambient temperature for 5 min. Then, K_3PO_4 (0.5 M, 1 ml) was added, and the reaction mixture was stirred at 60 °C for two days. The mixture was cooled to room temperature, extracted with ethyl acetate, washed with H_2O and brine successively. The organic layer was collected, dried over Na_2SO_4 and evaporated to dryness under reduced pressure. The crude sample was purified by silica gel column chromatography (ethyl acetate: hexane 1: 4) to afford dark green solid **2.5** (18 mg) in 31% yield. ^{1}H-NMR (400 MHz,

$CDCl_3$): δ (ppm) = 8.23 (d, *J* = 4.1 Hz, 2H), 7.61 (d, *J* = 8.6 Hz, 4H), 7.42 (d, *J* = 8.4 Hz, 4H), 7.36 (d, *J* = 4.0 Hz, 2H), 7.30~7.24 (m, 1H), 7.15 (d, *J* = 7.8 Hz, 2H), 6.78 (d, *J* = 4.4 Hz, 2H), 6.55 (bs, 2H), 6.52 (d, *J* = 4.4 Hz, 2H), 2.21 (s, 6H), 1.54 (s, 18H). ESI-FTMS (*m*/*z*): $[M - H]^+$ calculated for $C_{47}H_{44}BF_2N4O_4S_2$: 841.29, found: 841.29.

Synthesis of 8-(2,6-Dimethylphenyl)-3,5-di[5-(4-aminophenyl)-2-thienyl)]-BODIPY (**2.6**)

Dye **2.5** (26 mg, 0.03mmol) was dissolved in 1 ml dichloromethane (DCM) was stirred under N_2 for 5 min at 0 °C, followed by dropwise addition of TFA (60 μL), and the reaction mixture was stirred for 24 h at room temperature. After cooling to 0 °C, the reaction was quenched with 1 ml saturated solution of $NaHCO_3$, extracted with ethyl acetate, washed with H_2O and brine successively. The organic layer was collected, dried over Na_2SO_4, and evaporated to dryness under reduced pressure. The crude sample was purified by silica gel column chromatography ($CHCl_3$ 100%) to afford black solid **2.6** (11 mg) in 79% yield. ^{1}H-NMR (400 MHz, $CDCl_3$): δ (ppm) = 8.23 (d, *J* = 4.2 Hz, 2H), 7.49 (d, *J* = 8.4 Hz, 4H), 7.30~7.24 (m, 3H), 7.14 (d, *J* = 7.7 Hz, 2H), 6.76 (d, *J* = 4.3 Hz, 2H), 6.70 (d, *J* = 8.4 Hz, 4H), 6.49 (d, *J* = 4.3 Hz, 2H), 2.20 (s, 6H). ESI-FTMS (*m*/*z*): $[M - H]^+$ calculated for $C_{37}H_{28}BF_2N_4S_2$: 641.19; Found: 641.19.

*2.3.3. Synthesis of cyclictriol boronates (**2.9** and **2.13**) and MIDA boronate (**2.17**)*

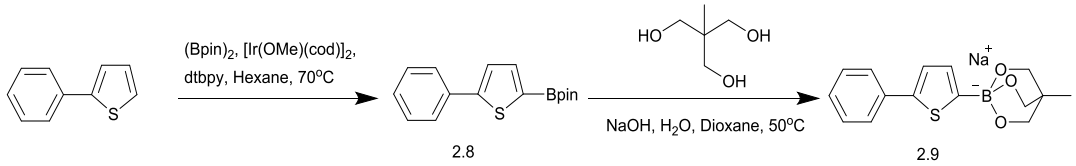

Figure 2.3. Synthesis scheme of compound **2.9**

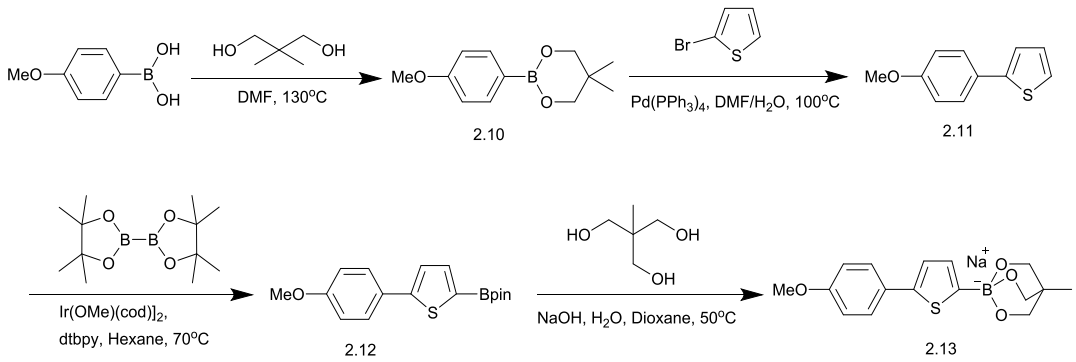

Figure 2.4. The **s**ynthesis scheme of **2.13**

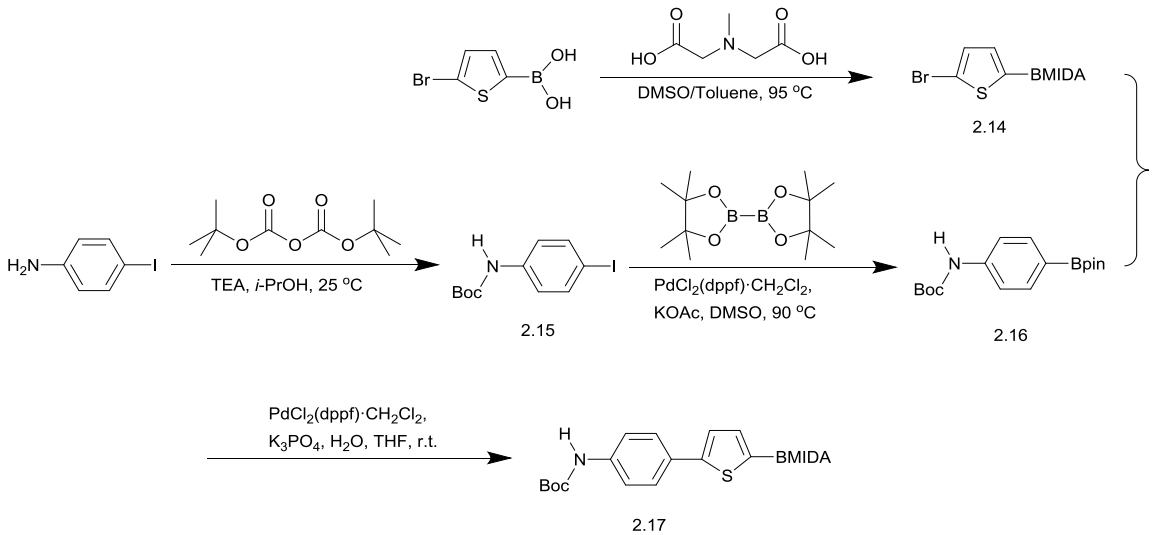

Figure 2.5. The synthesis scheme of **2.17**

Synthesis of 4,4,5,5-tetramethyl-2-(5-phenylthiophen-2-yl)-1,3,2-dioxaborolane (**2.8**)

2-Phenylthiphene (400 mg, 2.5 mmol, 1 equiv), bis(pinacolato)diboron (1.268 g, 5.0 mmol, 2 equiv), $[Ir(OMe)(cod)]_2$ (33 mg, 0.05 mmol, 2 mol%) and dtbpy (33.5 mg, 0.12 mmol, 5 mol%) were dissolved in hexane (150 ml), flushed with nitrogen gas three times in an oven-dried two-neck flask. The reaction mixture was stirred at 70 °C for 1 h. After cooling to room temperature, the mixture was extracted with EtOAc, washed with H_2O and brine successively. The organic layer was collected, dried over Na_2SO_4, filtered, and then concentrated. The crude sample was purified by silica gel column chromatography (EtOAc: hexane 1: 40) to give target compound **2.8** as grey solid (421 mg, 59%).

^{1}H-NMR (400 MHz, $CDCl_3$): δ (ppm) = 7.65 (d, J = 7.4 Hz, 2H), 7.61 (d, J = 3.4 Hz, 1H), 7.40~7.37 (m, 3H), 7.30 (t, J = 7.1 Hz, 1H), 1.37 (s, 12H). APCI-FTMS (*m/z*): $[M+H]^+$ calcd for $C_{16}H_{20}BO_2S$: 287.12; Found: 287.16.

Synthesis of 2-(5-phenylthiophene) Cyclic-triolborate Sodium salt (**2.9**)

Compound **2.8** (100 mg, 0.35 mmol, 1 equiv), 1,1,1-tris(hydroxymethyl)ethane (42 mg, 0.35 mmol, 1 equiv), crushed NaOH (14 mg, 0.35 mmol, 1 equiv) were placed in a two-necked round bottom flask. The flask was then purged with nitrogen gas three times before addition of dioxane (5 ml)

and H_2O (19 μL, 10.5 mmol, 3 equiv). The mixture was stirred at 50 °C for 24 h. After the reaction was complete, the mixture was cool to room temperature, and the white precipitate was collected by filtration, washed with diethyl ether (3 × 10 ml) to give target compound **2.9** as grey solid (73 mg, 68%).

^{1}H-NMR (400 MHz, DMSO): δ (ppm) = 7.53 (d, *J* = 7.3 Hz, 2H), 7.32 (t, *J* = 7.7 Hz, 2H), 7.18 (d, *J* = 3.3 Hz, 1H), 7.14 (t, *J* = 7.4 Hz, 1H), 6.69 (d, *J* = 3.2 Hz, 1H), 3.56 (s, 6H), 0.48 (s, 3H). ESI-FTMS (*m/z*): $[M-Na]^+$ calcd for $C_{15}H_{16}BO_3S$: 287.09; Found: 287.09.

Synthesis of 5,5-dimethyl-2-(4-methoxyphenyl)-1,3,2-dioxaborinane (**2.10**)

p-Methoxyphenyl boronic acid (1.00 g, 6.6 mmol, 1 equiv), 2,2-Dimethyl-1,3-propanediol (0.822 g, 7.9 mmol, 1.2 equiv) were dissolved in DMF (20 ml), flushed with nitrogen gas three times in an oven-dried two-neck flask. The mixture was stirred at 130 °C for 2 h. After cooling to room temperature, the mixture was extracted with EtOAc, washed with H_2O and brine successively. The organic layer was collected, dried over Na_2SO_4, filtered, and then concentrated. The crude sample was purified by silica gel column chromatography (EtOAc: Hexane 1: 40) to give target compound **S3** as white solid (1.50 g, 100%). ^{1}H-NMR (400 MHz, $CDCl_3$): δ (ppm) = 7.72 (dt, *J* = 8.5 Hz, *J* = 2.3 Hz, 2H), 6.87 (dt, *J* = 8.7 Hz, *J* = 2.4 Hz, 2H), 3.80 (s, 3H), 3.73 (s, 4H), 1.00 (s, 6H). APCI-FTMS (*m/z*): $[M+H]^+$ calcd for $C_{12}H_{18}BO_3$: 221.13; Found: 221.14.

Synthesis of 2-(4-methoxyphenyl)-thiophene (**2.11**)

Compound **2.10** (1.50 g, 6.82 mmol, 1 equiv), bromothiophene (1.334 g, 8.18 mmol, 1.2 equiv), Cs_2CO_3 (4.442 g, 18.36 mmol, 2 equiv), $Pd(PPh_3)_4$ (394 mg, 0.34 mmol, 5 mol%) were placed in a two-necked round bottom flask. The flask was then purged with nitrogen gas three times before the addition of DMF (20 ml) and H_2O (2 ml). The mixture was stirred at 100 °C for 3 h. After the reaction was complete, the mixture was cool to room temperature, extracted with EtOAc, washed with H_2O and brine successively. The organic layer was collected, dried over Na_2SO_4, filtered, and then concentrated. The crude sample was purified by silica gel column chromatography (DCM: hexane 1: 5) to give target compound **2.11** as yellowish solid (1.185 g, 91%).

^{1}H-NMR (400 MHz, $CDCl_3$): δ (ppm) = 7.55 (dt, J = 6.7 Hz, J = 3.0 Hz, 2H), 7.23-7.20 (m, 2H), 7.22-7.20 (m, 1H), 6.92 (dt, J = 6.7 Hz, J = 3.0 Hz, 2H), 3.83 (s, 3H). APCI-FTMS (*m/z*): $[M+H]^+$ calcd for $C_{11}H_{11}OS$: 191.05; Found: 191.05.

Synthesis of 4,4,5,5-tetramethyl-2-[5-(4-methoxylphenyl)thiophen-2-yl)-1,3,2-dioxaborolane (**2.12**)

The synthesis of **2.12** (light green solid, 660 mg, yield 66%) is the same as the synthesis of **2.8**, using **2.11** (600 mg, 3.15 mmol, 1 equiv), Bis(pinacolato)diboron (916 mg, 3.78 mmol, 1.2 equiv), $[Ir(OMe)(cod)]_2$ (42 mg, 0.06 mmol, 2 mol%) and dtbpy (42 mg, 0.16 mmol, 5 mol%) and hexane (150 ml).

^{1}H-NMR (400 MHz, $CDCl_3$): 7.59-7.56 (m, 3H), 7.27 (d, *J* = 3.7 Hz, 1H), 6.91 (d, *J* = 8.9 Hz, 2H), 3.83 (s, 3H), 1.36 (s, 12H). ESI-FTMS (*m/z*): $[M+H]^+$calcd for $C_{17}H_{22}BO_3S$: 317.13; Found: 317.14.

Synthesis of 2-[5-(4-methoxylphenyl)thiophene] Cyclic-triolborate Sodium salt (**2.13**)

The synthesis of **2.13** (gray solid, 584 mg, yield 82%) is the same as the synthesis of **2.9,** using **2.12** (660 mg, 2.09 mmol), 1,1,1-tris(hydroxymethyl)ether (251 mg, 2.09 mmol, 1 equiv), crushed NaOH (84 mg, 2.09 mmol, 1 equiv) dioxane (20 ml) and H_2O (113 μL, 6.3 mmol, 3 equiv).

^{1}H-NMR (400 MHz, DMSO): δ (ppm) = 7.44 (d, *J* = 8.7 Hz, 2H), 7.03 (d, *J* = 2.9 Hz, 1H), 6.90 (d, *J* = 8.8 Hz, 2H), 6.64 (m, *J* = 2.9 Hz, 1H), 3.55 (s, 6H), 0.47 (s, 3H). ESI-FTMS (*m/z*): $[M-H]^+$ calcd for $C_{16}H_{17}BO_4SNa$: 340.09; Found: 339.20.

Synthesis of 4-bromothiophene-2-boronic acid MIDA ester (**2.14**)

The 4-bromothiophene-2-boronic acid (1.0 g, 4.83 mmol, 1 equiv), *N*-methyliminodiacetic acid (MIDA, 0.78 g, 5.31 mmol, 1.1 equiv) were dissolved in DMSO (3 ml) and Toluene (30 ml), flushed with nitrogen gas three times in an oven-dried two-neck flask. The flask was fitted with a Dean-Stark trap, and the mixture was stirred at 95 °C for 20 h, toluene was removed under reduced pressure. H_2O was added, and the resulting precipitate was collected by filtration. The precipitate was washed with H_2O (3 × 30 ml) and diethyl ether (3 × 30 ml) to give

the target compound **2.14** as a white crystalline solid (1.45 g, 94%).

^{1}H-NMR (400 MHz, acetone-6d): δ (ppm) = 7.19 (d, *J* = 3.5 Hz, 1H), 7.13 (d, *J* = 3.5 Hz, 1H), 4.39 (d, *J* = 17 Hz, 2H), 4.20 (d, *J* = 17 Hz, 2H), 2.92 (s, 3H). ESI-FTMS (*m/z*): $[M+H]^+$ calcd for $C_{20}H_{24}BN_2O_6S$: 317.95; Found: 317.94.

Synthesis of *tert*-butyl (4-iodophenyl) carbamate (*N*-Boc-4-Iodoaniline) (**2.15**)

The 4-Iodoaniline (2.0 g, 9.13 mmol, 1 equiv), di-*tert*-butyl dicarbonate ($(Boc)_2O$, 2.39 g, 10.96 mmol, 1.2 equiv), Triethylamine (1.08 g, 18.26 mmol, 2 equiv) were placed in a two-necked round bottom flask. The flask was then purged with nitrogen gas three times before addition of *i*-PrOH (50 ml). The mixture was stirred at 25 ^oC for 20 h. After the reaction was complete, the mixture was extracted with EtOAc, washed with H_2O and brine successively. The organic layer was collected, dried over Na_2SO_4, filtered, and then concentrated. The crude sample was purified by silica gel column chromatography (EtOAc: hexane 1: 9) to yield the target compound **2.15** as white solid (2.83 g, 99%).

^{1}H-NMR (400 MHz, $CDCl_3$): 7.58 (d, *J* = 8.9 Hz, 2H), 7.14 (d, *J* = 8.7 Hz, 2H), 6.44 (bs, 1H), 1.51 (s, 9H). ESI-FTMS (*m/z*) $[M-H]^+$ calcd for $C_{11}H_{13}INO_2$: 318.01; Found: 318.00.

Synthesis of tert-butyl (4-(4,4,5,5-tetramethyl-1,3,2-dioxaborolan-2-yl)-phenyl) carbamate (**2.16**)

Compound **2.15** (1.5 g, 4.70 mmol, 1 equiv), Bis(pinacolato)diboron (1.43 g,

5.64 mmol, 1.2 equiv), KOAc (2.31 g, 23.5 mmol, 5 equiv) and $PdCl_2(dppf)\cdot CH_2Cl_2$ (115 mg, 0.14 mmol, 3 mol%) were placed in a two-necked round bottom flask. The flask was then purged with nitrogen gas three times before the addition of DMSO (45 ml). The mixture was stirred at 90 °C for 20 h. After the reaction was complete, the mixture was extracted with EtOAc, washed with H_2O and brine successively. The organic layer was collected and dried over Na_2SO_4 and evaporated to dryness under reduced pressure. The crude sample was purified by silica gel column chromatography (EtOAc: hexane 1: 9) to yield the target compound **2.16** as white solid (1.43 g, 95%).

^{1}H-NMR (400 MHz, $CDCl_3$): δ (ppm) = 7.73 (d, *J* = 8.6 Hz, 2H), 7.36 (d, *J* = 8.8 Hz, 2H), 6.52 (bs, 1H), 1.52 (s, 9H), 1.33 (s, 12H). ESI-FTMS (*m/z*): $[M+Na]^+$ calcd for $C_{17}H_{26}BNO_4Na$: 342.00; Found: 342.00.

Synthesis of 4-(Boc-amino) phenylthiophene-2-boronic MIDA ester (**2.17**)

Compound **2.14** (1.0 g, 3.15 mmol, 1 equiv), **2.16** (1.21 g, 3.80 mmol, 1.2 equiv), K_3PO_4 (1.0 g, 9.42 mmol, 3 equiv), $PdCl_2(dppf)\cdot CH_2Cl_2$ (103 mg, 0.13 mmol, 4 mol%) were placed in a two-necked round bottom flask. The flask was then purged with nitrogen gas three times before the addition of THF (5 ml) and H_2O (0.28 ml, 15.75 mmol, 5 equiv). The mixture was stirred at r.t. for 24 h. The reaction mixture was diluted with acetone (5ml), dried over Na_2SO_4, filtrated through a pad Celite, washed with acetone, and then concentrated. The crude sample was purified by silica gel column chromatography (Acetone: Hexane 1:2)

to yield the target compound **2.17** as yellow solid (0.94 g, 75%).

^{1}H-NMR (400 MHz, acetone-6*d*): δ (ppm) = 8.52 (bs, 1H), 7.61 (s, 4H), 7.42 (d, *J* = 3.8 Hz, 1H), 7.26 (d, *J* = 3.6 Hz, 1H), 4.29 (d, *J* = 17 Hz, 2H), 4.19 (d, *J* = 17 Hz, 2H), 3.21 (s, 3H), 1.50 (s, 9H). ESI-FTMS (*m/z*): $[M-H]^+$ calcd for $C_{20}H_{22}BN_2O_6S$: 429.14; Found: 429.13.

2.4. Results and Discussion

*2.4.1. Synthesis of dyes **2.1**–**2.6***

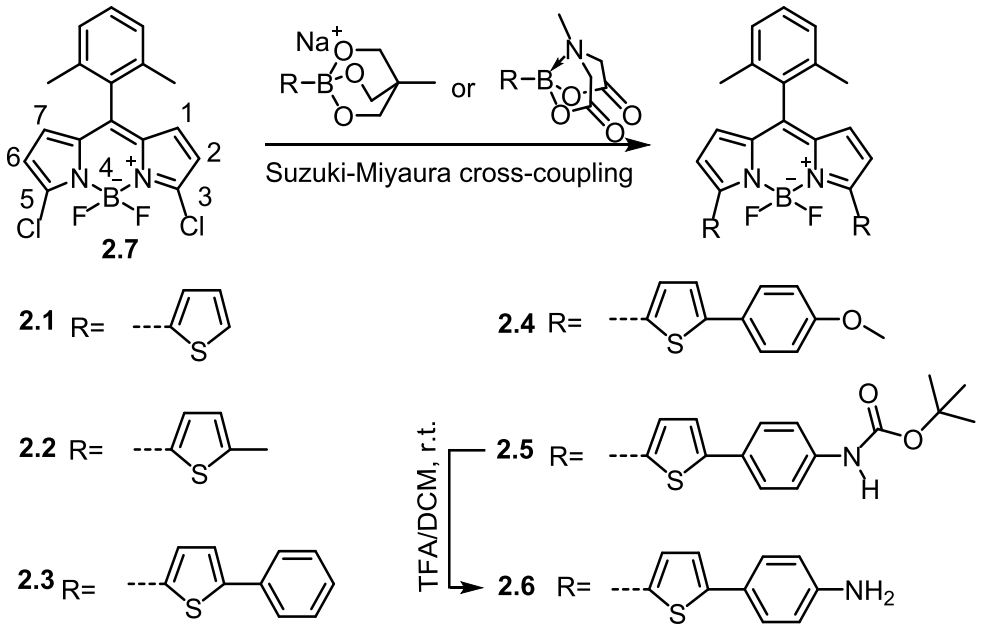

Figure 2.6. Synthetic scheme to NIR BODIPY dyes.

Introduction of a 2,6-dimethylphenyl moiety at the *meso*-position of BODIPY core is an efficient way to increase the fluorescence quantum yield by restricting the internal rotation of the phenyl ring caused by the two ortho methyl groups [31].

Suzuki–Miyaura cross-coupling often gives an undesirable result for heteroaromatic boronate due to the accelerated hydrolytic B–C bond cleavage in basic aqueous condition during Suzuki–Miyaura cross-coupling [32-34]. Cyclictriol boronate is superior as it can undergo Suzuki–Miyaura cross-coupling even in the absence of a base [35], which would diminish the competitive hydrolytic B–C bond cleavage during the reaction. In addition, cyclictriol boronate is an air- and water-stable boron reagent. This easy-handling boronate, which has extremely high nucleophilicity [36] and good solubility in organic solvents, tends to have high reactivity coupling with halogens [37]. Thus, the cyclictriol boronate was applied to this study.

It has been demonstrated that electron-rich and bulky ligands could facilitate the Suzuki–Miyaura cross-coupling by increasing the rate of the oxidative addition and reductive elimination process [38,39]. Moreover, the addition of copper(I) can promote Suzuki–Miyaura cross-coupling [35,40]. Based on this information, dyes **2.1**–**2.4** were synthesized under the optimized conditions and isolated in relatively high yields ranging from 35% to 51%, considering the fact that electron-neutral or electron-rich aryl chlorides have low reactivity and are regarded as inactivated chlorides [41]. In this disubstitution reaction, an electron donating group at the first substitution step inhibited the reactivity of the monosubstituted intermediates as the donating groups increased the electron density via a resonance donating effect.

The MIDA boronate, obtained from boronic acid [42,43], was also synthesized as an alternative boron reagent for the modification of the BODIPY core. MIDA

boronate ester is stable under various conditions and can slowly release the corresponding boronic acid in a mild basic aqueous solution[42]. This ester is more effective than the corresponding boronic acid when coupling with chlorides under mild basic aqueous condition [44]. Dye **2.5** was synthesized with a yield of 31%, and dye **2.6** was obtained a 79% yield via reaction of dye **2.5** with trifluoroacetic acid at room temperature.

Compared to the reported methods using Stille coupling [21-24], the synthetic method described here is advantageous as the reactions were conducted in mild condition (60 °C) with competitive yields, and no toxic regent is involved in the reactions.

*2.4.2. Spectroscopic and Photophysical Properties of dyes **2.1–2.6***

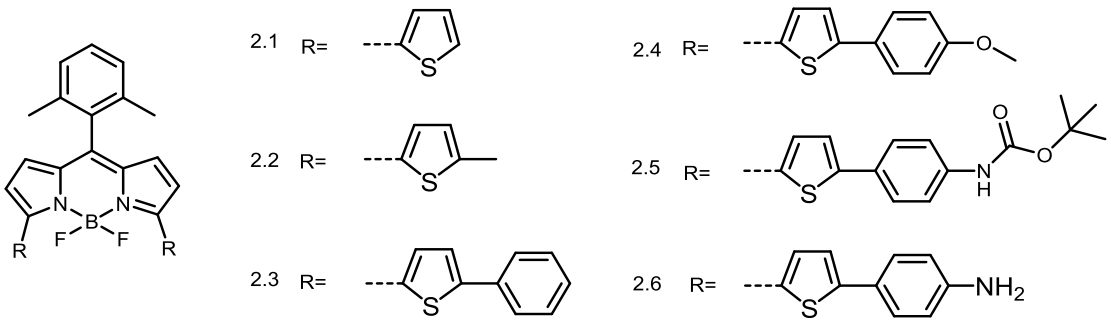

Figure **2.7**. The structure of BODIPY dyes **2.1–2.6**

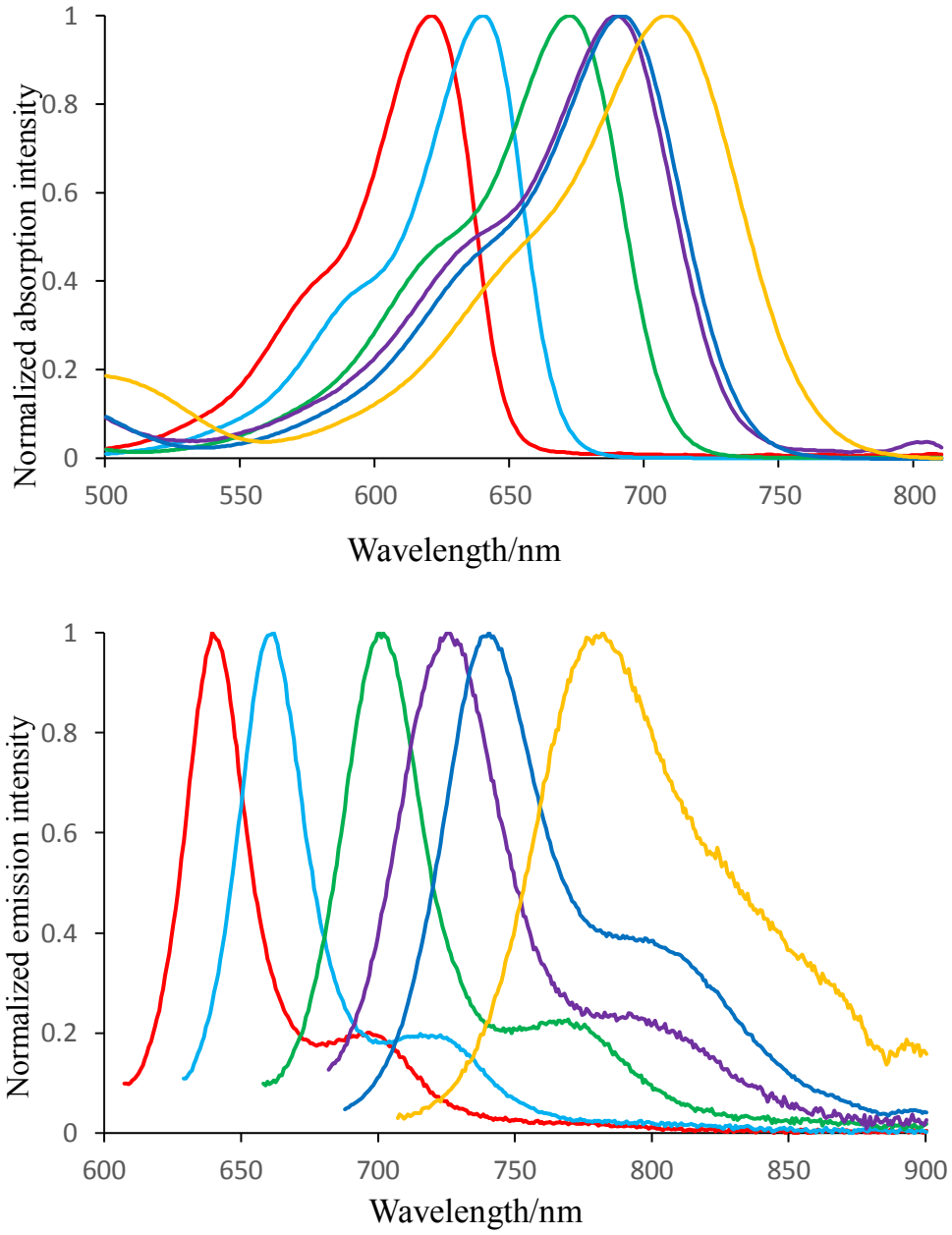

Figure 2.8. Normalized absorption and fluorescence (uncorrected) spectra of BODIPYs **2.1**–**2.6** in dichloromethane (DCM). They were excited at 600 nm, 620 nm, 650 nm, 680nm, 650nm and 670 nm, respectively. (red, **2.1**; light blue, **2.2**; green, **2.3**; purple, **2.4**; blue, **2.5**; and yellow, **2.6**, respectively).

The spectroscopic characterization of these BODIPY dyes was performed in DCM as shown in Figure **2.8** and are summarized in Table **2.1**. The absorption and emission maxima could be greatly affected by the introduction of electron donating substitution at 3,5-position [4,5,8]. The absorption and emission bands of dyes **2.1**–**2.6** were in the red to NIR regions. The absorption spectra showed a strong S_0 to S_1 transition with absorption maxima varying between 621 nm and 708 nm, and the shoulder peak located at shorter wavelength was ascribed to the S_0 to S_2 transition. The emission bands were the mirror images of the absorption ones with moderate Stokes shift; emission maxima were in the range of 640–780 nm.

Table 2.1. Spectroscopic data of dyes **2.1**–**2.6** in dichloromethane

Dye	λ_{abs}/nm	λ_{em}/nm	Φ_f	$\varepsilon/M^{-1}\,cm^{-1}$	Stokes Shift/cm^{-1}
2.1	621	640	0.85	69,000	4.78×10^2
2.2	640	662	0.81	66,000	5.19×10^2
2.3	672	701	0.71	75,000	6.16×10^2
2.4	689	725	0.68	78,000	7.21×10^2
2.5	691	740	0.53	82,000	9.58×10^2
2.6	708	780	0.19	72,000	13.0×10^2

Unexpectedly, comparing to dye **2.1** the methyl group at the α-position of the thiophene in dye **2.2** induced appreciable bathochromic shifts of 4.78×10^2 cm^{-1} in the absorption and 5.20×10^2 cm^{-1} in the emission. A similar phenomenon was also found in a previous report, i.e., one additional methyl group red-shifted the

absorption and emission maxima by about 2.01×10^2 cm^{-1} and 1.64×10^2 cm^{-1}, respectively [45]. It violated the general assertion that as a weak electron donating group, the methyl group generally has little effect on wavelengths of fluorescent dyes.

The extension of π-conjugation also led to a remarkable bathochromic shift (12.23×10^2 cm^{-1} and 13.60×10^2 cm^{-1} for the absorbance and emission band, respectively), dye **2.3** showed an absorption maximum at 672 nm and the emission at 701 nm. As expected, further extension of the π-conjugation and the addition of electron donating group increased the bathochromic shift. As a result, the absorption and the emission maxima of dye **2.6** were shifted to 708 nm and 780 nm, respectively.

Interestingly, dyes **2.4** and **2.5** showed similar absorption maximum (c.a. 690 nm), but their emission maxima were at 725 nm and 740 nm, respectively. The difference between the emission maxima may arise from the geometry relaxation of the dyes upon photoexcitation [46]. The author anticipates that compared to the methoxy group, the bulky *tert*-butyloxycarbonyl protecting amine group could induce larger geometry relaxation at the excited state (S_1 state), and the decreased energy gap will produce a larger Stokes shift. The increased wavelengths were likely caused by the combined effects of the extension of the π-electrons delocalization, the strength of the π-electron donors, and the sulfur atoms. Therefore, the wavelengths of the synthesized dyes could be fine-tuned using a

stronger donating group and/or achieving a longer extension of the π-conjugation, giving rise to the wavelengths that shifted to lower energy.

Fluorescence quantum yield is one of the most important parameters to evaluate fluorophores. It directly reflects the efficiency of the conversion of absorbed photons into emitted ones. In addition, many far-red and NIR chromophores encounter low fluorescence quantum yield [3,16]. To our delight, the bathochromic shift was achieved without compromising the fluorescence quantum yield: dyes **2.1**–**2.5** were quite high in the range of 0.53 to 0.85. Although for dye **2.6**, which was synthesized by removing the BOC group from dye **2.5**, a decrease in the fluorescence quantum yield was observed (0.19 in DCM), it remained at a moderate level. This decrease may result from the formation of hydrogen bonds between the amine groups and hence invoke rapid quenching of the singlet state through intermolecular charge transfer [47,48]. On the whole, no obvious fluorescence quenching was observed, indicating that the modification method is a feasible way to develop NIR BODIPY dyes.

2.5. Conclusions

In this chapter, a facile approach to develop red and NIR BODIPY dyes were proposed. Six different red and NIR BODIPY dyes were rationally designed and synthesized from readily available 3,5-dichloroBODIPY via a one-step Suzuki–Miyaura cross-coupling. Dyes **2.1**–**2.6** showed different absorption (621–708 nm) and emission (640–780 nm) with relatively high quantum yields (19–85%) in DCM. Extension of π-conjugation and the addition of electron donating group

increased the bathochromic shift. Dye **2.6** bearing amine groups exhibited the longest absorption maximum λ_{abs} (708 nm) and emission maximum λ_{em} (780 nm) and the longest Stokes shift (72 nm).

References

1. Escobedo, J.O.; Rusin, O.; Lim, S.; Strongin, R.M. Nir dyes for bioimaging applications. *Curr. Opin. Chem. Biol.* **2010**, *14*, 64–70.
2. Peng, X.; Song, F.; Lu, E.; Wang, Y.; Zhou, W.; Fan, J.; Gao, Y. Heptamethine cyanine dyes with a large stokes shift and strong fluorescence: A paradigm for excited-state intramolecular charge transfer. *J. Am. Chem. Soc.* **2005**, *127*, 4170–4171.
3. Pansare, V.J.; Hejazi, S.; Faenza, W.J.; Prud'homme, R.K. Review of long-wavelength optical and nir imaging materials: Contrast agents, fluorophores, and multifunctional nano carriers. *Chem. Mater.* **2012**, *24*, 812–827.
4. Boens, N.; Leen, V.; Dehaen, W. Fluorescent indicators based on bodipy. *Chem. Soc. Rev.* **2012**, *41*, 1130–1172.
5. Ulrich, G.; Ziessel, R.; Harriman, A. The chemistry of fluorescent bodipy dyes: Versatility unsurpassed. *Angew. Chem.* **2008**, *47*, 1184–1201.
6. Descalzo, A.B.; Xu, H.-J.; Xue, Z.-L.; Hoffmann, K.; Shen, Z.; Weller, M.G.; You, X.-Z.; Rurack, K. Phenanthrene-fused boron− dipyrromethenes as bright long-wavelength fluorophores. *Org. Lett.* **2008**, *10*, 1581–1584.
7. Jiao, L.; Yu, C.; Liu, M.; Wu, Y.; Cong, K.; Meng, T.; Wang, Y.; Hao, E. Synthesis and functionalization of asymmetrical benzo-fused bodipy dyes. *J. Org. Chem.* **2010**, *75*, 6035–6038.
8. Loudet, A.; Burgess, K. Bodipy dyes and their derivatives: Syntheses and spectroscopic properties. *Chem. Rev.* **2007**, *107*, 4891–4932.
9. Hayashi, Y.; Obata, N.; Tamaru, M.; Yamaguchi, S.; Matsuo, Y.; Saeki, A.; Seki, S.; Kureishi, Y.; Saito, S.; Yamaguchi, S.; et al. Facile synthesis of biphenyl-fused bodipy and its property. *Org. Lett.* **2012**, *14*, 866–869.
10. Zhao, W.; Carreira, E.M. Conformationally restricted aza-bodipy: Highly fluorescent, stable near-infrared absorbing dyes. *Chemistry* **2006**, *12*, 7254–7263.
11. McDonnell, S.O.; O'Shea, D.F. Near-infrared sensing properties of dimethlyamino-substituted bf2-azadipyrromethenes. *Org. Lett.* **2006**, *8*, 3493–3496.

12. Xuan, S.; Zhao, N.; Ke, X.; Zhou, Z.; Fronczek, F.R.; Kadish, K.M.; Smith, K.M.; Vicente, M.G. Synthesis and spectroscopic investigation of a series of push-pull boron dipyrromethenes (bodipys). *J. Org. Chem.* **2017**, *82*, 2545–2557.
13. Yu, Y.H.; Descalzo, A.B.; Shen, Z.; Röhr, H.; Liu, Q.; Wang, Y.W.; Spieles, M.; Li, Y.Z.; Rurack, K.; You, X.Z. Mono‐and di (dimethylamino) styryl‐substituted borondipyrromethene and borondiindomethene dyes with intense near‐infrared fluorescence. *Chem.-Asian J.* **2006**, *1*, 176–187.
14. Zhang, X.; Yu, H.; Xiao, Y. Replacing phenyl ring with thiophene: An approach to longer wavelength aza-dipyrromethene boron difluoride (aza-bodipy) dyes. *J. Org. Chem.* **2012**, *77*, 669–673.
15. Poirel, A.; De Nicola, A.; Ziessel, R. Oligothienyl-bodipys: Red and near-infrared emitters. *Org. Lett.* **2012**, *14*, 5696–5699.
16. Ni, Y.; Wu, J. Far-red and near infrared bodipy dyes: Synthesis and applications for fluorescent ph probes and bio-imaging. *Org. Biomol. Chem.* **2014**, *12*, 3774–3791.
17. Son, S.H.; Abe, Y.; Yuasa, M.; Yamagishi, Y.; Sakai, N.; Ayabe, T.; Yamada, K. A systematic analysis of aromatic heterocyclic rings in solvatochromic fluorophores. *Chem. Lett.* **2011**, *40*, 378–380.
18. Diwu, Z.; Lu, Y.; Zhang, C.; Klaubert, D.H.; Haugland, R.P. Fluorescent molecular probes ii. The synthesis, spectral properties and use of fluorescent solvatochromic dapoxyl dyes. *Photochem. Photobiol.* **1997**, *66*, 424–431.
19. Weber, G.; Farris, F.J. Synthesis and spectral properties of a hydrophobic fluorescent probe: 6-propionyl-2-(dimethylamino) naphthalene. *Biochemistry* **1979**, *18*, 3075–3078.
20. Slavik, J. Anilinonaphthalene sulfonate as a probe of membrane-composition and function. *Biochim. Biophys. Acta* **1982**, *694*, 1–25.
21. Forgie, J.C.; Skabara, P.J.; Stibor, I.; Vilela, F.; Vobecka, Z. New redox stable low band gap conjugated polymer based on an EDOT–BODIPY–EDOT repeat unit. *Chem. Mater.* **2009**, *21*, 1784–1786.
22. Liao, J.; Wang, Y.; Xu, Y.; Zhao, H.; Xiao, X.; Yang, X. Synthesis, optical and electrochemical properties of novel *meso*-triphenylamine-bodipy dyes with aromatic moieties at 3,5-positions. *Tetrahedron* **2015**, *71*, 5078–5084.

23. Mirloup, A.; Leclerc, N.; Rihn, S.; Bura, T.; Bechara, R.; Hébraud, A.; Lévêque, P.; Heiser, T.; Ziessel, R. A deep-purple-grey thiophene–benzothiadiazole–thiophene bodipy dye for solution-processed solar cells. *New J. Chem.* **2014**, *38*, 3644–3653.
24. Sengupta, S.; Pandey, U.K.; Athresh, E.U. Regioisomeric donor–acceptor–donor triads based on benzodithiophene and bodipy with distinct optical properties and mobilities. *RSC Adv.* **2016**, *6*, 73645–73649.
25. Rihn, S.; Retailleau, P.; Bugsaliewicz, N.; De Nicola, A.; Ziessel, R. Versatile synthetic methods for the engineering of thiophene-substituted bodipy dyes. *Tetrahedron Lett.* **2009**, *50*, 7008–7013.
26. Rohand, T.; Qin, W.; Boens, N.; Dehaen, W. Palladium‐catalyzed coupling reactions for the functionalization of bodipy dyes with fluorescence spanning the visible spectrum. *Eur. J. Org. Chem.* **2006**, *2006*, 4658–4663.
27. Lakhe, D.; Jairaj, K.K.; Pradhan, M.; Ladiwala, U.; Agarwal, N. Synthesis and photophysical studies of heteroaryl substituted-bodipy derivatives for biological applications. *Tetrahedron Lett.* **2014**, *55*, 7124–7129.
28. Kinzel, T.; Zhang, Y.; Buchwald, S.L. A new palladium precatalyst allows for the fast suzuki-miyaura coupling reactions of unstable polyfluorophenyl and 2-heteroaryl boronic acids. *J. Am. Chem. Soc.* **2010**, *132*, 14073–14075.
29. Barder, T.E.; Walker, S.D.; Martinelli, J.R.; Buchwald, S.L. Catalysts for suzuki-miyaura coupling processes: Scope and studies of the effect of ligand structure. *J. Am. Chem. Soc.* **2005**, *127*, 4685–4696.
30. Hafuka, A.; Kando, R.; Ohya, K.; Yamada, K.; Okabe, S.; Satoh, H. Substituent effects at the 5-position of 3-[bis (pyridine-2-ylmethyl) amino]-bodipy cation sensor used for ratiometric quantification of cu^{2+}. *Bull. Chem. Soc. Jpn.* **2014**, *88*, 447–454.
31. Yamada, K.; Toyota, T.; Takakura, K.; Ishimaru, M.; Sugawara, T. Preparation of bodipy probes for multicolor fluorescence imaging studies of membrane dynamics. *New J. Chem.* **2001**, *25*, 667–669.
32. Brown, R.D.; Buchanan, A.S.; Humffray, A.A. Protodeboronation of thiophenboronic acids. *Aust. J. Chem.* **1965**, *18*, 1521–1525.

33. Campeau, L.-C.; Fagnou, K. Applications of and alternatives to π-electron-deficient azine organometallics in metal catalyzed cross-coupling reactions. *Chem. Soc. Rev.* **2007**, *36*, 1058–1068.
34. Tyrrell, E.; Brookes, P. The synthesis and applications of heterocyclic boronic acids. *Synth.-Stuttg.* **2003**, *2003*, 469–483.
35. Yamamoto, Y.; Takizawa, M.; Yu, X.Q.; Miyaura, N. Cyclic triolborates: Air‐ and water‐stable ate complexes of organoboronic acids. *Angew. Chem. Int. Ed.* **2008**, *47*, 928–931.
36. Lennox, A.J.; Lloyd-Jones, G.C. Selection of boron reagents for suzuki-miyaura coupling. *Chem. Soc. Rev.* **2014**, *43*, 412–443.
37. Li, G.Q.; Yamamoto, Y.; Miyaura, N. Double-coupling of dibromo arenes with aryltriolborates for synthesis of diaryl-substituted planar frameworks. *Tetrahedron* **2011**, *67*, 6804–6811.
38. Galardon, E.; Ramdeehul, S.; Brown, J.M.; Cowley, A.; Hii, K.K.; Jutand, A. Profound steric control of reactivity in aryl halide addition to bisphosphane palladium(0) complexes. *Angew. Chem.* **2002**, *41*, 1760–1763.
39. Martin, R.; Buchwald, S.L. Palladium-catalyzed suzuki-miyaura cross-coupling reactions employing dialkylbiaryl phosphine ligands. *Acc. Chem. Res.* **2008**, *41*, 1461–1473.
40. Deng, J.Z.; Paone, D.V.; Ginnetti, A.T.; Kurihara, H.; Dreher, S.D.; Weissman, S.A.; Stauffer, S.R.; Burgey, C.S. Copper-facilitated suzuki reactions: Application to 2-heterocyclic boronates. *Org. Lett.* **2009**, *11*, 345–347
41. Littke, A.F.; Fu, G.C. Palladium-catalyzed coupling reactions of aryl chlorides. *Angew. Chem.* **2002**, *41*, 4176–4211
42. Gillis, E.P.; Burke, M.D. A simple and modular strategy for small molecule synthesis: Iterative suzuki-miyaura coupling of b-protected haloboronic acid building blocks. *J. Am. Chem. Soc.* **2007**, *129*, 6716–6717.
43. Grob, J.E.; Nunez, J.; Dechantsreiter, M.A.; Hamann, L.G. One-pot reductive amination and suzuki-miyaura cross-coupling of formyl aryl and heteroaryl mida boronates in array format. *J. Org. Chem.* **2011**, *76*, 4930–4940.

44. Knapp, D.M.; Gillis, E.P.; Burke, M.D. A general solution for unstable boronic acids: Slow-release cross-coupling from air-stable mida boronates. *J. Am. Chem. Soc.* **2009**, *131*, 6961–6963.
45. Sobenina, L.N.; Petrova, O.V.; Petrushenko, K.B.; Ushakov, I.A.; Mikhaleva, A.I.; Meallet‐Renault, R.; Trofimov, B.A. Synthesis and optical properties of difluorobora‐s‐diazaindacene dyes with trifluoromethyl *meso*‐substituents. *Eur. J. Org. Chem.* **2013**, *2013*, 4107–4118.
46. Chen, Y.; Zhao, J.; Guo, H.; Xie, L. Geometry relaxation-induced large stokes shift in red-emitting borondipyrromethenes (bodipy) and applications in fluorescent thiol probes. *J. Org. Chem.* **2012**, *77*, 2192–2206.
47. Musser, A.J.; Neelakandan, P.P.; Richter, J.M.; Mori, H.; Friend, R.H.; Nitschke, J.R. Excitation energy delocalization and transfer to guests within mii 4l6 cage frameworks. *J. Am. Chem. Soc.* **2017**, *139*, 12050–12059.
48. Neelakandan, P.P.; Jiménez, A.; Nitschke, J.R. Fluorophore incorporation allows nanomolar guest sensing and white-light emission in m 4 l 6 cage complexes. *Chem. Sci.* **2014**, *5*, 908–915.

Chapter 3 Synthesis and photophysical properties of NIR chemiluminescent boron dipyrromethene dyes

3.1. Abstract

In this chapter, a series of three luminol-based NIR chemiluminescent BODIPY dyes were developed by conjugating a luminol part at the 2-position of the NIR fluorescent BODIPY dyes through a direct bond. The dyes showed sharp chemiluminescence bands in NIR regions with emission maxima in 670–736 range. No chemiluminescence derived from the luminol parts was detected (around 400 nm). As expected, a longer extension of π-conjugation and the addition of an electron-donating groups lead to a red-shifted chemiluminescence band. The varied emission bands of the different dyes indicating that various NIR chemiluminescent BODIPY dyes can be developed by simply exchanging the parent fluorescent dyes.

3.2. Introduction

Chemiluminescence is generated through a certain chemical reaction rather than the excitation light. Therefore, there is no background noise arising from autofluorescence. Its sensitivity and high signal-to-noise ratio make it widely utilized in various chemical and biological application[1,2] and recently in noninvasive whole-body imaging[3]. As maintained in the previous chapters, in practical bio-application, NIR dyes process unique advantages over other dyes for the NIR light can better penetrate through tissue and less damage on the biological specimen.

The chemiluminogens can be mainly classified into several types as oxalate ester, acridinium ester, dioxetanes and luminol derivatives[4,5]. However, they

emit lights at relatively short wavelengths, which is not suitable for bio-applications. As luminol, for example, emits around 400 nm depending on the solvent media[6].

Efforts have been devoted to design and prepare long wavelength chemiluminescent dyes, however, most of the synthesized dyes are still in the visible light regions[7-12]. Most recently, a dioxetane based NIR chemiluminescent dye has been synthesized by composing of dioxetane tethered with the quinone-cyanine[3]. Which emits the chemiluminescence light at 714 nm through chemically initiated electron exchange luminescence (CIEEL) mechanism. However, due to the intrinsic structural sensitivity of dioxetanes, the dye decomposed rapidly even under normal room illumination condition at room temperature.

Luminol, as an extensively studied chemiluminogens, has been widely utilized in the field of analytical chemistry and biotechnology[6,13,14]. Up to date, efforts have been made to prepare long-wavelength luminol-based chemiluminescent dyes[7-9]. To the best of my knowledge, no NIR luminol-based chemiluminescent dye has been reported. K.Burgess and co-workers have synthesized a red luminol chemiluminescent dye by conjugating the luminol moiety and the Nile red via acetylene linker. However, its poor solubility precluded the study in aqueous media.

In this chapter, three kinds of luminol-based NIR chemiluminescent BODIPY dyes were synthesized by conjugating luminol parts at the 2-position of the NIR

BODIPYs through a direct bond. The synthesized dyes emit different chemiluminescence in the NIR regions under identical conditions. It indicated that the emitted light of the conjugated BODIPYs can be varied by choice of fluorophore.

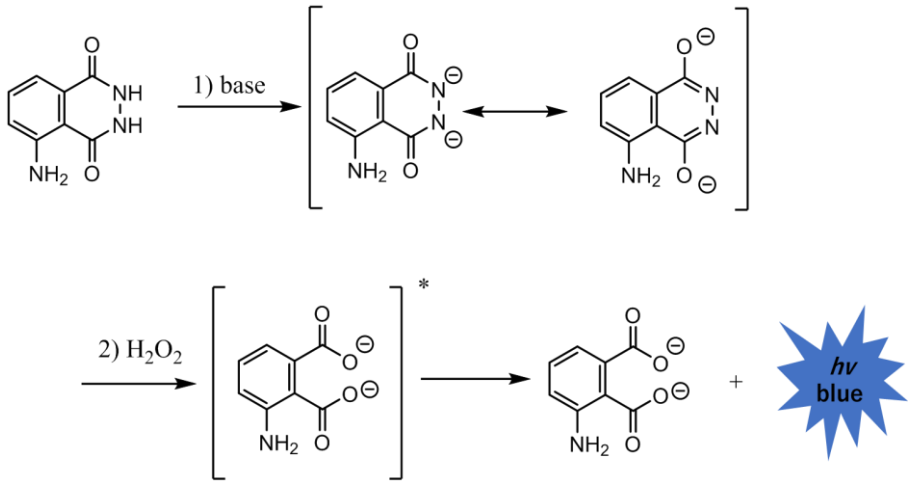

Figure 3.1. Mechanism and chemiluminescence activation pathway of luminol.

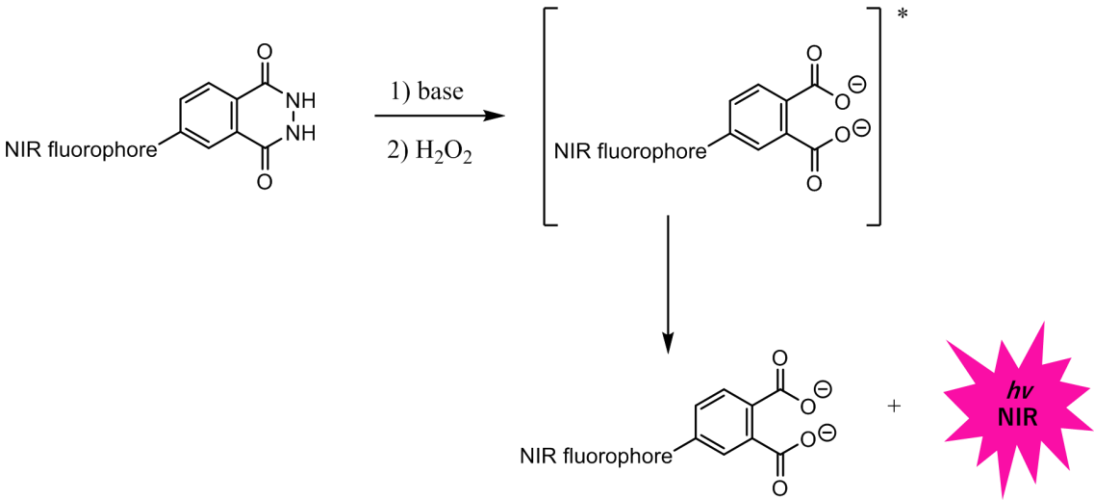

Figure 3.2. General design and chemiluminescence activation pathway of NIR luminophore based on luminol. The emitting light is expected to be varied by the choice of fluorophore.

3.3. Materials and methods

3.3.1 General experimental

UV/visible absorption spectra were measured with Agilent Technologies Cary 60 spectrophotometer (Agilent Technologies, Santa Clara, CA. USA) (scan speed, 600 nm/min; data interval, 1 nm). Chemiluminescence spectra were recorded using an ATTO AB-1850 spectrophotometer (ATTO Corporation, Tokyo, Japan) or PMA-12 Photonic multichannel analyzer C10027-02 (Hamamatsu Photonics K.K., Hamamatsu, Japan). Chemiluminescence kinetic were measured with Luminescencer-Octa AB-2270 (ATTO Corporation, Tokyo, Japan).

Other materials and methods used in this chapter were the same as described in chapter 2.

*3.3.2. Synthesis of chemiluminescent BODIPY dyes **3.1a-3.1c***

3.3.2.1. General procedure A: Synthesis of **3.3a-3.3c**

Compound **2.2, 2.4 or 2.5** was dissolved in dichloromethane (DCM) and stirred at 0 ^{o}C for 5 min, followed by addition of *N*-Bromosuccinimide (NBS) (1 equiv) slowly. The reaction mixture was stirred at room temperature for several hours. The reaction was quenched with an ice-cold saturated solution of $NaHCO_3$, extracted with DCM, washed with H_2O and brine successively, the organic layer was collected, dried over Na_2SO_4 and evaporated to dryness under reduced pressure. The crude sample was purified by silica gel column chromatography using eluent gradients with the eluent pair hexane/ethyl acetate.

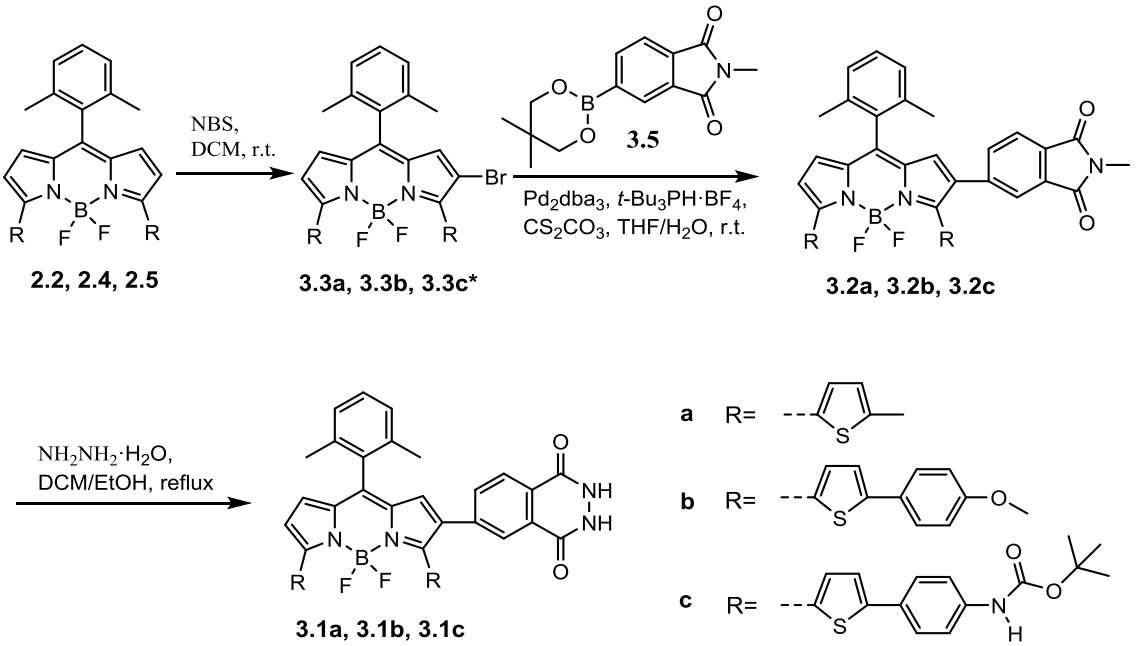

Figure 3.3. Synthesis scheme for chemiluminescent NIR BODIPY dyes **3.1a-3.1c.**

*: Used for the next reaction without purification.

Synthesis of compound **3.3a**

Prepared according to the general procedure A using compound **2.2** (118 mg, 0.24 mmol), NBS (43 mg, 0.24 mmol) and DCM (5 ml) to afford the desired product as a dark red solid (133 mg, 97%). ^{1}H-NMR (400 MHz, $CDCl_3$): δ (ppm) = 8.03 (d, *J* = 3.9 Hz, 1H), 7.65 (d, *J* = 4.0 Hz, 1H), 7.31~7.26 (m, 1H), 7.14 (d, *J* = 7.6 Hz, 2H), 6.88~6.85 (m, 2H), 6.75 (d, *J* = 4.4 Hz, 1H), 6.60 (d, *J* = 4.4 Hz, 1H), 2.59 (s, 3H), 2.54 (s, 3H), 2.20 (s, 6H). ^{13}C-NMR (100 MHz, $CDCl_3$) δ: 153.4, 147.1, 145.3, 144.3, 139.1, 137.5, 137.0, 133.6, 132.7, 132.6, 131.2, 130.7, 129.0, 128.4, 128.3, 127.4, 127.3, 125.8, 122.1, 107.7, 20.2, 15.7, 15.5. HRMS (ESI) m/z: $[M+Na]^+$ Calcd for $C_{27}H_{22}N_2{}^{10}BBrF_2NaS_2$ 588.04012, Found 588.04022.

Synthesis of compound **3.3b**

Prepared according to the general procedure A using compound **2.4** (150 mg, 0.22 mmol), NBS (40 mg, 0.22 mmol) and DCM (4 ml) to afford the desired product as a black solid (157 mg, 95%). ^{1}H-NMR (400 MHz, $CDCl_3$): δ (ppm) = 8.24 (d, *J* = 4.1 Hz, 1H), 7.88 (d, *J* = 3.9 Hz, 1H), 7.62 (dd, *J* = 22.3 Hz, *J* = 8.7 Hz, 4H), 7.34~7.28 (m, 3H), 7.16 (d, *J* = 7.6 Hz, 2H), 6.94 (dd, *J* = 8.7 Hz, *J* = 6.0 Hz, 4H), 6.85 (d, *J* = 4.4 Hz, 1H), 6.64 (d, *J* = 4.5 Hz, 1H), 6.56 (s, 1H), 3.86 (s, 3H), 3.85 (s, 3H), 2.23 (s, 6H). ^{13}C-NMR (100 MHz, $CDCl_3$) δ: 160.2, 159.6, 152.8, 150.2, 148.2, 145.0, 138.6, 137.8, 137.1, 134.4, 134.0, 133.6, 132.7, 131.6, 130.6, 129.2, 129.0, 127.5, 127.46, 127.42, 126.2, 124.8, 122.5, 122.3, 114.5, 144.3, 107.9, 55.41, 55.36, 20.2. HRMS (ESI) m/z: $[M+Na]^+$ Calcd for $C_{39}H_{30}O_2N_2{}^{10}BBrF_2NaS_2$ 772.09217, Found 772.09314.

3.3.2.2. General procedure B: Synthesis of **3.2a-3.2c**

Compound **3.3**, compound **3.5** (1.5 equiv), Tris(dibenzylideneacetone)dipalladium(0) (Pd_2dba_3) (0.1 equiv), Tri-*tert*-butylphosphonium tetrafluoroborate ([(*t*-Bu)$_3$PH]BF_4) (0.2 equiv) and Cs_2CO_3 (4 equiv) were placed in a two-necked round bottom flask. Prior to the addition of THF/H_2O = 150/1 (v/v), the flask was purged with N_2 three times. The reaction was stirred at 25 °C for 24 h, then extracted with DCM and washed with H_2O and brine successively. The organic layer was collected and dried over Na_2SO_4 and evaporated to dryness under reduced pressure. The crude sample was purified by

silica gel column chromatography using eluent gradients with the eluent pair hexane/DCM.

Synthesis of compound **3.2a**

Prepared according to the general procedure B using compound **3.3a** (96 mg, 0.17 mmol), compound **3.5** (70 mg, 0.26 mmol), Pd_2dba_3 (16 mg, 0.017 mmol), [(*t*-Bu)$_3$PH]BF_4 (10 mg, 0.034 mmol), Cs_2CO_3 (222 mg, 0.68 mmol) and THF/H_2O (3 ml/20 µl) to afford the desired product as a dark red solid (96 mg, 88%). ^{1}H-NMR (400 MHz, $CDCl_3$): δ (ppm) = 8.06 (d, *J* = 3.8 Hz, 1H), 7.65~7.63 (m, 2H), 7.39 (dd, *J* = 7.6 Hz, *J* = 1.6 Hz, 1H), 7.33~7.29 (m, 2H), 7.17 (d, *J* = 7.8 Hz, 2H), 6.87 (d, *J* = 3.9 Hz, 1H), 6.79 (d, *J* = 4.1 Hz, 2H), 6.65 (d, *J* = 4.6 Hz, 1H), 6.57 (s, 1H), 3.14 (s, 3H), 2.55 (s, 3H), 2.50 (s, 3H), 2.25 (s, 6H). ^{13}C-NMR (100 MHz, $CDCl_3$): 168.4, 168.3, 153.7, 147.3, 145.0, 144.1, 141.1, 140.0, 137.9, 137.0, 134.1, 133.8, 133.7, 132.9, 132.4, 132.0, 131.6, 131.2, 130.9, 129.9, 129.2, 129.0, 128.4, 127.5, 126.1, 124.6, 123.0, 122.9, 122.3, 23.9, 20.3, 15.7, 15.5. HRMS (ESI) m/z: $[M+Na]^+$ Calcd for $C_{36}H_{28}O_2N_3{}^{10}BF_2NaS_2$ 669.16216, Found 669.16217.

Synthesis of compound **3.2b**

Prepared according to the general procedure B using compound **3.3b** (120 mg, 0.16 mmol), compound **3.5** (65 mg, 0.24 mmol), Pd_2dba_3 (15 mg, 0.016 mmol), [(*t*-Bu)$_3$PH]BF_4 (9 mg, 0.032 mmol), Cs_2CO_3 (209 mg, 0.64 mmol) and THF/H_2O (3 ml/20 µl) to afford the desired product as a dark green solid (115 mg, 87%). ^{1}H-NMR (400 MHz, $CDCl_3$): δ (ppm) = 8.26 (d, *J* = 4.3 Hz, 1H), 7.70 (s, 1H), 7.64

(d, *J* = 7.8 Hz, 1H), 7.59 (d, *J* = 8.7 Hz, 2H), 7.54 (d, *J* = 3.8 Hz, 1H), 7.51 (d, *J* = 8.7 Hz, 2H), 7.45 (d, *J* = 7.8 Hz, 1H), 7.34~7.30 (m, 2H), 7.26~7.24 (m, 1H), 7.19 (d, *J* = 7.6 Hz, 2H), 6.94~6.87 (m, 5H), 6.68 (d, *J* = 4.6 Hz, 1H), 6.60 (s, 1H), 3.84 (s, 3H), 3.82 (s, 3H), 3.14 (s, 3H), 2.27 (s, 6H). ^{13}C-NMR (100 MHz, $CDCl_3$) δ: 168.3, 168.2, 160.1, 159.5, 153.1, 150.4, 148,0, 144.4, 140.9, 139.5, 138.2, 137.0, 134.6, 134.4, 133.8, 132.9, 132.8, 132.4, 131.9, 131.4, 130.8, 130.0, 129.8, 129.0, 127.5, 127.4, 127.2, 126.6, 126.0, 124.8, 124.7, 123.0, 122.9, 122.6, 122.5, 114.40, 114.2, 55.3, 22.3, 23.9, 20.2. HRMS (ESI) m/z: $[M+Na]^+$ Calcd for $C_{48}H_{36}O_4N_3{}^{10}BF_2NaS_2$ 853.21369, Found 853.21552.

Synthesis of compound **3.2c**

The starting material **3.3c** was prepared according to the general procedure A using compound **2.5** (60 mg, 0.07 mmol), NBS (13 mg, 0.07 mmol) and DCM (2 ml), and the crude compound was used for the next reaction without purification.

Compound **3.2c** was prepared according to the general procedure B using compound **3.3c**, compound **3.5** (29 mg, 0.1 mmol), Pd_2dba_3 (6 mg, 0.007 mmol), $[(t\text{-Bu})_3PH]BF_4$ (4 mg, 0.014 mmol), Cs_2CO_3 (91 mg, 0.28 mmol) and THF/H_2O (1.5 ml/10 μl) to afford the desired product as a dark red solid (51 mg, two step overall yield 72 %). ^{1}H-NMR (400 MHz, $CDCl_3$): δ (ppm) = 8.26 (d, *J* = 4.2 Hz, 1H), 7.70 (s, 1H), 7.65 (d, *J* = 7.8 Hz, 1H), 7.58 (d, *J* = 8.6 Hz, 2H), 7.53~7.49 (m, 3H), 7.45 (d, *J* = 7.8 Hz, 1H), 7.41 (d, *J* = 8.6 Hz, 1H), 7.37~7.31 (m, 4H), 7.28~7.26 (m, 1H), 7.18 (d, *J* = 7.6 Hz, 2H), 6.88 (d, *J* = 4.6 Hz, 1H), 6.69 (d, *J* =

4.6 Hz, 1H), 6.60 (s, 1H), 6.57 (s, 1H), 6.52 (s, 1H), 3.14 (s, 3H), 2.18 (s, 6H), 1.53 (s, 18H). ^{13}C-NMR (100 MHz, $CDCl_3$) δ: 168.4, 168.3, 153.1, 152.5, 152.4, 150.2, 147.9, 144.5, 141.0, 139.7, 139.0, 138.3, 137.1, 134.6, 134.5, 133.9, 133.0, 132.8, 132.5, 131.8, 130.9, 130.2, 130.1, 129.1, 128.6, 128.1, 12.6126.9, 126.6, 125.1, 124.8, 123.1, 123.0, 122.6, 118.65, 118.59, 80.9, 80.7, 28.3, 24.0, 20.3. HRMS (ESI) m/z: $[M+Na]^+$ Calcd for $C_{56}H_{50}O_6N_5{}^{10}BF_2NaS_2$ 1023.31922, Found 1023.32123.

3.3.2.3. General procedure C: Synthesis of **3.1a-3.1c**

Excess of hydrazine monohydrate ($NH_2NH_2{\cdot}H_2O$) was added to a stirred solution of compound **3.2** in ethanol/DCM at room temperature under N_2. The reaction mixture was refluxed for 24 h. After cooling to room temperature, the solvent was removed under reduced pressure. The residue was purified by silica gel column chromatography using eluent gradients with the eluent pair hexane/acetone.

Synthesis of compound **3.1a**

Prepared according to the general procedure C using compound **3.2a** (65 mg, 0.10 mmol), $NH_2NH_2{\cdot}H_2O$ (50 µl, 1 mmol), and ethanol/DCM (3 ml/6 ml) to afford the desired product as a dark purple solid (64 mg, 98%). ^{1}H-NMR (400 MHz, $CDCl_3$): δ (ppm) = 13.59 (bs, 1H), 12.28 (bs, 1H), 8.15 (s, 1H), 8.08~8.05 (m, 2H), 7.54 (d, J = 8.4 Hz, 1H), 7.34~7.31 (m, 2H), 7.19 (d, J = 7.6 Hz, 2H), 6.87 (d, J =

3.7 Hz, 1H), 6.80~8.79 (m, 2H), 6.69~6.66 (m, 2H), 2.56 (s, 3H), 2.51 (s, 3H), 2.27 (s, 6H). ^{13}C-NMR (100 MHz, $CDCl_3$) δ: 158.2, 157.5, 153.5, 147.1, 145.3, 144.2, 140.3, 140.1, 137.9, 137.0, 134.3, 133.74, 133.68, 132.9, 132.1, 131.8, 131.2, 130.8, 129.3, 129.0, 128.3, 127.6,127.2, 126.1, 125.4, 125.1, 124.9, 122.2, 20.3, 15.7, 15.5. HRMS (ESI) m/z: $[M+Na]^+$ Calcd for $C_{35}H_{27}O_2N_4{}^{10}BF_2NaS_2$ 670.15651, Found 670.15741.

Synthesis of compound **3.1b**

Prepared according to the general procedure C using compound **3.2b** (42 mg, 0.05 mmol), $NH_2NH_2{\cdot}H_2O$ (28 μl, 0.75 mmol), and ethanol/DCM (5 ml/3 ml) to afford the desired product as a dark purple solid (38 mg, 90%). ^{1}H-NMR (400 MHz, $CDCl_3$): δ (ppm) = 13.60 (bs, 1H), 12.29 (bs, 1H), 8.28 (d, *J* = 4.1 Hz, 1H), 8.20 (s, 1H), 8.06 (d, *J* = 8.4 Hz, 1H), 7.62~7.59 (m, 3H), 7.55~7.51 (m, 3H), 7.33~7.31 (m, 2H), 7.26~7.25 (m, 1H), 7.20 (d, *J* = 7.6 Hz, 2H), 6.94 (d, *J* = 8.8 Hz, 2H), 6.90~6.88 (m, 3H), 6.71~7.69 (m, 2H), 3.85 (s, 3H), 3.81 (s, 3H), 2.29 (s, 6H). ^{13}C-NMR (100 MHz, $CDCl_3$) δ: 160.2, 159.5, 158.3, 157.4, 152.9, 150.2, 148.2, 144.8, 140.2, 139.8, 138.2, 137.1, 134.6, 134.5, 133.1, 132.9, 132.1, 131.6, 131.0, 130.8, 130.0, 129.1, 127.6, 127.5, 127.3, 126.7, 126.2, 125.4, 125.3, 125.0, 124.9, 122.7, 122.4, 114.5, 114.3, 55.4, 55.3, 20.3. HRMS (ESI) m/z: $[M+Na]^+$ Calcd for $C_{47}H_{35}O_4N_4{}^{10}BF_2NaS_2$ 854.20894, Found 854.21050.

Synthesis of compound **3.1c**

Prepared according to the general procedure C using compound **3.2c** (30 mg, 0.015 mmol), $NH_2NH_2 \cdot H_2O$ (45 μl, 0.45 mmol), and ethanol/DCM (3 ml/3 ml) to afford the desired product as a dark purple solid (29 mg, 95%). ^{1}H-NMR (400 MHz, $CDCl_3$): δ (ppm) = 13.57 (bs, 1H), 12.29 (bs, 1H), 8.26 (d, *J* = 4.0 Hz, 1H), 8.19 (s, 1H), 8.06 (d, *J* = 8.7 Hz, 1H), 7.61~7.57 (m, 3H), 7.54 (d, *J* = 3.6 Hz, 1H), 7.49 (d, *J* = 8.6 Hz, 2H), 7.41 (d, *J* = 8.5 Hz, 2H), 7.36~7.31 (m, 4H), 7.28~7.26 (m, 1H), 7.20 (d, *J* = 7.8 Hz, 2H), 6.88 (d, *J* = 4.5 Hz, 1H), 6.71~6.69 (m, 2H), 6.62 (s, 2H), 2.28 (s, 6H), 1.53 (s, 9H), 1.50 (s, 9H). ^{13}C-NMR (100 MHz, $CDCl_3$) δ: 158.2, 157.4, 152.9, 152.6, 152.5, 149.9, 147.9, 144.9, 140.1, 139.9, 139.0, 138.3, 137.0, 134.7, 134.4, 133.9, 133.1, 132.8, 132.2, 131.9, 131.0, 130.8, 130.2, 129.1, 128.6, 128.1, 127.6, 126.8, 126.7, 125.5, 125.4, 125.1, 123.0, 122.4, 118.7, 118.6, 80.9, 80.6, 28.3, 20.3. HRMS (ESI) m/z: $[M+Na]^+$ Calcd for $C_{55}H_{49}O_6N_6{}^{10}BF_2NaS_2$ 1024.31446, Found 1024.31604.

*3.3.3. Synthesis of compounds **3.4, 3.5***

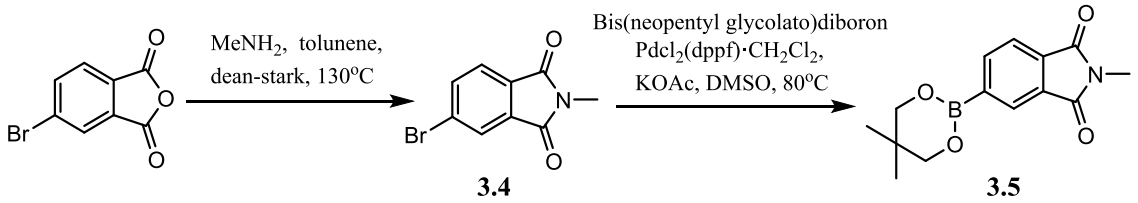

Figure 3.4 synthesis scheme for compound **3.5**

Synthesis of 5-Bromo-2-methylisoindoline-1,3-dione (**3.4**)

Compound **3.4** was synthesized according to previously published method[10], 5-bromophthalic anhydride (1.135 g, 5 mmol), methylamine (0.65 ml of 40 wt% in H_2O, 7.5 mmol) and toluene (25 ml) were placed in a round bottom flask, and purged with N_2 three times. The flask fitted with a Dean-Stark trap, and the mixture was refluxed for 12 h. After cooling to room temperature, the solvent was evaporated under reduced pressure. The residue was purified by silica gel column chromatography (ethyl acetate: hexane 1: 9) to yield target compound **3.4** as white solid (1.515 g, 90%). ^{1}H-NMR (400 MHz, $CDCl_3$): δ (ppm) = 7.93 (d, *J* = 1.4 Hz, 1H), 7.84 (dd, *J* =7.9 ,1.4 Hz, 4H), 7.68 (d, *J* = 7.9 Hz, 1H), 3.17 (s, 3H). ^{13}C-NMR (100 MHz, $CDCl_3$) δ: 167.6, 167.0, 136.9, 133.8, 130.7, 128.8, 126.6, 124,6, 24.1. HRMS (ESI) m/z: $[M+H]^+$ Calcd for $C_9H_7O_2NBr$ 239.9655, Found 239.9660.

Synthesis of 5-(5,5-Dimethyl-1,3,2-dioxaborinan-2-yl)-2-methylisoindole-1,3-dione (**3.5**)

Compound **3.4** (1.51 g, 6.29 mmol, 1 equiv), Bis(neopentyl glycolato)diboron (1.420 g, 6.29 mmol, 1 equiv), potassium acetate (KOAc) (1.850 g, 18.87 mmol, 3 equiv) and $PdCl_2(dppf)\cdot CH_2Cl_2$ (154 mg, 0.19 mmol, 3 mol%) were placed in a two-necked round bottom flask. The flask was then purged with N_2 three times before addition of 16 ml of dimethyl sulfoxide. The mixture was stirred at 80 ^{o}C for 22 h. After the reaction was complete, the mixture was extracted with ethyl acetate, washed with H_2O and brine successively, the organic layer was collected,

dried over Na_2SO_4 and evaporated to dryness under reduced pressure. The crude sample was purified by silica gel column chromatography (ethyl acetate: hexane 1: 9 to 1:4) to yield target compound **3.4** as white solid (1.04 g, 61%). ^{1}H-NMR (400 MHz, $CDCl_3$): δ (ppm) = 8.27 (s, 1H), 8.13 (d, *J* = 0.7 Hz, 1H), 7.80 (d, *J* = 0.8 Hz, 1H), 3.80 (s, 4H), 3.18 (s, 3H), 1.04 (s, 6H). ^{13}C-NMR (100 MHz, $CDCl_3$) δ: 168.8, 168.7, 139.5, 133.9, 131.2, 128.4, 122.1, 72.5, 31.9, 23.9, 21.8. HRMS (ACPI) m/z: $[M+H]^+$ Calcd for $C_{14}H_{17}O_2N^{10}B$ 273.12815, Found 273.12824.

3. 4. Results and discussion

*3.4.1. Synthesis of CL dyes **3.1a-3.1c***

To synthesize long-wavelength luminol derivatives, luminol parts have been connected to some probes. Obviously, conjugated luminol derivatives are more attractive due to the chemiluminescence wavelength is no longer limited by the necessary overlap between the luminol and connected probe. However, an imine conjugated luminol-BODIPY proved too insoluble to purify[8], another ethynyl conjugated luminol-Nile red also has poor solubility, which precludes studies in aqueous media[9]. The issue perhaps aroused via π-stacking and aggregation between molecules[8].

To obtain chemiluminescence dyes **3.1a-3.1c**, initial efforts were the design of the synthesis route. As most luminol derivatives are insoluble in most organic solvents, it is difficult to handle during synthesis procedures. In the previous studies, some strategies have been proposed to solve the problem, including bis(*N*-

protection) of luminol parts with 4-methoxybenzyl groups and using *N*-alkylated phthalimide as the intermediate of luminol[7,9,10].

Commercially available 5-bromophthalic anhydride was alkylated with methylamine to give phthalimide **3.4**, followed by a Miyaura–Ishiyama–Hartwig borylation to afford boronate **3.5**, which was coupled with mono-brominate BODIPYs **3.3**. The BODIPYs **3.3** were synthesized from BODIPYs by treating with 1 equivalent of NBS. The last step is the functionalization of BODIPYs **3.2** by reacting with an excess amount of hydrazine monohydrate. The intermediates and final targets have good solubility in many organic solvents, and all of them were purified and characterized.

*3.4.2. Spectroscopic and photophysical properties of dyes **3.1a-3.1c***

3.4.2.1 Absorption and fluorescence emission

Before investigating chemiluminescence of the dyes, the spectroscopic (absorption and fluorescence emission) properties of the CL BODIPYs were investigated in acetone and DMSO, and the results were summarized in **Figure 3.5, 3.6** and **Table 3.1.** The absorption and emission bands spanned a wide range over red to NIR regions. The absorption spectra showed strong S_0 to S_1 transitions between 617–678 nm with an absorption coefficient in the range of 56,000–81,000 M^{-1} cm^{-1}. Weaker and broader shoulder peak located at shorter wavelength was assigned to the S_0 to S_2 transition. Emission maxima were in the 667–761 nm range with moderate Stokes shift.

As the polarity of the solvent increased from acetone (E_T^N 0.335) to DMSO (E_T^N 0.444)[15], the absorption and emission band were red-shifted for 9–16 nm and 12–21 nm, respectively. The red-shift of the absorption and emission band is probably due to an increased dipole moment of the dye in an excited state, indicating that the excited state is better stabilized by the polar solvent (DMSO)[15]. The intramolecular charge transfer (ICT) is known to influence the rate of non-radioactive decay of excited fluorophores, resulting in lower quantum yields[16]. The fluorescence quantum yields in DMSO were about 1/3–1/2 times as that in acetone. The decreased fluorescence quantum yields in higher polarity solvent are consistent with the results from previous studies, the ICT excited state is more likely to relax by non-radiative decay than by fluorescence emission in a more polar solvent[17-21].

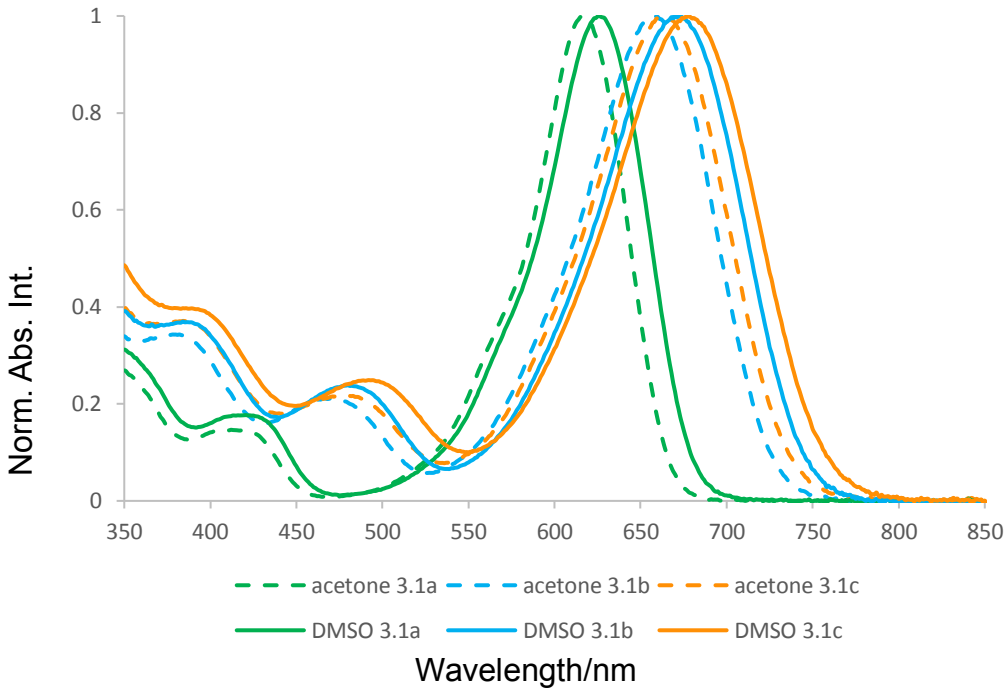

Figure 3.5. Normalized absorption spectra of dyes **3.1a-3.1c** in acetone and DMSO.

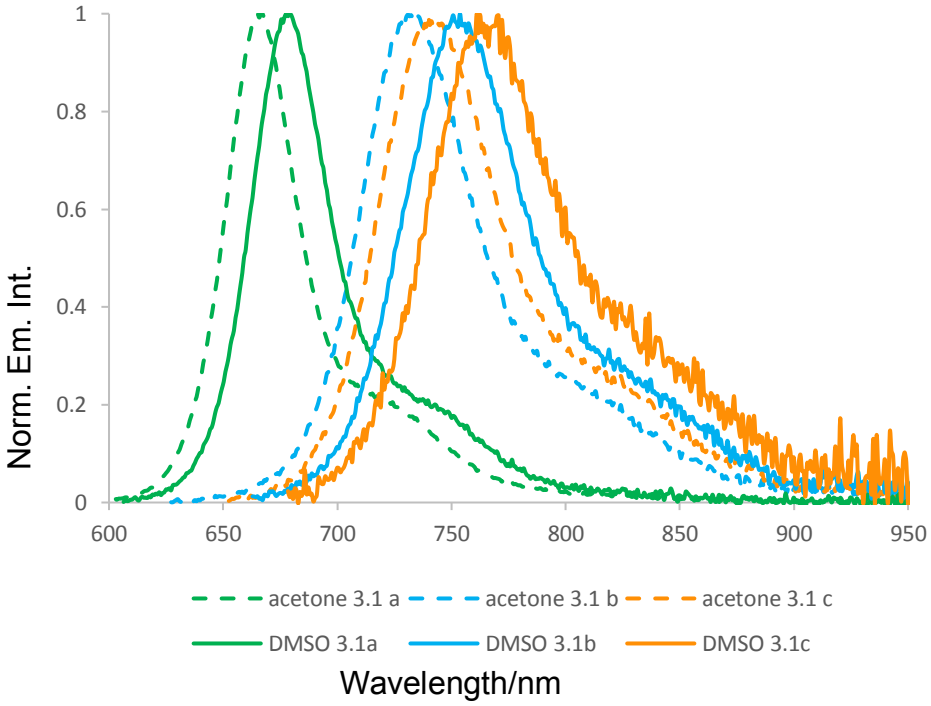

Figure 3.6. Normalized emission spectra of dyes **3.1a-3.1c** in acetone and DMSO.

Table 3.1. Spectroscopic data of dyes **3.1a**–**3.1c** in acetone

dye	solvent	λ_{abs}[a]/nm	λ_{ex}[b]/nm	λ_{fl}[c]/nm	Φ_f[d]	ε[e]/M^{-1} cm^{-1}	Stokes Shift/cm^{-1}
3.1a	acetone	617	580	667	0.85	81,000	1215
	DMSO	626	580	679	0.39	72,000	1247
3.1b	acetone	657	610	733	0.55	63,000	1578
	DMSO	670	625	754	0.27	56,000	1663
3.1c	acetone	662	625	740	0.31	66,000	1592
	DMSO	678	650	761	0.09	60,000	1609

a: absorption maxima. b: excitation wavelength. c: fluorescence emission maxima. d: fluorescence quantum yield. e: molar absorption coefficient.

3.4.2.2. Chemiluminescence

To our delight, all the CL BODIPYs emitted red chemiluminescence under conditions: the mixture of the dye (80 μM in MeOH, 500 μl), H_2O_2 (0.12 M in H_2O, 17 μl) and horseradish peroxidase (HRP) (10 μM in 0.1 M K_2CO_3 aq., 500 μl). **Figure 3.9** shows normalized chemiluminescence spectra. All the dyes showed sharp single chemiluminescence band in NIR regions with emission maxima in 670–738 range. And no chemiluminescence derived from the luminol parts was observed.

As expected, a longer extension of π-conjugation and the addition of electron-donating groups red-shifted the chemiluminescence band. The varied emission bands of the different dyes demonstrate that various chemiluminescence

wavelengths could be achieved by exchanging different substitution groups at the 3,5-positions.

The chemiluminescence of the CL BODIPYs as a function of time was measured. After a short time of fluctuation, the probes exhibited a typical chemiluminescent kinetic file, the signal decreased to zero gradually (**Figure 3.8** A-D). Total photo count emitted from each of the probes was shown in **Figure 3.8** E-H.

The chemiluminescence quantum yield (Φ_{CL}) of the CL BODIPYs was calculated using luminol as a standard. Dye **3.1a** showed much stronger light emission than that of luminol (c.a. 3-fold). However, weaker light emission was observed for dye **3.1b** and **3.1c** (1/3-fold for **3.1b**, 1/6 for **3.1c**), which coincide with the previous conclusion that slight modification on the structure of luminol tend to decrease its quantum yield[6].

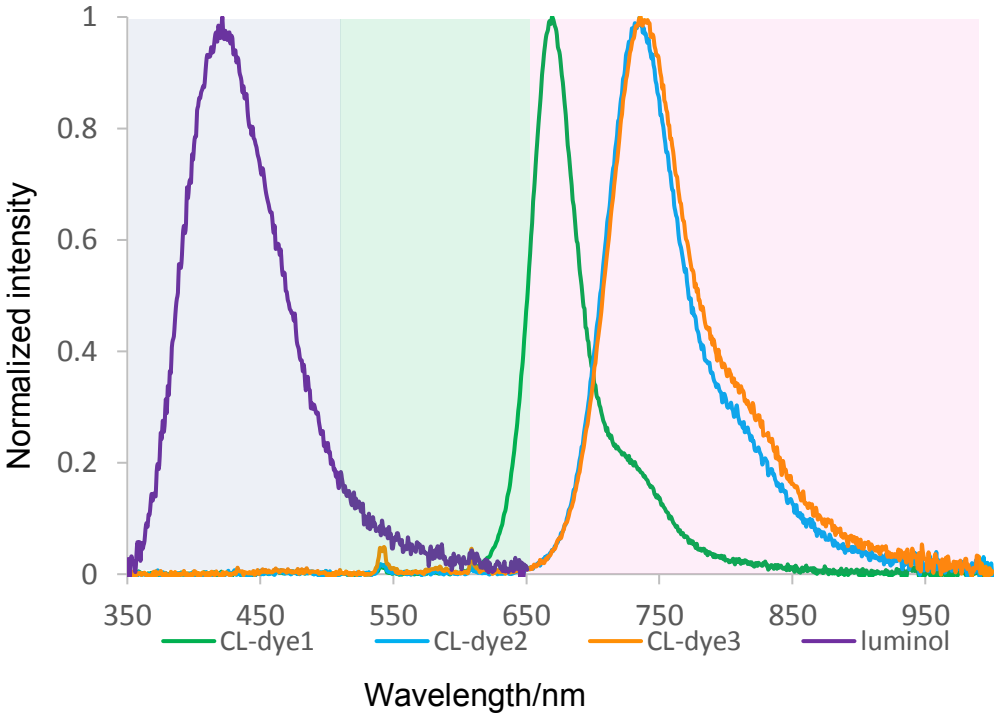

Figure 3.7. Normalized chemiluminescence emission spectra of dyes **3.1a**–**3.1c** and luminol[#]. #: the spectra of luminol was recorded as the following condition: the mixture of the dye (80 μM in 0.1M K_2CO_3 aq., 500 μl), H_2O_2 (0.12 M in H_2O, 17 μl) and HRP (10 μM in 0.1M K_2CO_3 aq., 500 μl).

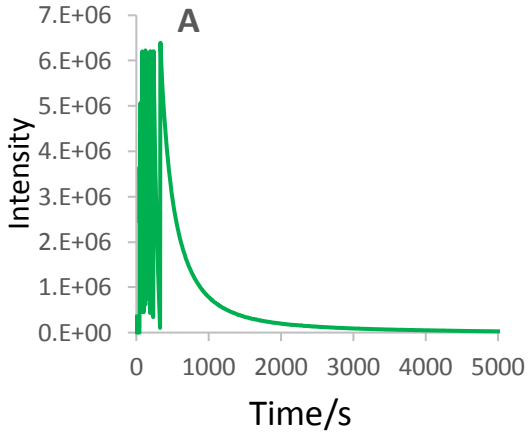
A
Intensity
7.E+06
6.E+06
5.E+06
4.E+06
3.E+06
2.E+06
1.E+06
0.E+00
0
1000
2000
3000
4000
5000
Time/s

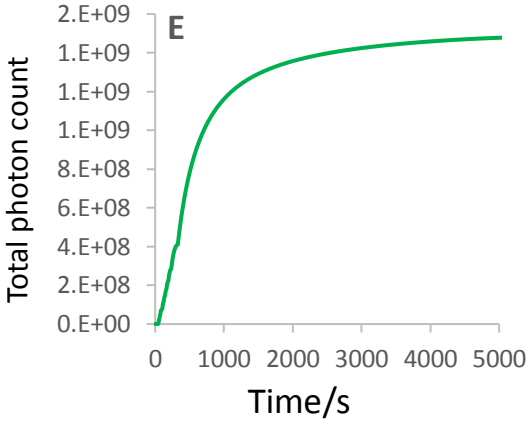
E
Total photon count
2.E+09
1.E+09
1.E+09
1.E+09
8.E+08
6.E+08
4.E+08
2.E+08
0.E+00
0
1000
2000
3000
4000
5000
Time/s

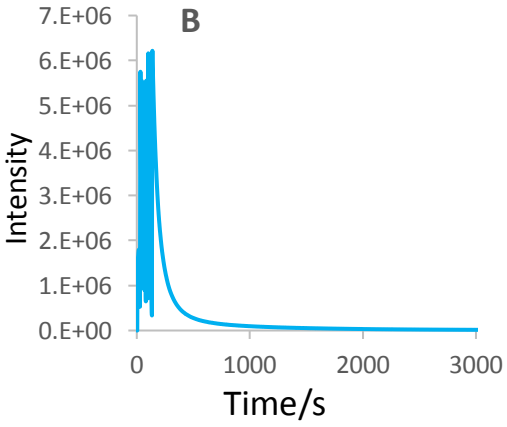
B
Intensity
7.E+06
6.E+06
5.E+06
4.E+06
3.E+06
2.E+06
1.E+06
0.E+00
0
1000
2000
3000
Time/s

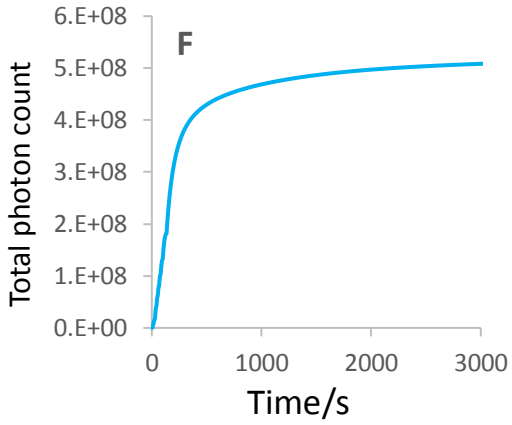
F
Total photon count
6.E+08
5.E+08
4.E+08
3.E+08
2.E+08
1.E+08
0.E+00
0
1000
2000
3000
Time/s

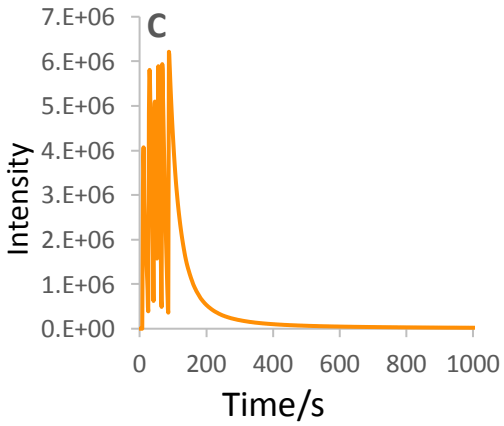
C
Intensity
7.E+06
6.E+06
5.E+06
4.E+06
3.E+06
2.E+06
1.E+06
0.E+00
0
200
400
600
800
1000
Time/s

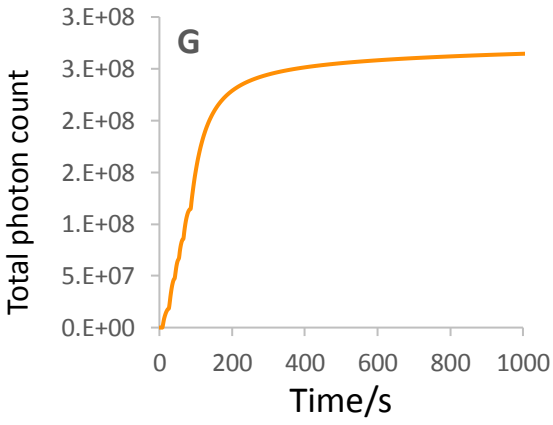
G
Total photon count
3.E+08
3.E+08
2.E+08
2.E+08
1.E+08
5.E+07
0.E+00
0
200
400
600
800
1000
Time/s

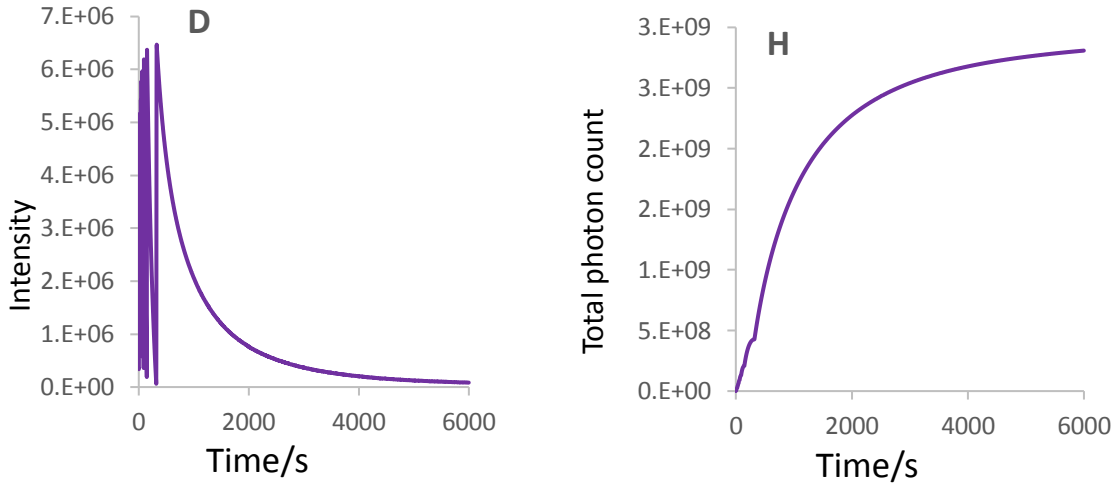

Figure 3.8. (A-D) Chemiluminescent kinetic profiles of 80 μM (A) dye **3.1a**, (B) dye **3.1b**, (C) dye **3.1c** (D) luminol (green, blue, yellow, purple lines, respectively). (E-H) Total photon counts emitted from (E) dye **3.1a**, (F) dye **3.1b**, (G) dye **3.1c**, (H) luminol.

Table 3.3. Chemiluminescence data of dyes **3.1a–3.1c**

dye	λ_{CL}/nm[a]	$T_{1/2}$/s[b]	Φ_{CL}[c]	Relative Φ_{CL}
3.1a	670	480	8.3×10^{-5}	3.55
3.1b	735	165	8.2×10^{-6}	0.35
3.1c	736	95	4.0×10^{-6}	0.17
luminol	421	800	2.3×10^{-5}	1

a: chemiluminescence maxima. b: half-lives of light emission. c: chemiluminescence quantum yield.

3.5. Conclusion

In this chapter, a simple and practical synthesis route for luminol-based NIR chemiluminescence BODIPY dyes were developed. The luminol precursors were introduced on to the NIR BODIPYs via a Suzuki–Miyaura cross-coupling. The late-stage functionalization was carried out at the last synthesis step, the intermediates and all target compounds were easily purified by silica gel chromatography. Following the synthesis route, a series of three kinds of luminol-based NIR chemiluminescent BODIPY dyes were prepared by connecting the luminol part to the NIR BODIPY dyes though direct bond. The synthesized dyes produced chemiluminescence of various wavelengths in the NIR regions under the identical condition, which indicates various NIR chemiluminescent dyes can be developed by simply exchanging the substitution groups on parent BODIPY fluorescent dyes.

Reference

1. Roda, A.; Guardigli, M. Analytical chemiluminescence and bioluminescence: Latest achievements and new horizons. *Analytical and bioanalytical chemistry* **2012**, *402*, 69-76
2. Roda, A.; Guardigli, M.; Pasini, P.; Mirasoli, M.; Michelini, E.; Musiani, M. Bio- and chemiluminescence imaging in analytical chemistry. *Analytica chimica acta* **2005**, *541*, 25-35
3. Hananya, N.; Eldar Boock, A.; Bauer, C.R.; Satchi-Fainaro, R.; Shabat, D. Remarkable enhancement of chemiluminescent signal by dioxetane–fluorophore conjugates: Turn-on chemiluminescence probes with color modulation for sensing and imaging. *Journal of the American Chemical Society* **2016**, *138*, 13438-13446
4. Dodeigne, C.; Thunus, L.; Lejeune, R. Chemiluminescence as diagnostic tool. A review. *Talanta* **2000**, *51*, 415-439
5. Kricka, L. Clinical applications of chemiluminescence. *Analytica chimica acta* **2003**, *500*, 279-286
6. White, E.H.; Roswell, D.F. Chemiluminescence of organic hydrazides. *Accounts of Chemical Research* **1970**, *3*, 54-62
7. Degirmenci, A.; Algi, F. Synthesis, chemiluminescence and energy transfer efficiency of 2, 3-dihydrophthalazine-1, 4-dione and bodipy dyad. *Dyes and Pigments* **2017**, *140*, 92-99
8. Bag, S.; Tseng, J.-C.; Rochford, J. A bodipy-luminol chemiluminescent resonance energy-transfer (cret) cassette for imaging of cellular superoxide. *Organic & biomolecular chemistry* **2015**, *13*, 1763-1767
9. Han, J.; Jose, J.; Mei, E.; Burgess, K. Chemiluminescent energy‐transfer cassettes based on fluorescein and nile red. *Angewandte Chemie International Edition* **2007**, *46*, 1684-1687
10. Yamagishi, Y.; Son, S.-H.; Yuasa, M.; Yamada, K. Design and synthesis of a chemiluminescent solvatochromic dye. *Chemistry Letters* **2012**, *41*, 504-506
11. Sekiya, M.; Umezawa, K.; Sato, A.; Citterio, D.; Suzuki, K. A novel luciferin-based bright chemiluminescent probe for the detection of reactive oxygen species. *Chemical communications* **2009**, 3047-3049

12. Watanabe, N.; Kino, H.; Watanabe, S.; Ijuin, H.K.; Yamada, M.; Matsumoto, M. Synthesis of bicyclic dioxetanes tethering a fluororescer through an ω-carbamoyl-substituted linker and their high-performance chemiluminescence in an aqueous system. *Tetrahedron* **2012**, *68*, 6079-6087
13. Yamaguchi, M.; Yoshida, H.; Nohta, H. Luminol-type chemiluminescence derivatization reagents for liquid chromatography and capillary electrophoresis. *Journal of Chromatography A* **2002**, *950*, 1-19
14. Marquette, C.A.; Blum, L.J. Applications of the luminol chemiluminescent reaction in analytical chemistry. *Analytical and Bioanalytical Chemistry* **2006**, *385*, 546-554
15. Reichardt, C. Solvatochromic dyes as solvent polarity indicators. *Chemical Reviews* **1994**, *94*, 2319-2358
16. Umezawa, K.; Matsui, A.; Nakamura, Y.; Citterio, D.; Suzuki, K. Bright, color‐tunable fluorescent dyes in the vis/nir region: Establishment of new "tailor‐made" multicolor fluorophores based on borondipyrromethene. *Chemistry–A European Journal* **2009**, *15*, 1096-1106
17. Qin, W.; Baruah, M.; Van der Auweraer, M.; De Schryver, F.C.; Boens, N. Photophysical properties of borondipyrromethene analogues in solution. *The Journal of Physical Chemistry A* **2005**, *109*, 7371-7384
18. Nano, A.; Ziessel, R.; Stachelek, P.; Harriman, A. Charge‐recombination fluorescence from push–pull electronic systems constructed around amino‐substituted styryl–bodipy dyes. *Chemistry–A European Journal* **2013**, *19*, 13528-13537
19. Shi, W.-J.; Lo, P.-C.; Singh, A.; Ledoux-Rak, I.; Ng, D.K. Synthesis and second-order nonlinear optical properties of push-pull bodipy derivatives. *Tetrahedron* **2012**, *68*, 8712-8718
20. Ulrich, G.; Barsella, A.; Boeglin, A.; Niu, S.; Ziessel, R. Bodipy‐bridged push–pull chromophores for nonlinear optical applications. *ChemPhysChem* **2014**, *15*, 2693-2700
21. Jiao, L.; Wu, Y.; Wang, S.; Hu, X.; Zhang, P.; Yu, C.; Cong, K.; Meng, Q.; Hao, E.; Vicente, M.G.a.H. Accessing near-infrared-absorbing bf2-azadipyrromethenes

via a push–pull effect. *The Journal of organic chemistry* **2014**, *79*, 1830-1835

Chapter 4 Cell imaging by NIR BODIPY dyes

4.1. Abstract

In this chapter, to investigate the performance of synthesized NIR BODIPY dyes in practical application, biological studies were carried out. Cellular imaging of NIR fluorescent BODIPY dyes was conducted using bovine cumulus cells. The fluorescence microscopy images indicated that the dyes penetrated the membrane of the cells and was exclusively localized in the cytoplasm rather than the nucleus. The major localization sites of dye **2.1** and **2.2** would be lipid-like drops according to morphology.

4.2. Introduction

Fluorescence imaging technique has become an indispensable tool for noninvasive visualization of molecular processes inside of living cell[1-4]. Particularly, NIR fluorescent dyes which active in the range of 650-900 nm have many advantages: greatly reduced the background signal due to lower autofluorescence in the NIR region, deeper penetration for decreased light scattering and less autoabsorption, and less damage to biological specimens.

Many NIR fluorophores, including NIR fluorescent sensors, have been applied for bio-applications, including specific organelle staining[5], intracellular reactive species sensing (Reactive oxygen species (ROS), reactive nitrogen species (RNS), thiol-containing molecules, ion, pH and enzyme)[6].

To investigate the potential biological usefulness of the developed NIR BODIPY dyes, cellular imaging experiments were performed using bovine cumulus cells. In this chapter, the performance of NIR **dyes 2.1-2.6** for biological

application was tested by staining the bovine cumulus cells. All the NIR dyes penetrated the membrane, and specifically accumulated in the cytoplasm.

4.3. Materials and methods

4.3.1. General Experimental

Fluorescence microscopy images were carried out on Leica DMi 8 fluorescence microscope (Leica Camera AG, Wetzlar, Germany).

4.3.2. Collection and Culture of Bovine Cumulus Cells

Bovine ovaries were obtained from a local slaughterhouse. The ovaries were washed in a sterile solution of saline containing 10 IU/mL of penicillin and streptomycin. After oocytes pick up, cumulus cells remaining in the follicular fluid were used for the experiment.

Collected cumulus cells were transferred to a Petri dish filled with Dulbecco's minimal essential medium (DMEM) containing 5% fetal bovine serum (FBS). Then, cells were cultured for 1–2 days at 38 °C in a humidified atmosphere of 95% air and 5% CO_2. After reaching 70–90% of confluency, the medium was removed. After treated with phosphate buffered saline (PBS), the adherent cells were dissociated by trypsinization and collected after centrifuge (ca. 1,200 rpm, 170 g, 3 min). After dissolved in DMEM with containing 5% FBS, the cumulus cells were transferred to 8 well chamber slide (Watson, Tokyo, Japan). Then, cells were cultured for 1–2 days at 38 °C in a humidified atmosphere of 95% air and 5% CO_2. After reaching 70–80% of confluency, each well was washed and replaced with

fresh DMEM containing 5% FBS.

*4.3.3. Cellular Staining Study of dye **2.1-2.6***

Cell staining was carried out using dye **2.1-2.6**. Stock dye solution (1mM in dimethyl sulfoxide) was diluted with DMEM containing 5% FBS to make final concentration at 10 μM. Hoechst 33242 (Thermo Fisher Scientific, Waltham, MA, USA) was also added to the same medium to stain the nuclei. After incubation at 38 °C in 5% CO_2 incubator for a specific time, the culture medium was removed, and the cells were washed with PBS, and fresh culture medium was added to each well. Images were acquired using a fluorescent microscope with DAPI, TexasRed (TX2) and CY-5 filter cubes.

4.4. Results and discussion

*4.4.1. Cell-permeant of dyes **2.1-2.6***

To assert the performance of the NIR fluorescent dyes in practical use, cellular imaging was conducted using bovine cumulus cells to investigate the cellular uptake and the main subcellular localization site of the NIR dyes.

To simplify the cellular observation, dual staining experiments were performed. 10 μM dyes **2.1-2.6** and Hoechst (nucleus) were incubated with bovine cumulus cells at 38 °C, respectively. The images of the cells stained by the dyes **2.1-2.3** were obtained after incubation for 1 h, as shown in **Figure 4.1**, **4.2** and **4.3**. However, dyes **2.4-2.6** did not penetrate the membrane efficiently within 1h. Fluorescence images (**Figure 4.4, 4.5** and **4.6**) were obtained after extension the

incubation time to 7h. Low penetration efficiency of dyes **2.4-2.6** could be due to their high hydrophobicity and poor solubility in aqueous solution. And their staining images were dim with high background. It suggested that dyes **2.1-2.3** are more useful for cell imaging.

Excitation and observation of dye **2.1** and Hoechst were achieved using TX2 and DAPI filter cubes. Dye **2.1** appeared to be accumulated in the cytoplasm (red color) of the cell, but not in the nucleus (black area), as shown in **Figure 4.1c**. We further merged these two images, and an image of clear contrast (**Figure 4.1d**) was obtained. As we know that Hoechst specifically stains the nuclei other than the cytoplasm, the images indicated that dye **2.1** was exclusively localized in the cytoplasm.

A similar phenomenon was observed for other 5 dyes, the observations agree with previously reported studies[7,8].

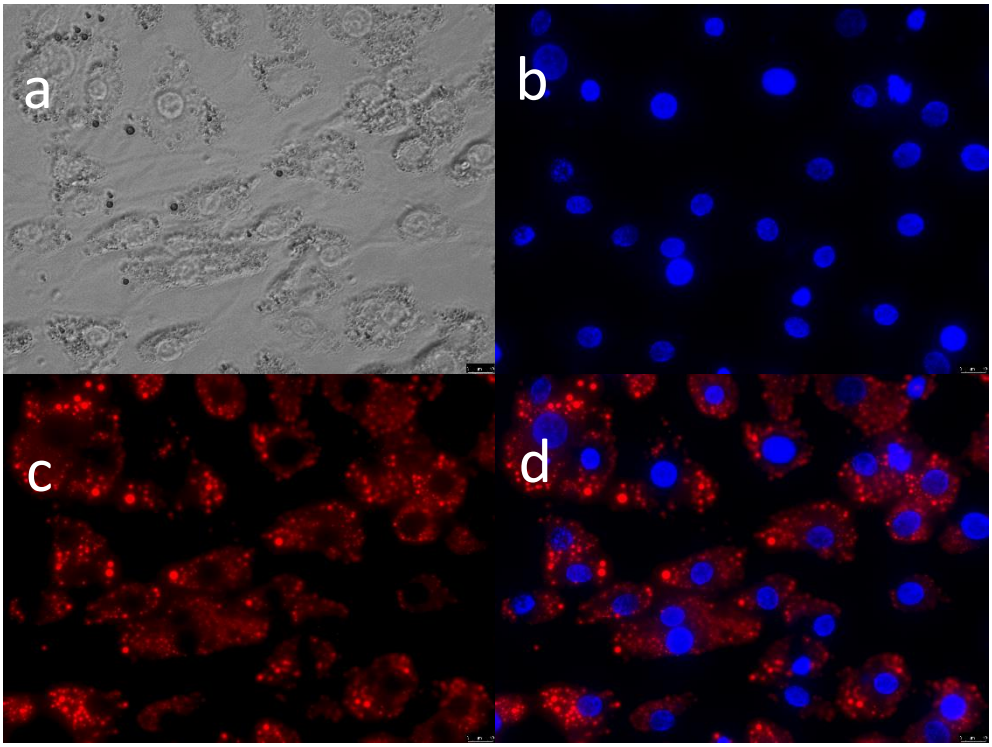

Figure 4.1. Fluorescence colocalization images of dye **2.1** and Hoechst 33242 in live bovine cumulus cells. (a) bright field. (b) Hoechst stained nuclei region, DAPI filters (BP 350/50, BP 460/50). (c) cellular uptake of dye **2.1** in the cytoplasm, TX2 filters (BP 560/40, BP 645/75). (d) overlay of b/c.

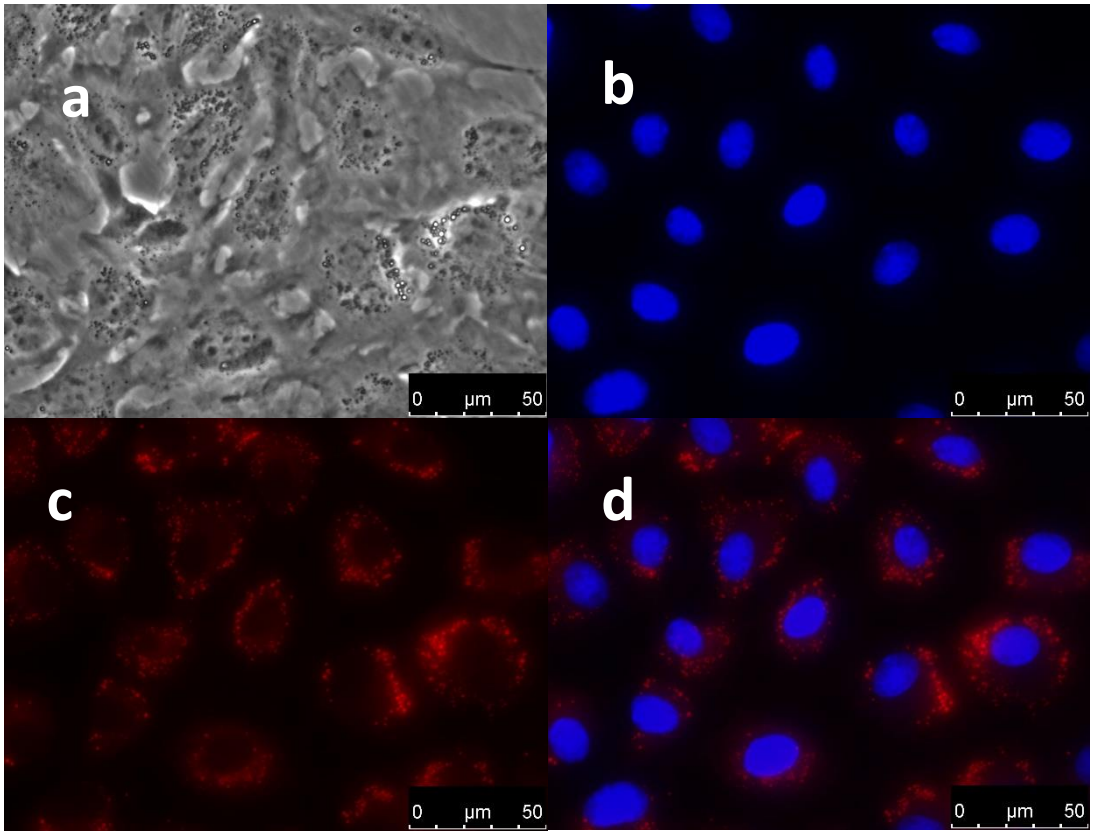

Figure 4.2. Fluorescence colocalization images of dye **2.2** and Hoechst 33242 in live bovine cumulus cells. (a) bright field. (b) Hoechst stained nuclei region, DAPI filters. (c) cellular uptake of dye **2.2** in the cytoplasm, TX2 filters. (d) overlay of b/c.

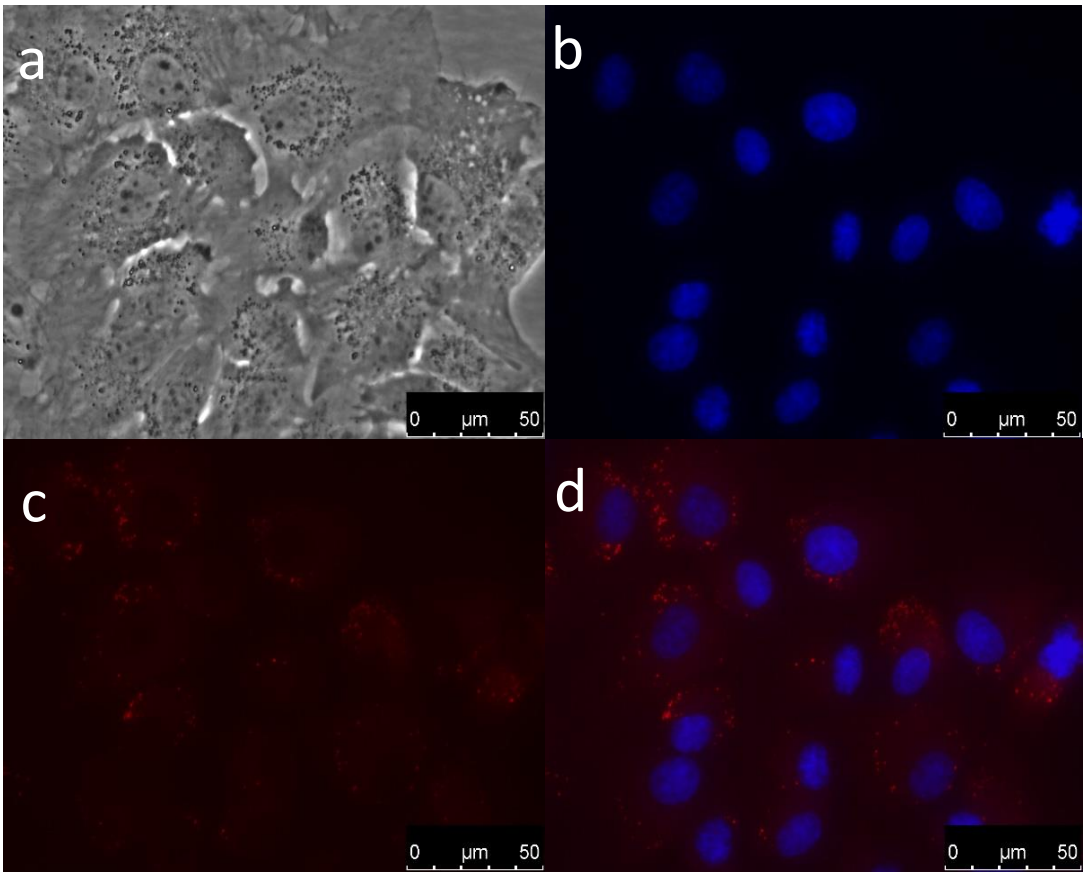

Figure 4.3. Fluorescence colocalization images of dye **2.3** and Hoechst 33242 in live bovine cumulus cells. (a) bright field. (b) Hoechst stained nuclei region, DAPI filters. (c) cellular uptake of dye **2.3** in the cytoplasm, TX2 filters. (d) overlay of b/c.

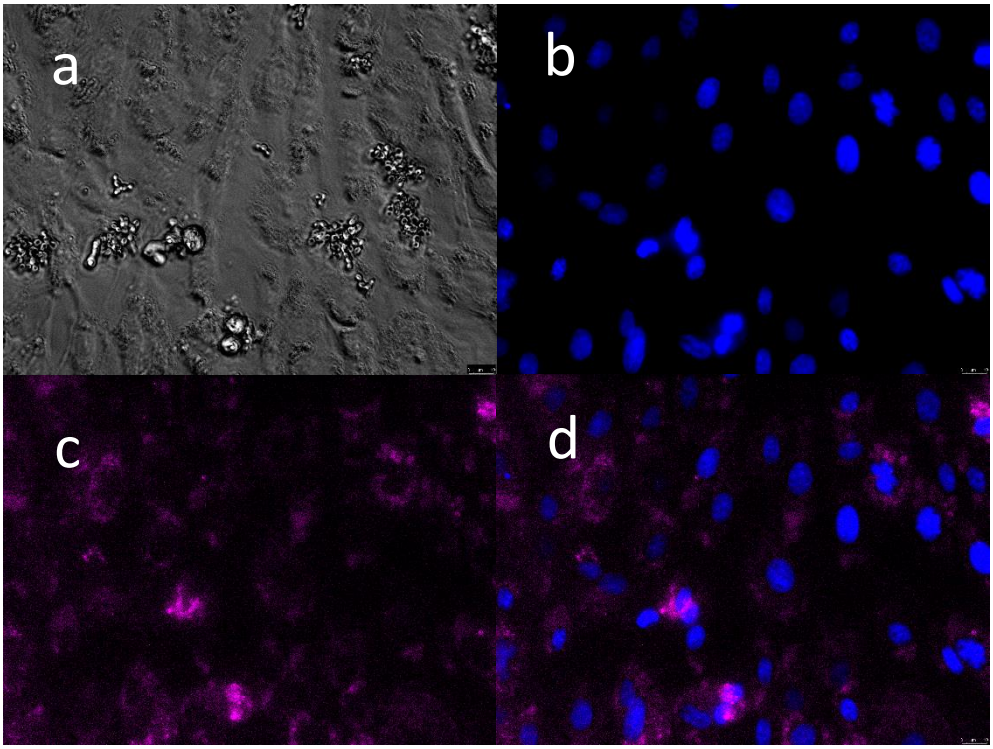

Figure 4.4. Fluorescence colocalization images of dye **2.4** and Hoechst 33242 in live bovine cumulus cells. (a) bright field. (b) Hoechst stained nuclei region, DAPI filters. (c) cellular uptake of dye **2.4** in the cytoplasm, CY-5 filters (BP 620/60, BP 700/75). (d) overlay of b/c.

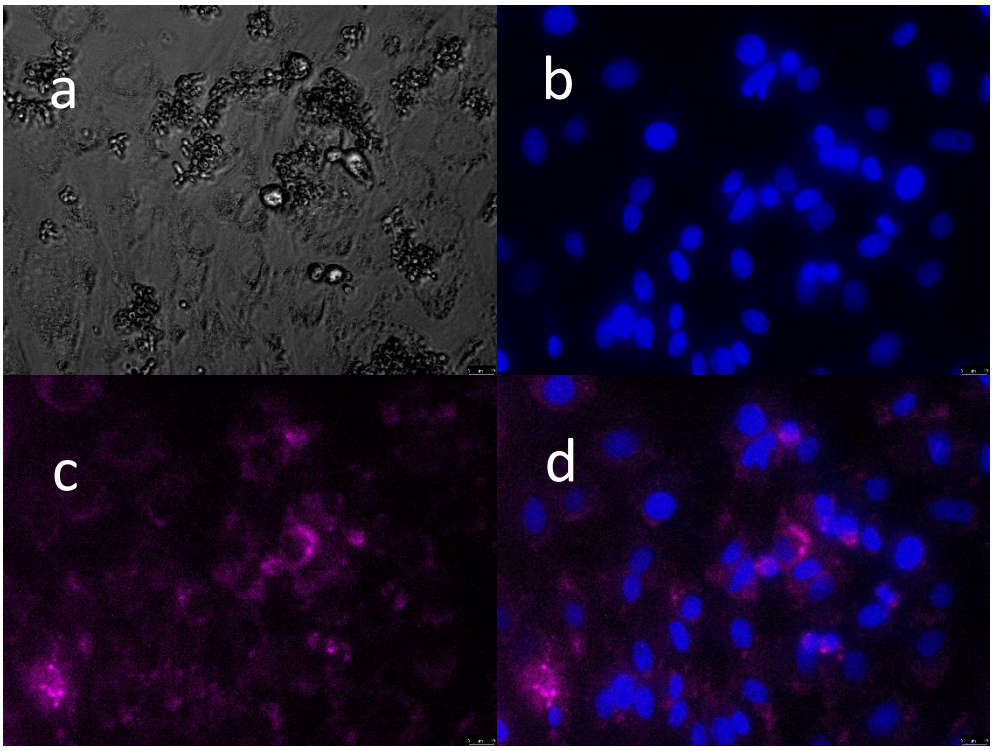

Figure 4.5. Fluorescence colocalization images of dye **2.5** and Hoechst 33242 in live bovine cumulus cells. (a) bright field. (b) Hoechst stained nuclei region, DAPI filters. (c) cellular uptake of dye **2.5** in the cytoplasm, CY-5 filters. (d) overlay of b/c.

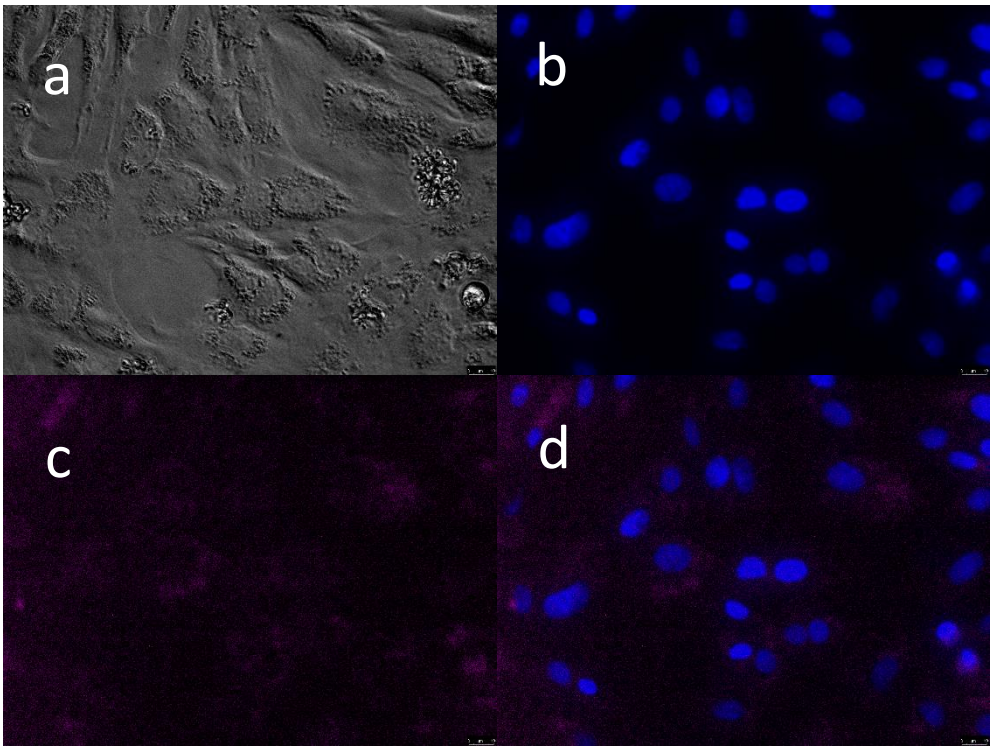

Figure 4.6. Fluorescence colocalization images of dye **2.6** and Hoechst 33242 in live bovine cumulus cells. (a) bright field. (b) Hoechst stained nuclei region, DAPI filters. (c) cellular uptake of dye **2.6** in the cytoplasm, CY-5 filters. (d) overlay of b/c.

4.4.2. Identification of staining targets in the cells.

To further investigate the subcellular location of dye **2.1-2.3**, identification of staining targets was carried out by comparison of organelle-specific probes. Commercially available LysoBrite™ Red (lysosome-staining dye) (Figure **4.7**) and MitoTracker green (mitochondria-staining dye) (Figure **4.8**) were used as reference dyes. The staining pattern of the dye **2**.**1** was different from these two reference probes, which suggested that dye **2.1** does not specifically localize in lysosome and mitochondria.

The figure **4.9-4.11** showed the enlarged representations of cells stained by dye **2.1**, **2.2**, and **2.3**, respectively. In figure **4.9**, we can find that the spots stained by dye **2.1** match the spots observed in the bright field (Figure **4.9a**), indicating that dye **2.1** may specific staining the lipid droplets in the cell. Dye **2.2** showed similar staining properties as that of dye **2.1**. Dye **2.3** stained some of the spots in the bright field, it does not show obvious organelle staining in the cells.

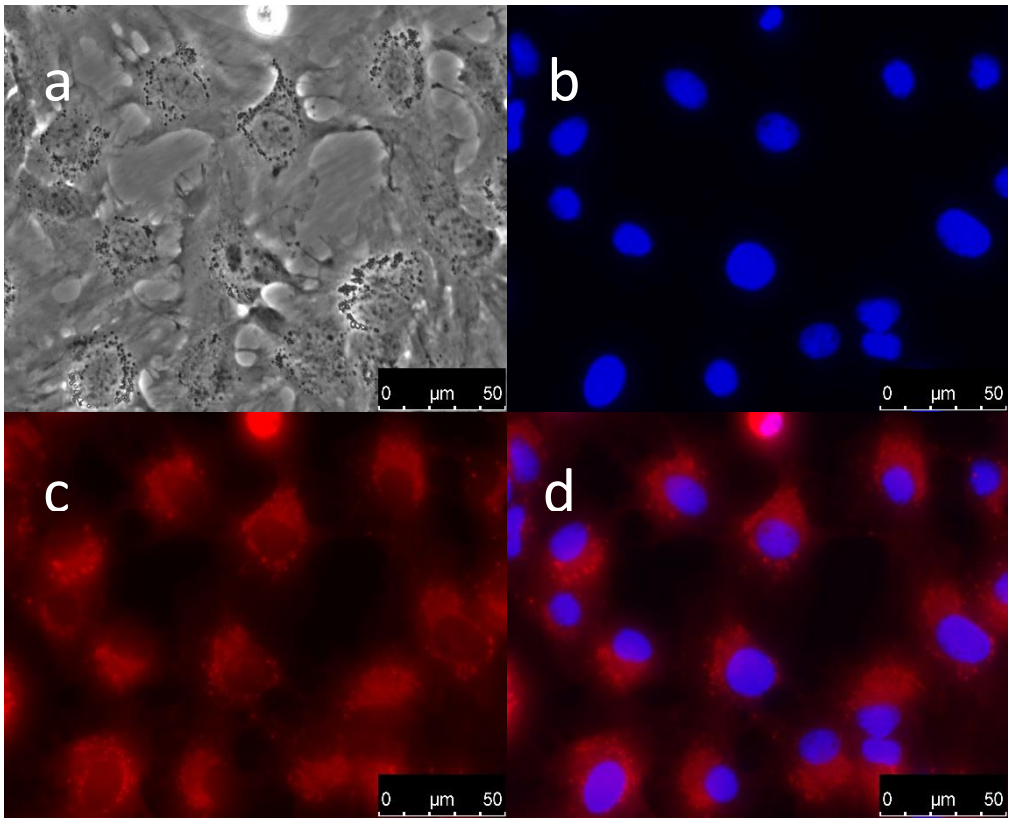

Figure 4.7. Fluorescence colocalization images of LysoBrite™ Red and Hoechst 33242 in live bovine cumulus cells. (a) bright field. (b) Hoechst stained nuclei region, DAPI filters. (c) cellular uptake of LysoBrite™ Red in lysosome, TX2 filters. (d) overlay of b/c.

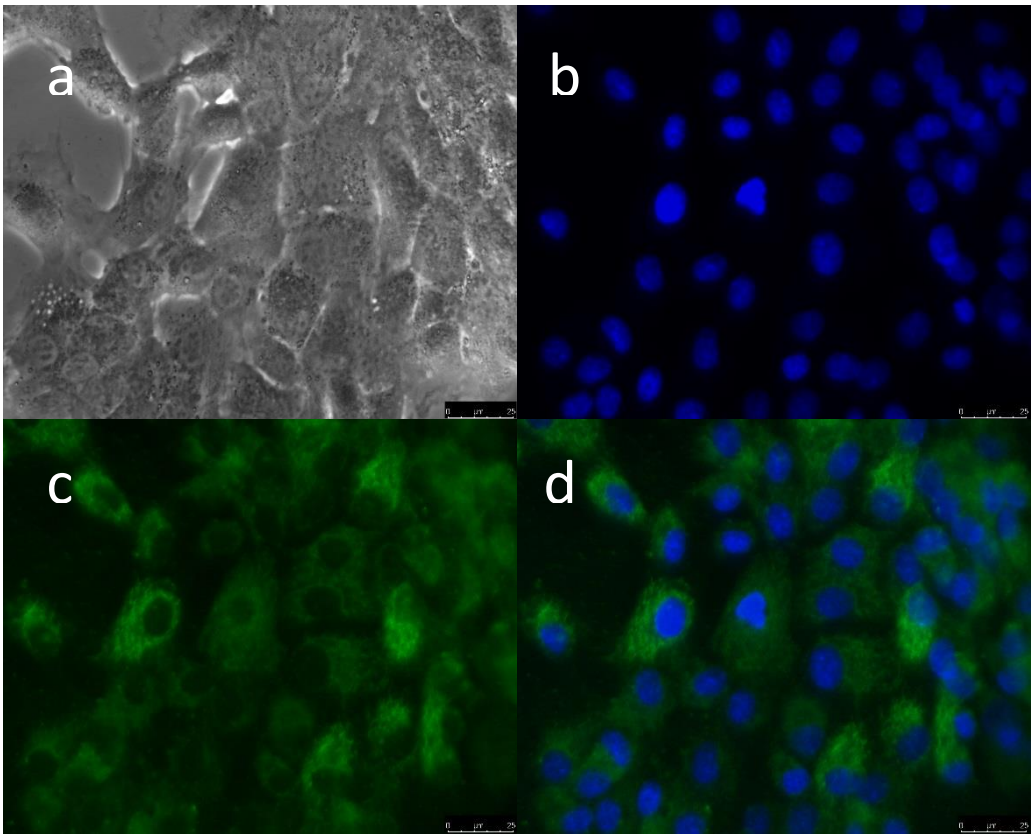

Figure 4.8. Fluorescence colocalization images of MitoTracker green and Hoechst 33242 in live bovine cumulus cells. (a) bright field. (b) Hoechst stained nuclei region. (c) cellular uptake of MitoTracker green in mitochondria, GFP filters (BP 470/40, BP 525/50). (d) overlay of b/c.

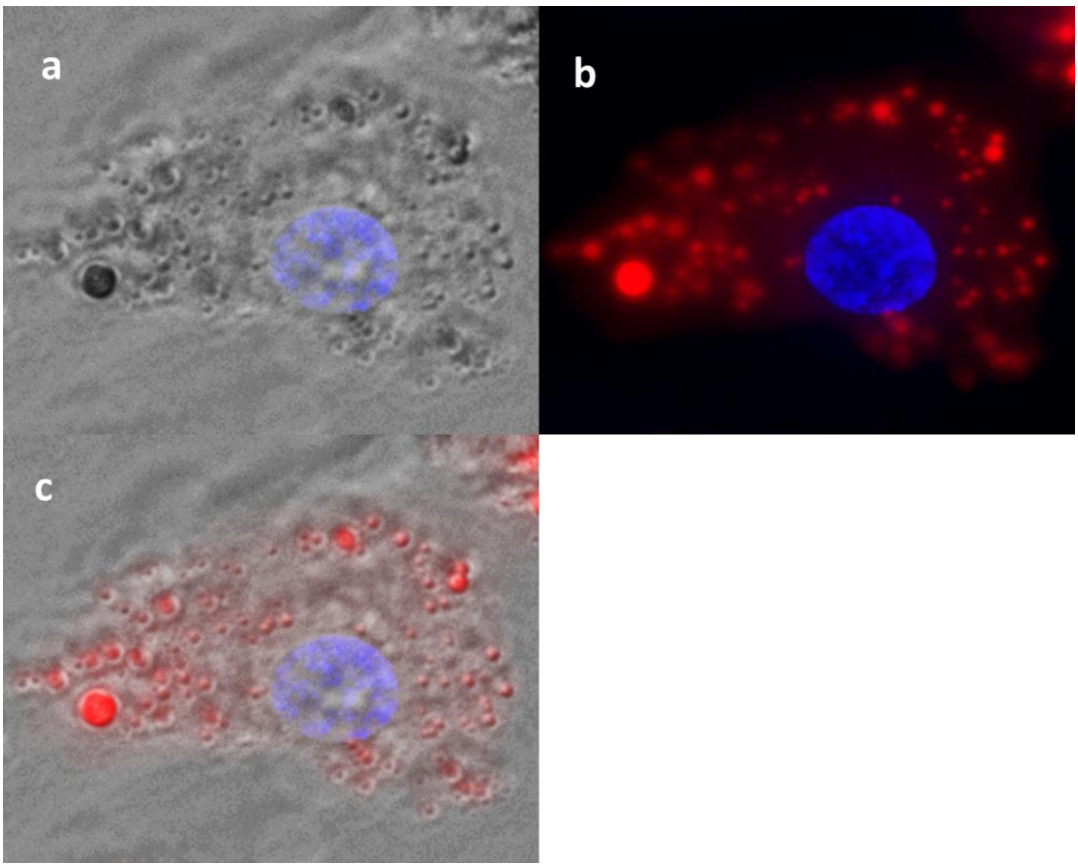

Figure **4.9**. The enlarged representations of cell in Figure **4.1**. (a) Bright field and Hoechst 33242, (b) dye **2.1** and Hoechst 33242, (c) overlay of a/b.

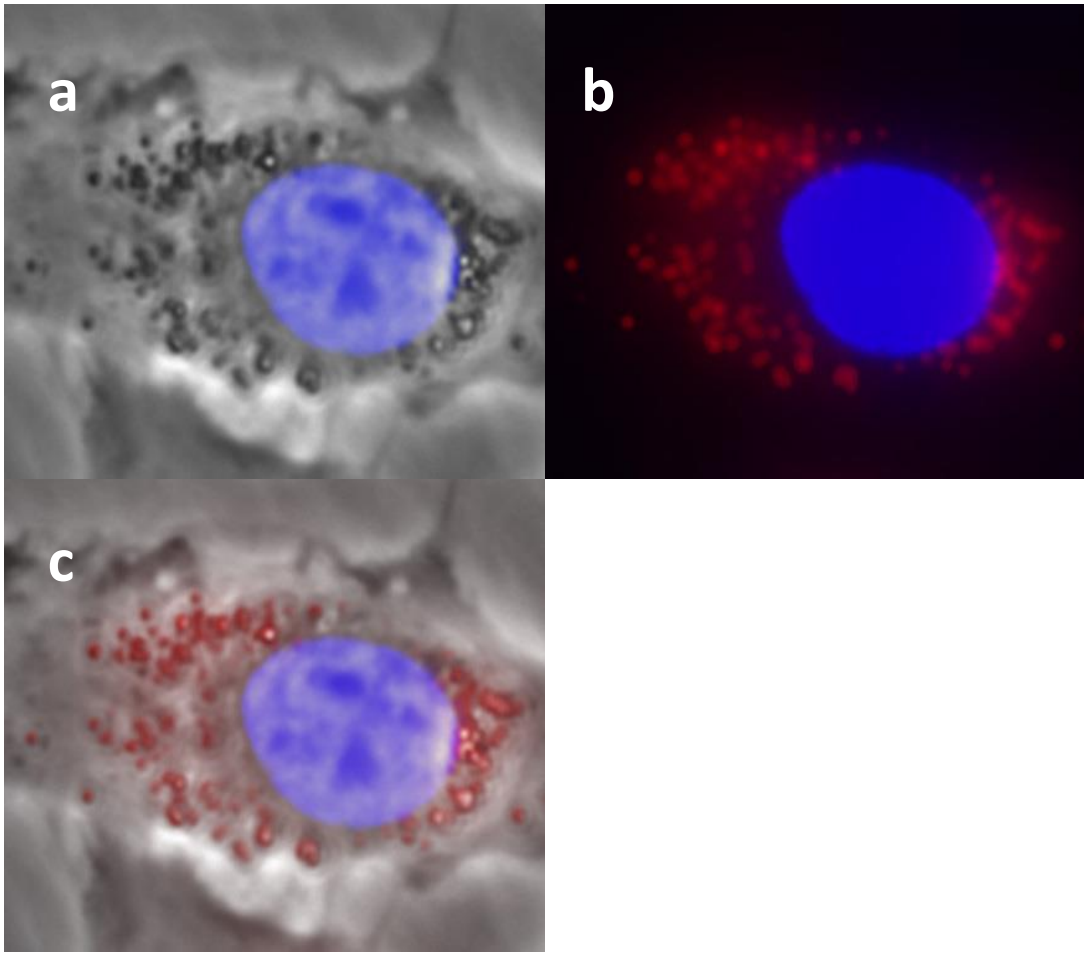

Figure **4.10**. The enlarged representations of cell in Figure **4.2**. (a) Bright field and Hoechst 33242, (b) dye **2.2** and Hoechst 33242, (c) overlay of a/b.

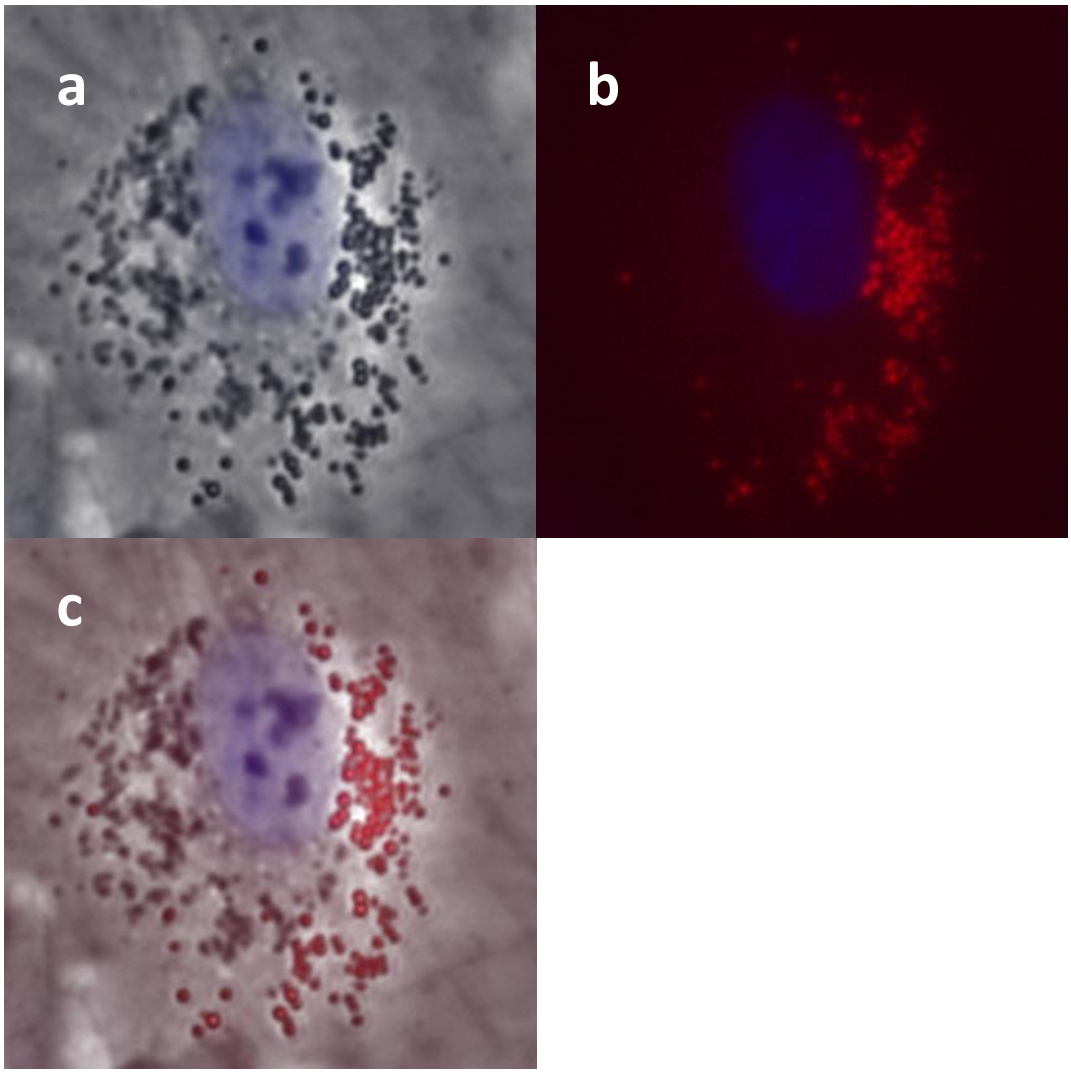

Figure **4.11**. The enlarged representations of cell in Figure **4.3**. (a) Bright field and Hoechst 33242, (b) dye **2.3** and Hoechst 33242, (c) overlay of a/b.

4.5. Conclusions

Cellular imaging of NIR fluorescent BODIPY dyes was conducted using bovine cumulus cells. The fluorescence microscopy images indicated that all the dyes penetrated the membrane of the cells, and exclusively localized in the cytoplasm rather than the nucleus. Dye **2.1-2.3** showed higher penetration efficiency through the cell membrane. On the morphological ground, dye **2.1** and **2.2** would specific stain the lipid-like drops in the cells.

Reference

1. Ettinger, A.; Wittmann, T. Fluorescence live cell imaging. In *Methods in cell biology*, Elsevier: 2014; Vol. 123, pp 77-94.
2. Yang, Y.; Zhao, Q.; Feng, W.; Li, F. Luminescent chemodosimeters for bioimaging. *Chemical Reviews* **2012**, *113*, 192-270
3. Escobedo, J.O.; Rusin, O.; Lim, S.; Strongin, R.M. Nir dyes for bioimaging applications. *Current opinion in chemical biology* **2010**, *14*, 64-70
4. Liu, Z.; Lavis, L.D.; Betzig, E. Imaging live-cell dynamics and structure at the single-molecule level. *Molecular cell* **2015**, *58*, 644-659
5. Jiang, N.; Fan, J.; Liu, T.; Cao, J.; Qiao, B.; Wang, J.; Gao, P.; Peng, X. A near-infrared dye based on bodipy for tracking morphology changes in mitochondria. *Chemical Communications* **2013**, *49*, 10620-10622
6. Guo, Z.; Park, S.; Yoon, J.; Shin, I. Recent progress in the development of near-infrared fluorescent probes for bioimaging applications. *Chemical Society Reviews* **2014**, *43*, 16-29
7. Zhu, L.; Xie, W.; Zhao, L.; Zhang, Y.; Chen, Z. Tetraphenylethylene-and fluorene-functionalized near-infrared aza-bodipy dyes for living cell imaging. *RSC Advances* **2017**, *7*, 55839-55845
8. Xuan, S.; Zhao, N.; Ke, X.; Zhou, Z.; Fronczek, F.R.; Kadish, K.M.; Smith, K.M.; Vicente, M.G.H. Synthesis and spectroscopic investigation of a series of push–pull boron dipyrromethenes (bodipys). *The Journal of organic chemistry* **2017**, *82*, 2545-2557

Chapter 5 Summary and Conclusion

A straightforward method to synthesize NIR BODIPY fluorophores by using a one-step Suzuki–Miyaura cross-coupling was proposed in chapter 2. Following the synthesis method, six kinds of thieno-expended red and NIR BODIPY fluorescent dyes were synthesized in acceptable yields. And all the dyes exhibited relatively high fluorescent quantum yield. It was the first time that electron-donating group modified thiophene parts were efficiently introduced onto the 3- and 5- positions of the BODIPY core.

In chapter 3, three kinds of luminol-based NIR chemiluminescent BODIPY dyes were developed by conjugating a luminol part at the 2-position of the NIR fluorescent BODIPY dyes through a direct bond. They emit different chemiluminescence in the NIR region under identical reaction conditions, indicating that various NIR chemiluminescent dyes can be developed by simply exchanging the parent NIR BODIPY fluorescent dyes.

Chapter 4 investigated the performance of synthesized NIR BODIPY dyes in practical use. The cell staining experiments were carried out by incubation of NIR fluorescent BODIPY dyes with bovine cumulus cells. The fluorescence microscope images indicated the all the dyes penetrated the membrane of the cells, and exclusively localized in the cytoplasm rather than the nucleus. They could be used as subcellular fluorescent probes in live cells.

Therefore, it can be expected that various NIR fluorescent and chemiluminescent dyes could be prepared following the proposed methods.

Acknowledgment

I would like to thank my supervisor Associate Professor Koji Yamada for his invaluable guidance, scholastic advice and earnest support. Thanks to his guidance on the research, I could experience a “colorful” world of photochemistry and organic chemistry.

I own my great appreciation to Prof. Nobuo Sakairi and Prof. Katsuaki Konishi for their helpful suggestion on the dissertation. I am grateful to Prof. Masashi Takahashi for his kind guidance, constructive suggestions and facilitation in his laboratory. Thanks to all the three professors for setting aside time in their busy schedules to review my thesis.

My sincere gratitude is extended to Prof. Takashi Hirano (The University of Electro-Communications) and Associate Prof. Toshikazu Kawaguchi for his useful suggestions and many help in my experiments. Also, I will appreciate Associate Prof. Taiki Umezawa and Assistant Prof. Tatsuya Morozumi for their help on 13C NMR measurement.

I would like to appreciate Prof. Min Yao and Prof. Isao Tanaka for their great help in my research and daily life.

I want to thank Mr. Jianye Li, Mr. Toshiyuki Suzuki and Ms. Shuang Li for helping me do some experiments and their useful suggestions.

I would like to show my sincere thanks to all the members of Sakairi and Yamada lab, especially Dr. Bin Han, Mr. Otsuka Yu, Mr. Takuya Matsumiya and

Mr. Yasuhide Fukuyo.

I would also like to thank my friends here. They made my life wonderful in Sapporo.

Finally, I would thank my family, thank you for your love and understanding.